PHOSPHORUS LEACHING FROM MANURE-IMPACTED SOILS AFFECTED BY FLUCTUATING WATER TABLES

By

JAIME MEJIAS-BASSALETTI

A dissertation submitted in partial fulfillment of
the requirements for the degree of

DOCTOR OF PHILOSOPHY

WASHINGTON STATE UNIVERSITY
Department of Biological Systems Engineering

August, 2005

To the Faculty of Washington State University:

The members of the Committee appointed to examine the dissertation of JAIME MEJIAS-BASSALETTI find it satisfactory and recommend that it be accepted.

_____
Chair

_____

_____

_____

_____

Acknowledgements

First, I would like to express my sincere appreciation to the Government of Chile and the "Instituto de Investigaciones Agropecuarias, INIA-Chile" for providing the financial assistance during my doctorate studies at Washington State University. Partial financial support for this work was also provided by The State of Washington Water Research Center (SWWRC).

I would like to express my gratitude to Dr. Markus Flury, whose expertise, ethics, understanding, and patience, helped considerably to my learning process. I appreciate his great assistance in writing grant proposals, and his technical support in correcting and editing this thesis. Special thanks goes out to my supervisor Claudio Stöckle for his support and direction during all these years. I would like to thank the other members of my committee, Dr. Harsh, Dr. Harrison, Dr. Manoranjan and Dr. Chen for the assistance they provided at all levels of this research. Appreciation also goes out to Dr. Jeff Boyle, and Dr. Deng for their invaluable assistance in soil chemical analyses. Thanks are also given to Dr. Kennedy for her continuous interest in this research and her technical support. I would also like to thank to Dr. VanWieringen for her invaluable help in contacting farmers and her assistance in taking soil and water samples.

I am also grateful to my parents, sister, and "tia Maria" for their infinite emotional support. My most important acknowledgement must go to my wife Claudia, for her understanding, efforts and whose love, encouragement and infinite patience provided

me with the strength needed to finish this project. Finally, I am indebted to my children, Paulina, Felipe, Pablo and my baby girl who have followed this process with enthusiasm, and tolerated my absence from home during this five years.

PHOSPHORUS LEACHING FROM MANURE-IMPACTED SOILS AFFECTED BY FLUCTUATING WATER TABLES

Abstract

by Jaime Mejias-Bassaletti, Ph.D.
Washington State University
August, 2005

Chair: Claudio Stöckle

The main objectives of this dissertation were:

1. Acquire relevant field data to determine the role of iron reduction in P transport in tile effluents.

2. Explore the relation of the soil redox potential to P release and transport in column studies under dynamic conditions.

3. Develop a P leaching indicator based on the estimate of the P sorption strength in highly P-impacted soils.

In the first study, we observed a significant positive correlation between P and Fe^{2+} concentrations in drainage water from the pasture, but not in that from the corn field. In the latter, a significant relation was found between P Fe^{3+} concentration. Phosphorus and Fe^{2+} were positively correlated to drain flow rate in the pasture system

and the same was true for P and Fe^{3+} in the corn field. In the second study, we demonstrated that an initially oxidized system saturated with P and under dynamic flow conditions can mobilize P after reductive dissolution of ferric iron. These results revealed that a reduced system presents a sink for P due to precipitation reactions but the system turns unstable after the redox potential increases, fixing less P than the oxidized control system. These findings suggest that alternating anoxic-oxic conditions play an important role in subsurface P transport. In the third study, we demonstrated that the inverse of the equilibrium P concentration at zero sorption ($1/c_e$) is a valid estimate of the soil sorption strength, which may be used as an indicator for P leaching potential. Below a threshold level of $1/c_e$=0.71 L/mg, desorbability parameters increased significantly.

Table of Contents

List of Tables

List of Figures

Chapter 1

Overall Introduction

1.1 Background

Phosphorus is an essential nutrient for plant growth and it is commonly applied to agricultural fields to increase crop yields. Fresh water eutrophication caused by agricultural non-point source pollution has been recognized as one of the leading water quality problems in the U.S. [*USEPA*, 2003]. Since Nitrogen (N) and phosphorus (P) are the main limiting nutrients for primary production in freshwater systems, its control and remediation strategies have been directed mainly to prevent these two nutrients becoming pollutants in the water systems [*Sharpley et al.*, 1999]. However, the exchange of N between the atmosphere and water makes N control more difficult than controlling P inputs. Thus, most attention has focused on P as the limiting factor leading to the accelerated growth of algae and aquatic plants [*Sharpley et al.*, 1999].

Phosphorus is strongly immobilized in soils by mean of ligand exchange reactions with hydroxyls groups in the surface of iron and aluminum hydr(oxides) [*Stumm and*

Sigg, 1979]. Oxide surfaces may adopt positive, negative or neutral charges as a function of the soil pH. The reaction of iron oxides and phosphate can be described according to *Sanchez and Uehara* [1980]:

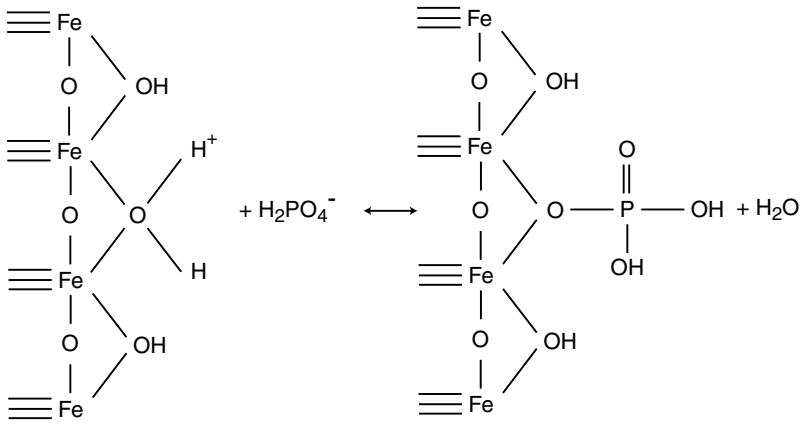

Figure 1.1: Mechanism of P adsorption on Fe(III) oxide surface by ligand exchange reaction.

The rapid growth and intensification of crop and animal farming has led an excessive application of P to land. The accumulation of P in soils at levels that are excessive from an agronomic and environmental point of view has been of major concern in the last few years, because this represents a potential risk for contamination of surface and ground water [*Shober and Sims*, 2003]. Although P is nearly immobile in the soil profile, at elevated soil P concentrations, P can be transported off site and reach fresh water.

Phosphorus is mainly transported via surface runoff attached to soil particles, but in the last few years, P transported via subsurface flow has been a major concern.

Phosphorus can be mobilized and transported in soluble forms after desorption or solubilization processes from the soil matrix. While many P sorption studies have been conducted, the influence of redox reactions on P chemistry and its potential impact on P movement into tile drains has not been investigated intensively. Periodic flooding induce special conditions on P dynamics. Phosphorus associated to iron oxides may be released to pore water upon reduction of ferric iron. The fate of P released by reductive dissolution of iron oxides has been a matter of controversy. Some authors suggests that upon reduction P is released to the pore water and transported through percolating water [*Pant et al.,* 2002]. *Patrick and Khalid* [1974], found that flooding increased the P retention but, after the soils were re-oxidized, P was released more easily and to a greater extent than permanently oxidized soils. As far as we know, no studies on the effect of redox potential on P release to surface water have been conducted in the northwestern Washington State. This dissertation aimed to generate new information on this area of research and contribute to the improvement of P management in this region.

1.2 Scope and Objectives

The overall goal of this dissertation is to study the transport of P in manure-impacted soils affected by periodic flooding. Specifically, we address the following objectives:

1. Acquire relevant field data to determine the role of iron reduction in P transport in tile effluents from a highly P-impacted soil.

2. Explore the relation of the soil redox potential to P release and transport in column studies under dynamic conditions.

3. Develop a P leaching indicator based on the estimate of the P sorption strength of highly P-impacted soils.

1.3 Thesis Outline

This dissertation is organized in three main chapters. The core of each chapter is a paper that has been prepared for submission to a peer reviewed journal.

In Chapter 2 we present field evidence of the effect of redox potential on P release in tile drain outflow, as indicated by the relationship between ferrous iron and P.

In Chapter 3 we present experimental results of the P release and transport affected by oxidation-reduction conditions in dynamic systems.

In Chapter 4 we provide theory and data to obtain a P leaching indicator that can be used as a predictor of risk of P loss via subsurface soils in soils affected by high P inputs.

A summary and overall conclusions are presented in Chapter 5. Tables and figures are presented at the end of each chapter following the format of manuscripts submitted to a journal.

Chapter 2

Phosphorus Leaching from a Tile-drained Histosol under Reductive Dissolution of Iron

2.1 Abstract

Long-term application of animal manure to farmland has caused an excessive accumulation of phosphorus (P) in soils. Under this conditions there is a potential risk of P release to the soil solution and subsequent leaching into surface and groundwater, especially where seasonal flooding occurs. During flooding, iron can be reduced from ferric (Fe^{3+}) to ferrous iron (Fe^{2+}). Phosphorus associated with Fe-minerals can thereby be released into the soil solution and transported to ground and surface waters. We monitored tile drain outflow from a Pangborn muck soil in northwestern Washington State, from April 28^{th} 2004 through February 1^{st} 2005 (279 days). Two systems were compared, a pasture and a corn field. The soil P concentrations (≈300 mg P/kg) were greater than agronomic requirements. Mean P concentration in drain

outflow was 0.02 mg/L for the pasture and 0.07 mg/L for the corn field. These values were higher than suggested critical environmental limits (<0.01 mg/L). During the time of the study, we estimated the loss of P to be 4.2 kg/ha for the pasture and 8.7 kg/ha for the corn field. The soil was periodically flooded as indicated by soil water tension measurements. During flooding, the redox potential of water drainage dropped to ≈180 mV. We observed a significant correlation between P and Fe^{2+} in drainage water from the pasture, but not for the corn field. Instead, in the corn field, P was positively related to Fe^{3+}. Phosphorus and Fe^{2+} in the pasture system, and P and Fe^{3+} in the corn field were related linearly to drain flow rates. We conclude that in the pasture system, P lost in tile drainage was associated with reductive dissolution of Fe. A different geochemical mechanism led to the P release in the corn field. Because no colloids were detected by light scattering analysis, we believe that P and iron were transported as dissolved phases possibly as ternary complexes with dissolved organic matter (DOM) (<1nm particle size).

2.2 Introduction

Phosphorus is considered fairly immobile in soils because of its strong sorption onto aluminum and iron hydroxides [*Sample et al.*, 1980*; Torrent*, 1997]. In the last few years, however, the impact of soil P accumulation on water quality has been of increasing concern. The over application of P in areas of intensive animal production has led to the accumulation of P in soils at levels that are excessive from an environ-

mental point of view [*Shober and Sims,* 2003]. Animal-based agriculture is one of the largest contributors of non-point P contamination of surface waters [*USEPA,* 2003]. A fraction of the accumulated P in soils can be transported via soil erosion, surface runoff, and subsurface transport processes [*Heathwaite and Dils,* 2000]. Phosphorus carried off site can be deposited in water bodies enhancing eutrophication of aquatic ecosystems [*McDowell et al.,* 2002b].

Although subsurface transport of P through soil is considered to be of minor concern, recent reports indicate elevated P concentrations in leachates and tile drainage from agricultural soils receiving high P inputs [*Beauchemin et al.,* 1998*; Heathwaite and Dils,* 2000*; Turner and Haygarth,* 2000*; Kleinman et al.,* 2003]. It has been reported that soils with excessive P levels, low P sorption capacity, high organic matter content, and shallow water tables, are vulnerable to P leaching [*Sims et al.,* 1998]. The risk of P leaching increases if soils are artificially drained [*Sims et al.,* 1998] and if the transport of P is facilitated by preferential flow [*Stamm et al.,* 1998*; Kleinman et al.,* 2003].

Soil P enrichment and anaerobic conditions have been reported as major factors controlling the mobilization of P in subsurface environments. Soils saturated with P are more vulnerable to release P via reductive dissolution of iron oxides during aerobic-anaerobic cycles [*Szilas et al.,* 1998*; Scalenghe et al.,* 2002*; Pant et al.,* 2002]. *Villapando and Graetz* [2001] found that fluctuating water tables increased P leaching in soils receiving intensive manure application. *Young and Ross* [2001] reported that

phosphorus concentration in pore water was directly related to soil P saturation of 14 soils used in a microcosm flooding experiment. *Olila et al.* [1997] reported environmental critical P losses in a constructed wetland after periodic water level drawdown and reflooding cycles.

The reductive transformation of iron–phosphates leading to P release can be described using the strengite dissolution example given by *Willett* [1985]:

$$\mathrm{Fe(III)PO_4}(s) \cdot 2\mathrm{H_2O} + e^- \rightleftharpoons \mathrm{Fe^{2+}}(aq) + \mathrm{H_2PO_4^-}(aq) + 2\mathrm{OH^-} \tag{2.1}$$

The reductive dissolution of iron oxides is commonly controlled by microbial respiration under anaerobic conditions [*Benner et al.,* 2002]. In absence of oxygen, microbes may use $\mathrm{Fe^{3+}}$ as an electron acceptor [*Frederickson et al.,* 1998], thereby releasing the sorbed P to the soil solution [*Pant et al.,* 2002]. Sources of carbon such as DOM, humic, and fulvic acids, have been shown to be effective in promoting iron reduction under anaerobic conditions [*Petruzzelli et al.,* 2005]. Equation 2.1 suggests that water table fluctuations may have a considerable effect on the P mobilization into the drainage system, promoting the pollution of surface waters [*Sims et al.,* 1998].

The Lower Nooksack River watershed in Whatcom county, WA is characterized by agricultural activities such as potato, blueberry, corn and permanent pasture for intensive dairy production [*Cox and Kahle,* 1999]. Soils are usually poorly drained, located on flood plains, and have fluctuating water tables, periodically rising to the soil surface [*Goldin,* 1992]. One third of the dairies of Washington State are located in Whatcom County on soils affected by periodic flooding [*Cox and Kahle,* 1999].

Long–term use of manure in these soils has been of environmental concern. Currently, the Washington Department of Ecology is applying restrictions and regulations on the amount and timing of manure applications on these soils [*Carey,* 2004].

The objective of this study was to acquire relevant field data to determine whether increased P release occurs into tile drains as a result of reductive dissolution of iron oxides. Specifically, we explore the relationship between P and ferrous iron (Fe^{2+}) in drainage water from a pasture and a corn field.

2.3 Materials and Methods

2.3.1 Field Sites

A dairy farm, near Everson, Washington typical of dairies in the region, was selected as the experimental site of this study. A schematic of the location of the Everson site is presented in Figure 2.1. The soil series was identified as the Pangborn muck [*Goldin,* 1992]. Pangborn mucks are defined as dysic, mesic Typic Medisaprists, have low pH, and have a high accumulation of organic matter that is dominated by fine, woody, partially decomposed organic deposits [*Goldin,* 1992]. These soils are usually located in flood plains with 0 to 2% slopes [*Goldin,* 1992]. There exist 2,778 ha of Pangborn muck soils in the Whatcom county area [*NRCS,* 2005].

This type of soil was selected as appropriate for the objective of this study for three reasons: (i) organic soils are recognized to be one of the most important contributors

of P to surface waters resulting from facilitated subsurface transport of P complexed with DOM [*Miller*, 1979]; (ii) these soils are hydric soils which turn anaerobic during the growing season due to wet conditions [*NRCS*, 2005]; and (iii) solute transport and fate in level soils with artificial drainage systems is thought to be controlled mostly by subsurface flow [*Sims et al.*, 1998]. A photograph of the Everson field site is shown in Figure 2.2.

Typical crop rotations in dairy systems of this area may include five years of permanent pasture followed by corn [*Mitchell et al.*, 2003]. This study was conducted from April 28^{th} 2004 through February 1^{st} 2005 (279 days). Half of an existing permanent pasture 70% fescue and 30% white clover, was sown with 13 ha of corn on May 2004 (corn field). The other half of the surface was left as the original pasture (pasture system) so that both systems were adjacent. Liquid manure was applied on April 3^{rd} by injection in both the pasture and the corn field at a rate of 220 m^3/ha (44 kg P/ha).

2.3.2 Soil Analysis

Physical and chemical soil analyses were performed before the manure application. Dry soil bulk density was measured in the top soil (0-10 cm) using the intact core method [*Blake and Hartge*, 1986], and soil texture was determined at two depths (0-30 cm and 30-60 cm) using a soil particle size analyzer (Mastersizer S, Malvern Instruments, Inc., Malvern, UK).

Soil samples for chemical analyses were taken at two soil depths (0-30 cm and 30-60 cm) with a manual auger. Before analysis, samples were air dried and sieved to < 2 mm diameter. Soil pH was measured in a 1:2 (w/v) soil:water solution. Total organic carbon (TOC) and total organic nitrogen (TON) were determined in a Leco FP2000 Nitrogen and Carbon Analyser. Plant available P was measured with the Bray and Kurtz P-1 (Bray-P1) method according to standard procedures [*Kuo,* 1996]. Phosphorus extracted by the Bray-P1 method is designed to dissolve P from Fe and Al complexes in acidic and neutral soils and inhibit the re-adsorption of solubilized P on soil colloids [*Sims,* 2000]. Calcium-chloride-extractable P (P_{CaCl_2}) was determined according to *Kuo* [1996]. The amount of P_{CaCl_2} in soils has been well correlated to the extent of P release and the risk of P leaching in soils [*Brookes et al.,* 1997]. Oxalate extractable P (P_{ox}), iron (Fe_{ox}), and aluminum (Al_{ox}) which are associated with organic and amorphous mineral phases were obtained by extracting soil samples with ammonium oxalate [*Loeppert and Inskeep,* 1996]. All the extracts were filtered through a 0.45 μm cellulose-nitrate-acetate (CNA) membrane [*Haygarth and Sharpley,* 2000]. Molybdate reactive P concentration was determined colorimetrically [*Kuo,* 1996]. The Fe_{ox} and Al_{ox} were determined by atomic absorption spectrophotometry (AAS) and P_{ox} concentration was obtained by colorimetry according to *Wolf and Baker* [1990].

2.3.3 Phosphorus Sorption Experiments

Soil P sorption characteristics were assessed by performing P sorption isotherms and calculating the degree of saturation of the P sorption capacity of the soils. Phosphorus sorption isotherms were performed following *Nair et al.* [1984]. Briefly, 1 g of air-dried soil, sieved < 2-mm was mixed with 25 mL of 0.01 M KCl P-free solution. The soil was then mixed with 0, 0.01, 0.1, 5, 10, 25, 50, and 100 mg/L of P as KH_2PO_4 in 50 mL centrifuge tubes and shaken for 24 h. After centrifugation for 10 min, the supernatant was filtered through 0.45 μm CNA filter and P concentration in the extracts was determined according to *Kuo* [1996]. Phosphorus sorption isotherms were described using the modified Langmuir equation [*Yli-Halla et al.*, 2002]:

$$q = \frac{kq_m c}{1 + kc} - q_i \tag{2.2}$$

where c is the equilibrium P concentration (mg/L), k is the P sorption strength (L/mg), q_m is the maximum P sorption capacity (mg/kg) and q_i is a fitting parameter accounting for the potential desorbable P (mg/kg) [*Hartikainen*, 1991]. Equation 2.2 allows one to account for the desorption of initially existing sorbed P.

The degree of P saturation (DPS) was calculated according to *van der Zee and van Riemsdijk* [1988].

$$\mathrm{DPS} = \frac{\mathrm{P_{ox}}}{0.5(\mathrm{Fe_{ox}} + \mathrm{Al_{ox}})} \tag{2.3}$$

where $\mathrm{P_{ox}}$, $\mathrm{Fe_{ox}}$ and $\mathrm{Al_{ox}}$ are in mmol/kg. The denominator of Equation 2.3 represents an estimate of the total P sorption capacity of the soil [*van der Zee and van Riemsdijk*,

1988]. *Szilas et al.* [1998] found that the DPS is a good predictor for the potential P loss after reductive dissolution of iron in flooded soils.

2.3.4 Field Instrumentation and Water Sampling

Nine tensiometers were installed to monitor the changes in the soil water status. We installed the tensiometers at soil depths of 25, 50, and 100 cm with three replicates each. The tensiometers were located five meters away from the open ditch (Figure 2.3). Each tensiometer was filled with degassed nanopure water, and sealed with a septum stopper at the top. The water tension inside the tensiometer was measured every 15 days with a digital portable tensimeter equipped with a transducer probe and a digital display (Tensimeter, Soil Measurement Systems, Tucson, AZ).

One tile drain was selected in each system and the outflow of the drains into the drainage ditch was monitored. The tile drain flow rates were measured manually every 15 days, using a bucket and a stop watch with three replicates per tile drain.

Water samples for chemical analysis were obtained in two ways: for P analysis, three different samples (replicates) were collected in 250 mL plastic bottles, previously washed in a P free detergent. Bottles were rinsed three times with drain water before the sample was retained. The bottles were fully filled and tightly capped; for Fe analysis, a water volume of 60 mL was filtered in situ <0.22 μm using a syringe filter and immediately acidified using 6 M HCl to prevent oxidation of Fe^{2+}. All water samples were then refrigerated, transferred to the laboratory, and stored at 4°C.

The maximum time between sampling and analysis was 24 h to avoid potential P transformations.

Weather data during sampling were collected in an automatic weather station (Davis Instruments, Hayward CA) located 5 miles southeast of the Everson sampling site and provided by courtesy of Chris Clark (Whatcom Conservation District Lynden, WA). Rainfall, air, and soil temperatures were collected hourly and the daily average used for data analysis. Soil temperature was measured at 15 cm soil depth below a grass surface, similar to the pasture system used in this study.

2.3.5 Analysis of Drain Outflow

Redox potential, and pH, were measured in the laboratory with a combination ORP electrode (Cole Parmer,Cat. EW-05658-70, USA) and a pH electrode (Cole Parmer, Cat. EW-05662-90 , USA) connected to a pH/voltmeter (Orion 720A voltmeter, Orion Research Inc., Beverly, MA).

Phosphorus concentration was measured after filtration (<0.45 μm) using CNA membrane filters. The P concentration in each sample was determined using the methodology described by *Pote and Daniel* [2000]. This fraction corresponds to the operationally defined Molybdate Reactive Phosphorus ($MRP_{<0.45}$) according to *Haygarth and Sharpley* [2000]. Iron concentrations ($[Fe^{2+}]$, $[Fe^{3+}]$, and $[Fe_{Total}]$) were measured using ferrozine analysis [*Stookey,* 1970].

Colloid facilitated transport has been identified as a potential and relevant mecha-

nism for P leaching [*Haygarth and Jarvis*, 1999; *Siemens et al.*, 2004; *Ilg et al.*, 2005]; therefore, samples as collected from the field were analyzed for scattering counts to detect suspended colloidal material (Zetasizer 3000 HSA, Malvern Instruments, Malvern, UK).

2.3.6 Data Analysis

Phosphorus concentrations in the water drainage outflow were correlated to Fe^{2+}, Fe^{3+}, and flow rate. Linear regression analyses were conducted using SigmaPlot® 2002 version 8.0. Sorption parameters in Equation 2.2 were optimized by nonlinear regression using the Solver utility provided by Microsoft Excel.

2.4 Results and Discussion

2.4.1 Soil Properties

Soil properties are depicted in Table 2.1. Mineral fractions were dominated by elevated amounts of silt (≈50%) and sand (≈45%). No differences were observed in the texture between the two depths. This soil is mainly characterized by its high organic matter content (SOM). The TOC and TON values measured in the two depths were 28% and 2%, respectively. The high organic matter content of this soil explained its elevated porosity and its low ρ_b (≈0.4 g/cm^3).

Soil pH was acidic with slightly higher values in surface soils (pH≈5.1) compared

to (pH≈4.8) the 30-60 cm soil depth. Soil P analyses revealed that the soil has been affected by high P inputs. Mean values of P Bray-P1 (≈300 mg/kg) are far higher than values considered optimum for plant growth (≈25 mg/kg) [*Sims*, 2000]. Amounts of P_{CaCl_2} were also high, indicating a potential risk of P loss in subsurface flow [*Brookes et al.*, 1997; *Hooda et al.*, 2000; *Hesketh and Brookes*, 2000].

2.4.2 Langmuir P Sorption Parameters and DPS

Phosphorus sorption isotherms for the two depths are given in Figure 2.4. Mean Langmuir P sorption parameters k, q_m, and q_i estimated using Equation 2.2 are listed in Table 2.1.

Maximum P sorption capacity (q_m) was similar in both pasture and the corn field, and also between the two soil depths. The DPS indicated high saturation of sorption sites with P in the surface soil than below 30 cm soil depth. The mean DPS was higher than 25% in all soil samples indicating a potential risk of P loss via leaching. A value of 25% of DPS has been suggested as a critical environmental limit above which enhancing P loss via subsurface transport may occur [*van der Zee and van Riemsdijk*, 1988].

The soil studied here contains elevated soil test P (Bray-P1 >25 mg/kg) and DPS values above suggested environmental critical limits (>25%). This implies that independent of the mechanism involved in P release (desorption or reductive dissolution of Fe), this soil presents a potential risk of P contamination for surface waters.

2.4.3 Soil Water Status and Flow Rates

Soil water tension, rainfall, and average air temperature measured during the sampling period are depicted in Figure 2.5. Soil water tension was less than -40 mbars from September to November 2004 but became less negative after heavier rainfalls occurred. In November 2004 and December 2004, soil water tension reached values near zero. In November 2004, the soil water tension was close to zero in the first 25 cm of soil depth. The same was true for a soil depth of 100 cm in January 2005. In the first case, the soil was close to saturation possibly as a result of water recharge from the soil surface. In the second case, the drainage system possibly was not able to drain the excess water and the water table may have risen above the drain lines. The near saturation conditions suggest that suboxic or anoxic conditions are likely during this time of the year.

The drain flow rates increased during the period of heavy rainfall, reaching a peak of $\approx$ 6 L/s (Figure 2.5). The mean flow rates were 2.19 L/s and 1.77 L/s for the pasture and the corn field, respectively (Table 2.2).

2.4.4 Phosphorus Loadings and Rate of P Transfer

An estimation of the rate of the reactive P ($MRP_{<0.45}$) transfer per drain (g/day) was obtained by multiplying the $MRP_{<0.45}$ sample concentration by the mean flow rate per drain. Although the mean drain flow rate in the pasture drain was 20% higher than in the corn field, the rate of P transfer was five times higher in the corn field than in the

pasture system (Table 2.2). This was due to the higher P concentration measured in the corn field water outflows. The mean rate of transfer of $MRP_{<0.45}$ was 5 g/day per drain for the pasture and 10.4 g/day per drain for the corn field. The total $MRP_{<0.45}$ exported in 279 days of flow was estimated in 4.2 kg/ha for the pasture, and 8.7 kg/ha for the corn field. These values are in the range of P losses measured in organic soils and considered detrimental for surface water quality [*Miller,* 1979]. Because the sampling methodology was not intended to calculate P transfer rates per land area, these data should be interpreted with caution. However, P concentrations measured in the drain water outflows can be considered high enough to trigger eutrophication in fresh waters (>0.01 mg/L) [*Sims et al.,* 1998*; USEPA,* 2003].

2.4.5 Redox Potential and pH of Drainage Water

Redox potential and pH of water samples are shown in Figure 2.6. In general, redox potential was lower in the spring (≈170 mV) and increased in the summer up to 220 mV. These values decreased during winter to about 180 mV, coinciding with the soil water saturation conditions discussed above. The decrease of the redox potential during the flooding period confirmed that reductive processes occurred in these soils. The ferric iron reduction occurs typically at these ranges of redox potential (150 to 200 mV) [*McBride,* 1994].

An inverse trend was observed with pH. The highest pH values were measured in the spring but rapidly decreased by the end of the summer. This can be attributed to an

increase in the mineralization rate of SOM induced by an increment of soil temperature. Because soil temperature was not measured at the sampling site, these values are used only as a reference. Figure 2.6 shows that pH was minimum when the soil temperatures taken at 15 cm soil depth were higher. As a result of microbial respiration, weak acids and CO_2 are released and cause the pH to drop [*Rowell,* 1981]. During fall, water pH increased again possibly due to reductive processes during anaerobic respiration. Anaerobic respiration releases OH^- groups during the reduction of iron hydroxides, increasing the soil solution pH [*Ponnamperuma,* 1972]. This is supported by the decrease in the redox potential measured in the outflows. During winter, pH values were as low as 5.6 and as high as 6.2 during May 2004.

In general, the water pH followed a similar trend in both the corn field and the pasture. Although no differences were found in the initial pH values between the pasture and the corn field (Table 2.1), we observed a slightly lower pH in water samples collected from the corn field. We believe that, due to cultivation, the soil in the corn field became more aerated than the pasture and, hence, we may expect higher microbial activity and higher SOM degradation.

2.4.6 Phosphorus and Iron in Drainage Water

Pasture System

The concentrations of Fe_{Total} measured in the drain outflows are in the range of values reported for the Whatcom county area (<0.1 mg/L) [*Cox and Kahle,* 1999]. Iron found

naturally in subsurface water in the Whatcom area originates from the parent material of the subsoil and soil organic matter [*Cox and Kahle,* 1999]. The variation of Fe^{2+}, Fe_{Total} ($[Fe_{Total}]= [Fe^{3+}] + [Fe^{2+}]$), and the ratio $[Fe^{2+}]/[Fe_{Total}]$ and $[Fe^{3+}]/[Fe_{Total}]$ as a function of time are shown in Figure 2.7. The concentration of Fe^{2+} in the pasture system was below detection limits from April 2004 through November 2004. During this period the only form of iron was Fe^{3+} ($Fe^{3+}/Fe_{Total}= 1$). After November 2004, Fe^{2+} was the dominant form of iron ($Fe^{2+}/Fe_{Total}= 0.7$), reaching a maximum of 0.035 mg/L on January 2005.

Corn Field

Concentrations of Fe^{2+} ($[Fe^{2+}]$) in the corn field were nearly constant (≈0.02 mg/L) between April 2004 to December 2004 (Figure 2.7). The ratio $[Fe^{2+}]/[Fe_{Total}]$ during this period increased from ≈0.4 to 0.7 in November 2004, where the concentration became ≈0.025 mg/L. After December 2004, $[Fe^{2+}]$ decreased to a minimum of 0.006 mg/L ($[Fe^{2+}]/[Fe_{Total}]$=0.2), due to an increase in $[Fe^{3+}]$. The $[Fe^{3+}]/[Fe_{Total}]$ increased from 0.3 to 0.8 from November 2004, reaching a maximum of ≈0.05 mg/L at the end of December 2004.

Phosphorus and Iron as a function of Flow Rate

Figure 2.8 shows the relationship between $MRP_{<0.45}$, $[Fe^{2+}]$, $[Fe^{3+}]$ and the flowrate. The $MRP_{<0.45}$ was linearly and positively correlated ($R^2 = 0.83$) to the flowrate in the pasture system (Figure 2.8(a)), and the same was true for Fe^{2+} ($R^2 = 0.96$).

Conversely, Fe^{3+} was not related to flow rate in this system (Figure 2.8(b)).

In the corn field, $MRP_{<0.45}$ increased linearly as a function of flow rate (May 2004 to October 2004) but negatively when the flow rates increased higher than $\approx$ 1 L/s (Figure 2.8 (c)). Concentrations of Fe^{3+} increased linearly as a function of flow rate up to $\approx$ 1 L/s. At higher flow rates, we identify a second linear relationship but with a lower slope (Figure 2.8 (d)).

P Release as a Function of Oxidation State of Fe

In the corn field, Fe^{3+} was the dominant form of iron (>60%), which is coincident when the maximum flow rates. In contrast, in the pasture system, Fe^{2+} was the dominant form of iron when the flow rates were the highest (December 2004 to January 2005) and the redox potential the lowest ($\approx$180 mV). As expected, in the pasture system, the variation of the $MRP_{<0.45}$ as a function of time followed the same trend as Fe^{2+} and both Fe^{2+} and $MRP_{<0.45}$ were positively correlated ($R^2 = 0.87$) (Figure 2.9, top). This suggests that, in the pasture system, the $MRP_{<0.45}$ and Fe^{2+} were released and transported off site as a result of similar chemical and physical processes. After the pasture system became anaerobic, reductive processes of ferric iron took place, releasing P and Fe^{2+} to the pore water. Because the soil solution is mobile, as indicated by the drain outflows, P and Fe^{2+} are transferred from the source to the percolating solution [*Jensen et al.,* 1999]. Because of the high DPS of this soil, P is translocated downward together with Fe^{2+}. Free Fe^{2+} is slightly soluble in water and can reach the

drainage system.

Light scattering analysis did not show evidence of colloids in the water drainage samples. Therefore, we concluded that, in the pasture, P was released by reductive dissolution of iron (given by the significant relation to Fe^{2+}) and transported into tile drains in dissolved forms or associated with organic colloids. There is evidence that, in reduced soils, Fe^{2+} also reacts with DOM forming an oxidation-resistant complex [*Theis and Singer,* 1974].

In the corn field, Fe^{2+} was not well correlated with $MRP_{<0.45}$ in drainage water (Figure 2.9, bottom). Instead, we observed good correlations between $MRP_{<0.45}$ and Fe^{3+} (Figure 2.10). Regression analysis indicated that these parameters were directly related from May 2004 to October 2004, but inversely from November 2004 to January 2005, coinciding with the increase of the drain flow rates.

The positive correlation between P and Fe^{3+} in the corn field, could result from P transported by iron-(hydr)oxide colloids. However, as stated before, colloids were not detected by light scattering analysis in the corn field water samples. Additionally, the P concentration, but not $[Fe^{3+}]$, decreased linearly when the flow rate was high. This revealed that P mobilization could have been controlled by diffusion mechanisms from immobile water in micropores [*Jensen et al.,* 1999].

Thus, although Fe^{2+} detected in the drainage water is indicative of reductive processes, the P release in the corn field may be dominated by additional desorption processes. The high P content and the elevated DPS of the soil favor desorption

processes and enhance the mobilization of P [*Hooda et al.,* 2000]. This may explain the higher P concentrations measured in the water drainage from the corn field (0.07 mg/L) as compared to the pasture system (0.02 mg/L), even though the flow rates were higher in this system.

Desorption processes and competitive interactions for sorption sites between DOM and P or dissolution of iron-P minerals by the presence of DOM may be additional processes affecting the P release in the corn field [*Hutchison and Hesterberg,* 2004]. Results reported for agricultural sandy soils indicate that more than 50% of $MRP_{<0.45}$ was associated to iron-aluminum-humic complexes [*Dolfing et al.,* 1999*; Hens and Merckx,* 2002]. Then the released P and Fe^{3+} in solution may form P-Fe^{3+}-DOM ternary complexes [*Hutchison and Hesterberg,* 2004], and be transported through soil as a mobile complex [*Hens and Merckx,* 2001].

2.5 Conclusions

The monitoring results showed that flooding played an important role in the release of P into the tile drainage system. The positive correlation found between P and Fe^{2+} in the pasture system was consistent with earlier reports. The results of this study indicate that in soils enriched with P and affected by fluctuating water tables, P is released as a result of iron reduction and transported off site via tile drains.

Although in the corn field we found Fe^{2+} in the outflows, this was not well related to P. This suggested that iron reduction was not the only process involved in the P

release. This was evident from the higher P concentration in the outflows in the corn field compared to the pasture.

Apparently, cultivation had an effect on the P loss from the corn field. Studies suggest that cultivation may increase the contact between P and reactive sorption sites, and hence decrease the P mobilization via leaching. However, in this soil with high DPS we observed the opposite. After cultivation more P was released compared to the pasture. Because P in the corn field was related to Fe^{3+}, it is possible that mobile P was associated with colloidal iron oxides. The cultivation in soils with high DPS, may increase the contact and sorption between P and small colloids. The adsorption of P to these iron oxides favor its dispersibility and mobility [*Siemens et al.*, 2004]. Cultivation of a soil with elevated DPS levels could favor Fe(III)-DOM complexes and P as a ternary complex with these by (i) stimulating oxidation of Fe or suppressing its reduction; or (ii) enhancing the mineralization of soil organic matter.

In addition to cultivation effects, differences in biological dynamics associated with crop and microbial activity in the corn and pasture fields may contribute to differences in the characteristics of P losses in both fields. For example, (a) the pattern (amounts and timing) of P uptake, (b) interaction of P uptake and organic matter mineralization and crop growth period (phenology), and (c) residual soil P before late fall/winter flooding, are all likely to be different in the two fields.

Elucidating the P and iron cycling in intensive agricultural systems affected by periodic flooding is important to improve the control of P losses from land to water.

Further research is required to elucidate the mechanisms involved and provide adequate interpretation of the results obtained in this study.

2.6 Tables and Figures

Table 2.1: Mean (standard error, s.e.) of selected soil properties for a Pangborn muck (Everson) soil at two soil depths for both the pasture and field corn.

	Pasture		Corn Field	
Soil Parameter	0-30 cm	30-60 cm	0-30 cm	30-60 cm
pH (H_2O)	5.1	4.7	5.1 (0.2)	4.8
Bray-P1 (mg/kg)	352 (39)	195 (59)	343 (19)	243 (25)
P_{CaCl_2}(mg/L)	2.1 (0.4)	0.9 (0.3)	2.8	1.7
Total organic C (TOC) (%)	28 (1)	24 (5)	28 (1)	30 (1)
Total organic N (TON) (%)	2.2 (0.03)	1.5 (0.27)	2.1 (0.07)	1.8 (0.06)
Phosphorus Sorption properties				
q_m (mg/kg)	2533 (152)	2664 (188)	2691 (511)	2600 (117)
k (L/mg)	0.03	0.05 (0.017)	0.02 (0.008)	0.02 (0.008)
q_i (mg/kg)	342 (35)	166 (10)	295 (76)	184 (31)
DPS (%)	40.0 (7)	21.2 (2)	42.7 (14)	25 (7)
Physical Properties				
Sand (%)♯	43.6 (0.8)	45 (2.6)		
Silt (%)♯	50.5 (0.7)	48.6 (2.1)		
Clay (%)♯	5.9 (0.1)	6.4 (0.5)		
Bulk Density (g/cm^3)†	0.4 (0.025)			

♯ Represents to both pasture and the corn field at two depths (0-30 cm and 30-60 cm.)

† Bulk density measured in the first 10 cm.

Table 2.2: Phosphorus losses and flow rates of the Everson field site from April to February 2004.

	Pasture			Corn Field		
	MRP† (mg/L)	Flow Rate (L/s)	MRP Rate† (g/day)	MRP† (mg/L)	Flow Rate (L/s)	MRP Rate† (g/day)
Mean	0.02	2.19	5.0	0.07	1.77	10.4
Max	0.04	6.00	21.5	0.11	5.86	28.2
Min	0.004	0.10	0.06	0.018	0.33	0.5

†:Molybdate reactive P ((< 0.45)).

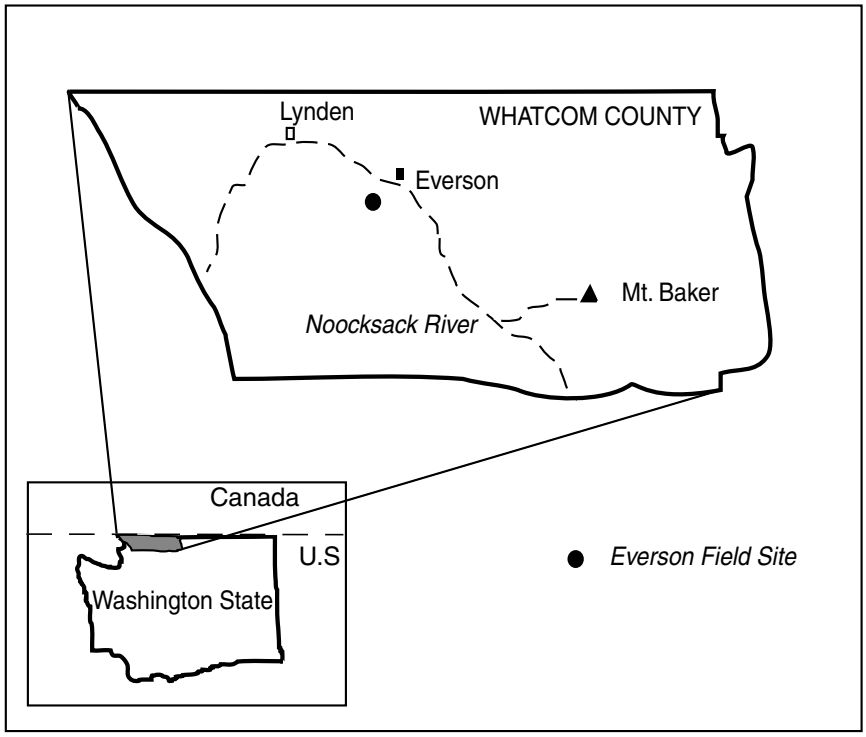

Figure 2.1: Schematic of location of Everson sampling site. Not to scale.

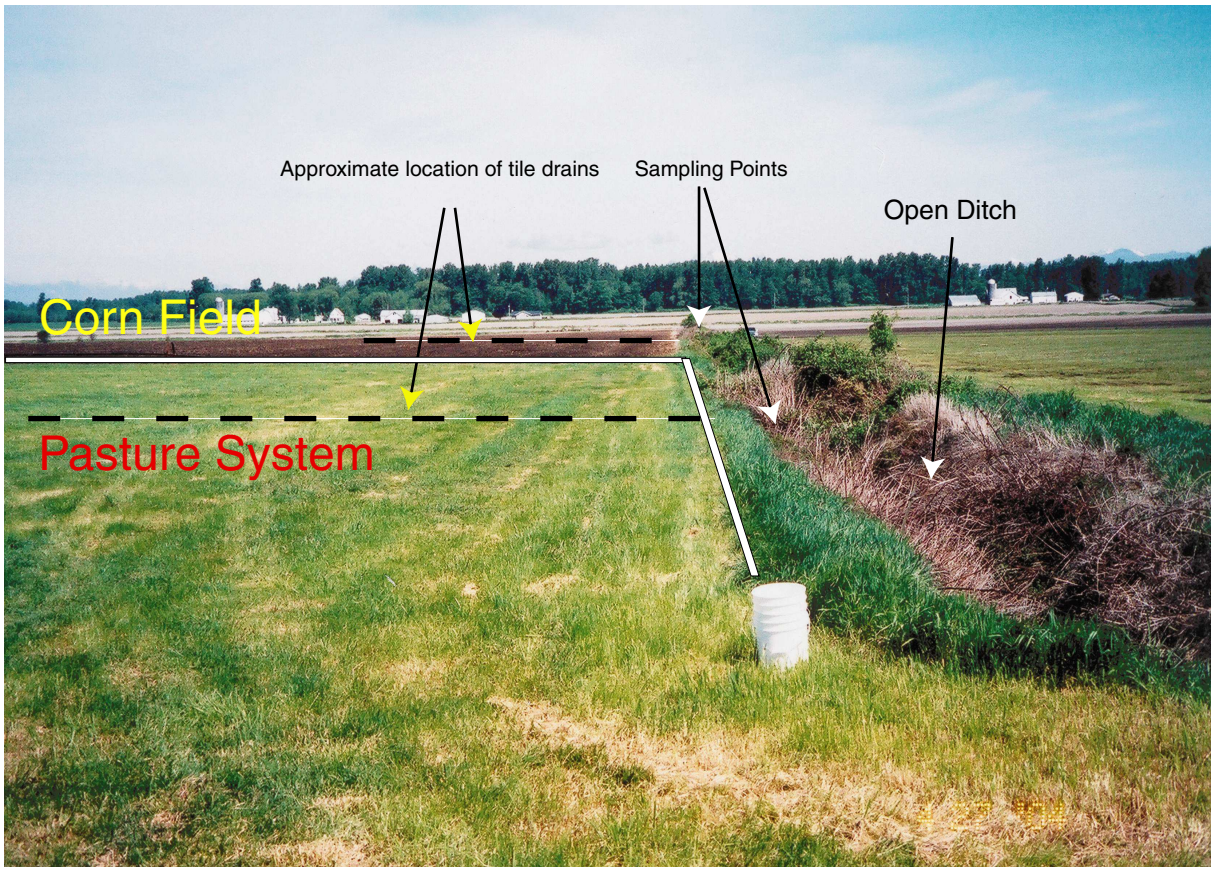

Figure 2.2: Photo of Everson site showing the pasture system, the corn field, ditch and the sampling points in each drain.

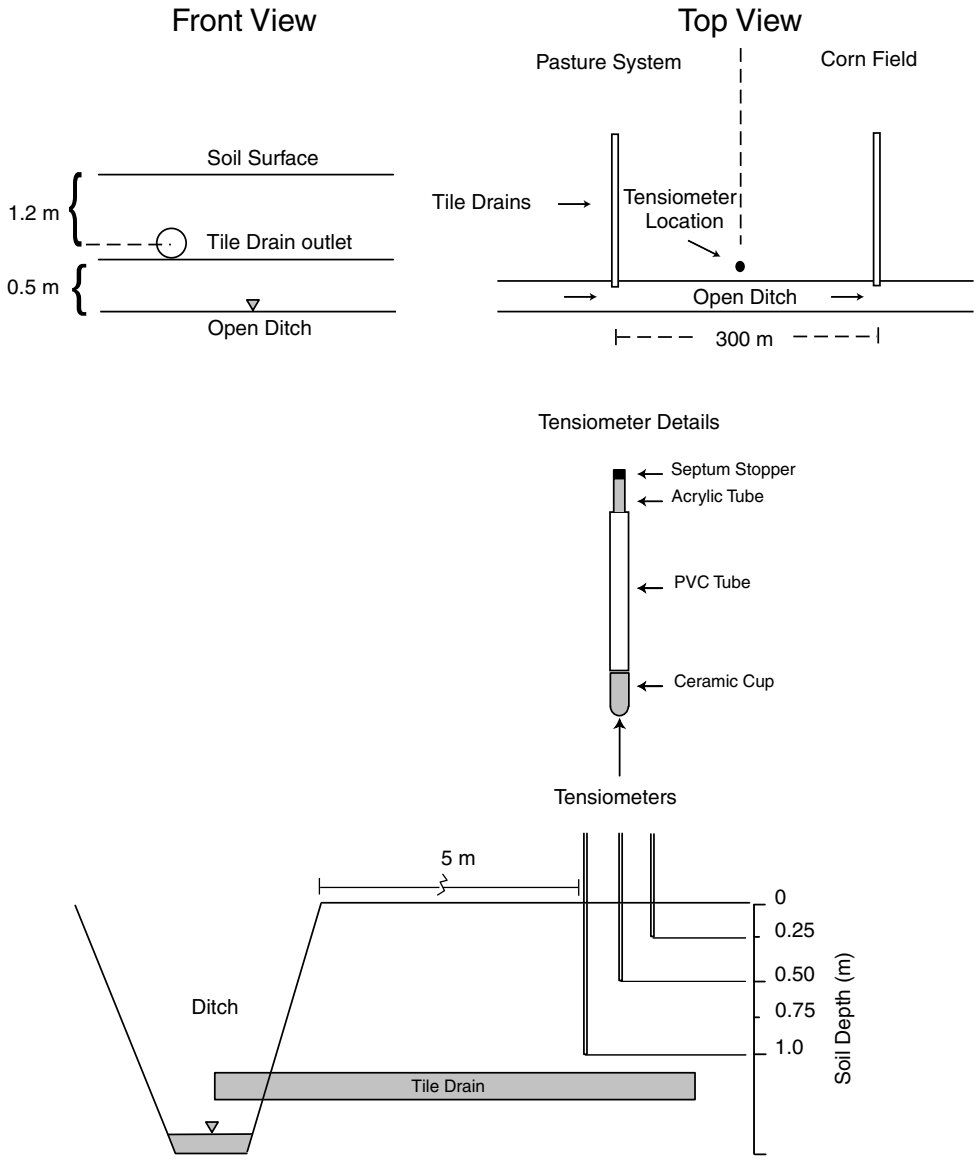

Figure 2.3: Front and top view of the location of the pasture system and corn field (top). Schematic of the location of tensiometers (bottom).

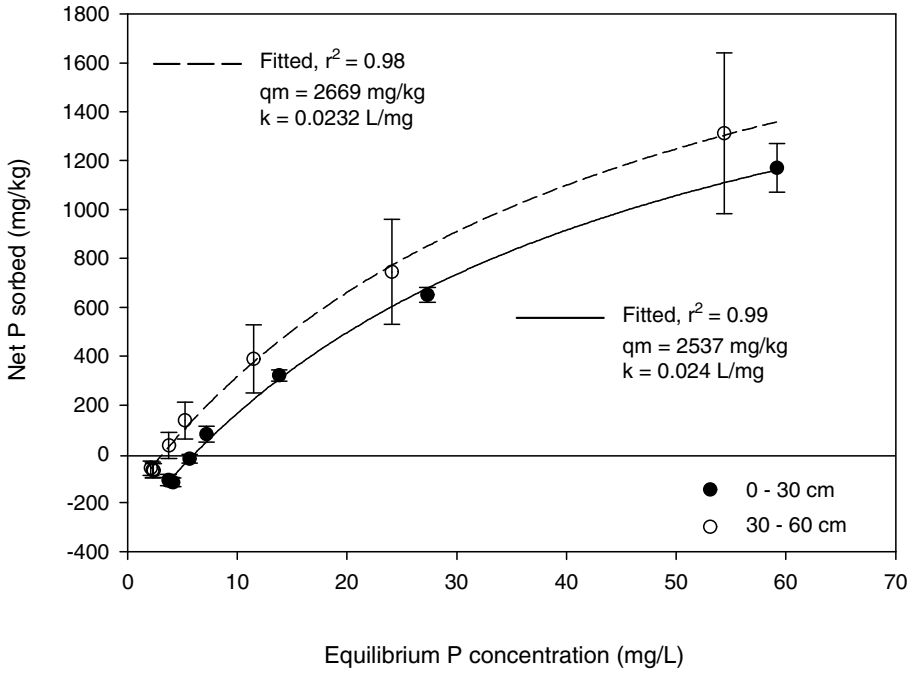

Figure 2.4: Sorption isotherms for Pangborn muck (Everson)at two soil depths. Fitted lines were generated from Equation 2.2. Errors bars are standard errors (s.e.) of 5 replicates.

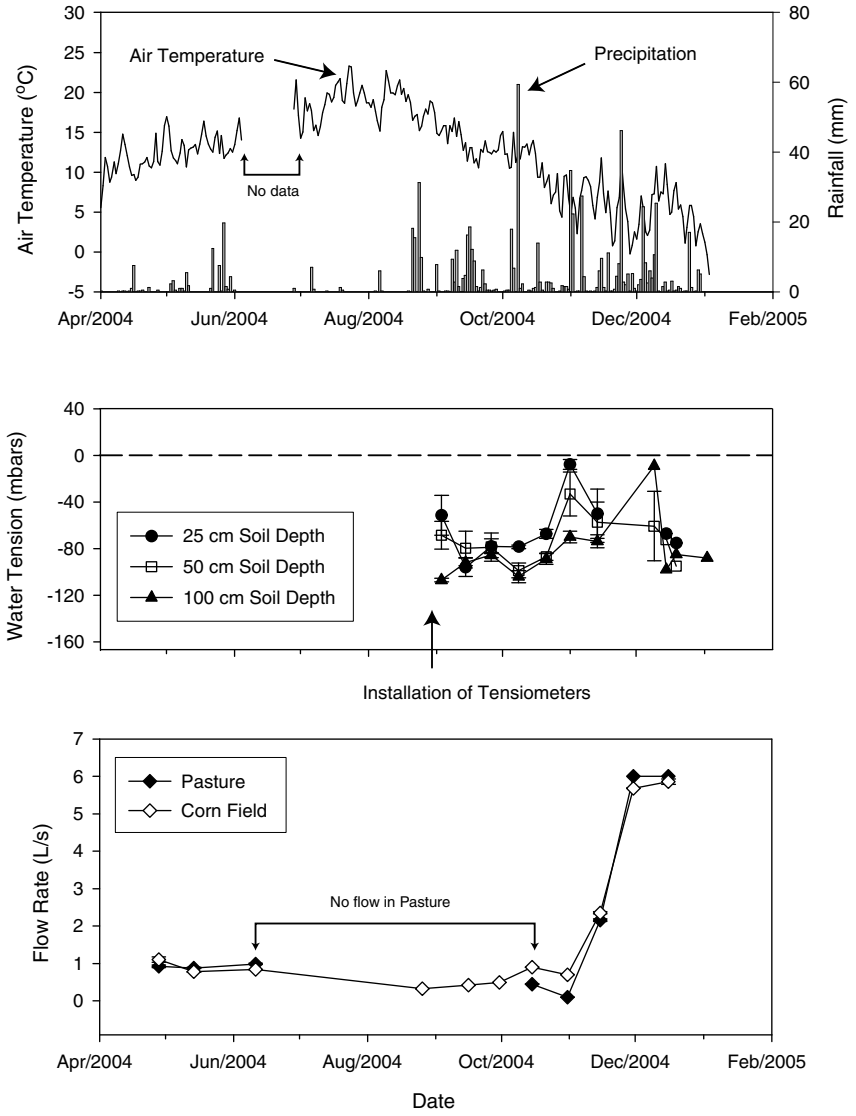

Figure 2.5: Daily rainfall and daily average air temperature observed during the sampling period (top). Average water tension at three soil depths at Everson. Error bars correspond to standard errors (s.e.) (middle). Flow rates measured in Everson site in the pasture system and corn field (bottom)

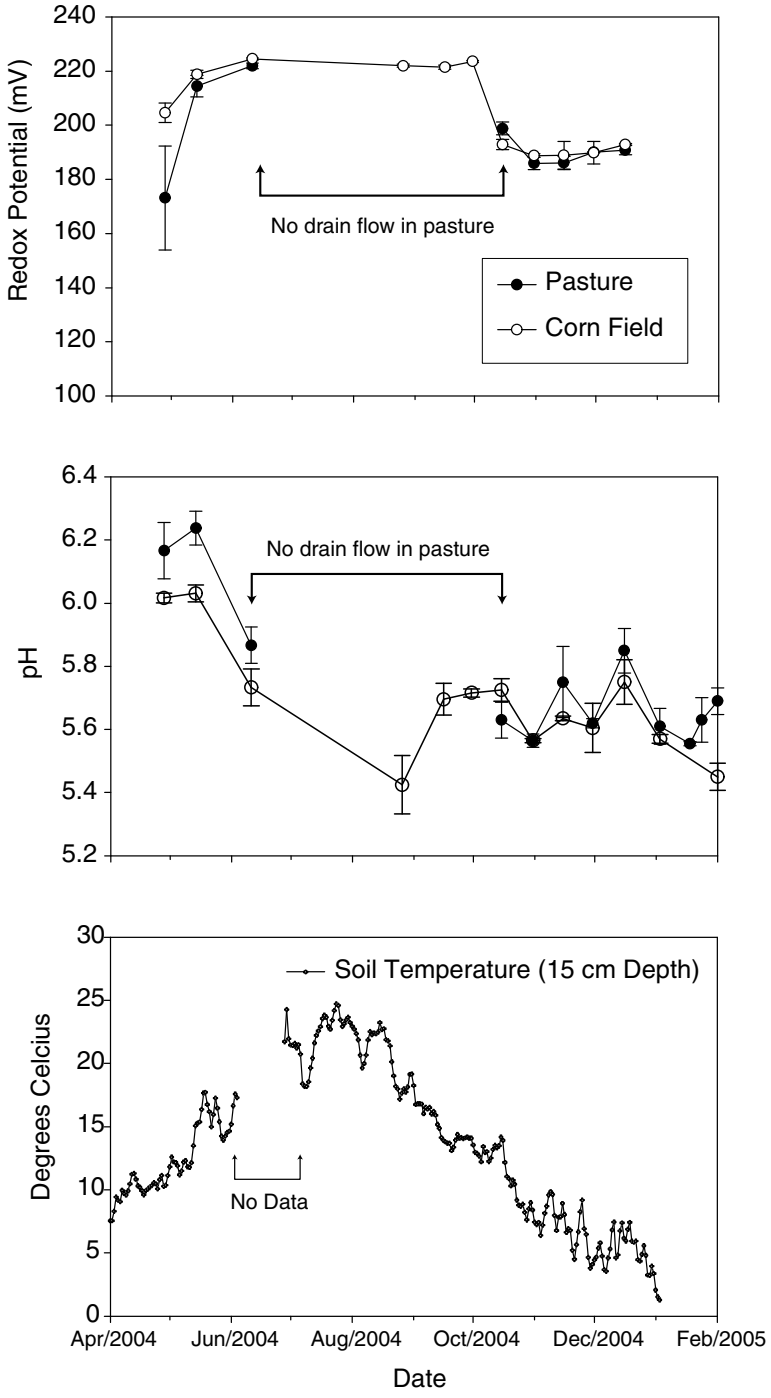

Figure 2.6: Redox potential (top) and pH (middle) on drainage water samples at Everson. Average soil temperature taken at 15 cm soil depth (bottom).

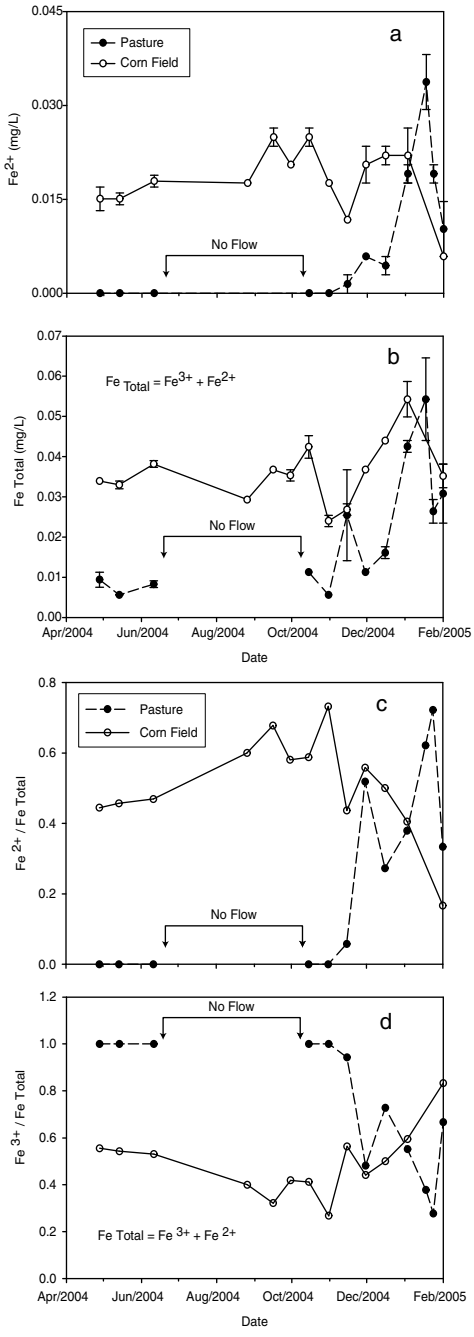

Figure 2.7: Ferrous iron (Fe^{2+}) (a), Total iron (b), Fe^{2+}/Fe_{Total} ratio (c) and Fe^{3+}/Fe_{Total} ratio (d), as a function of time in water samples at the Everson site for pasture and corn field. Error bars correspond to the standard errors (s.e.)

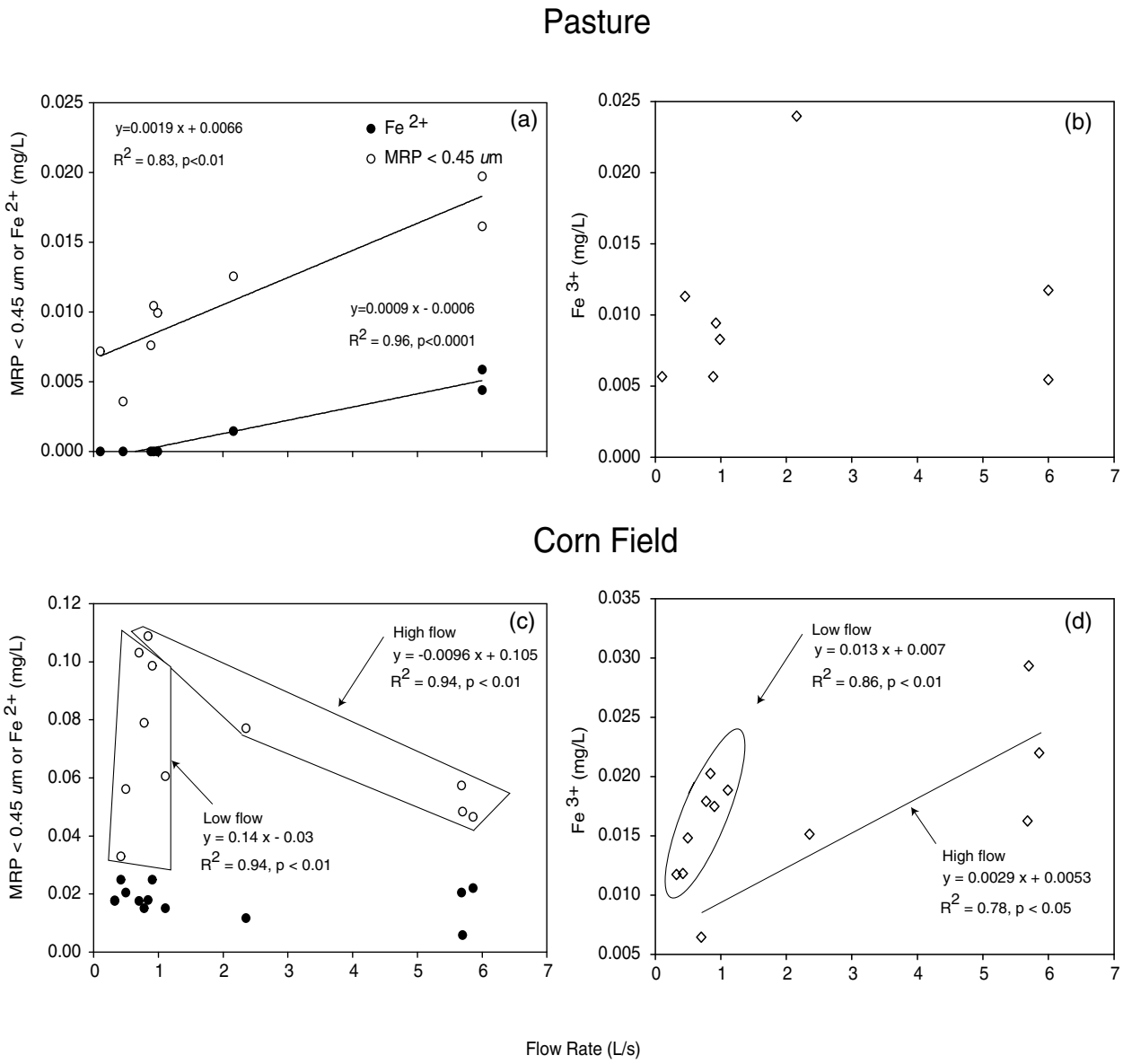

Figure 2.8: Ferrous iron (Fe^{2+}), $MRP_{<0.45}$ and Ferric iron (Fe^{3+}), as a function of drain flow rate in the pasture (a and b), and in the corn field (c and d).

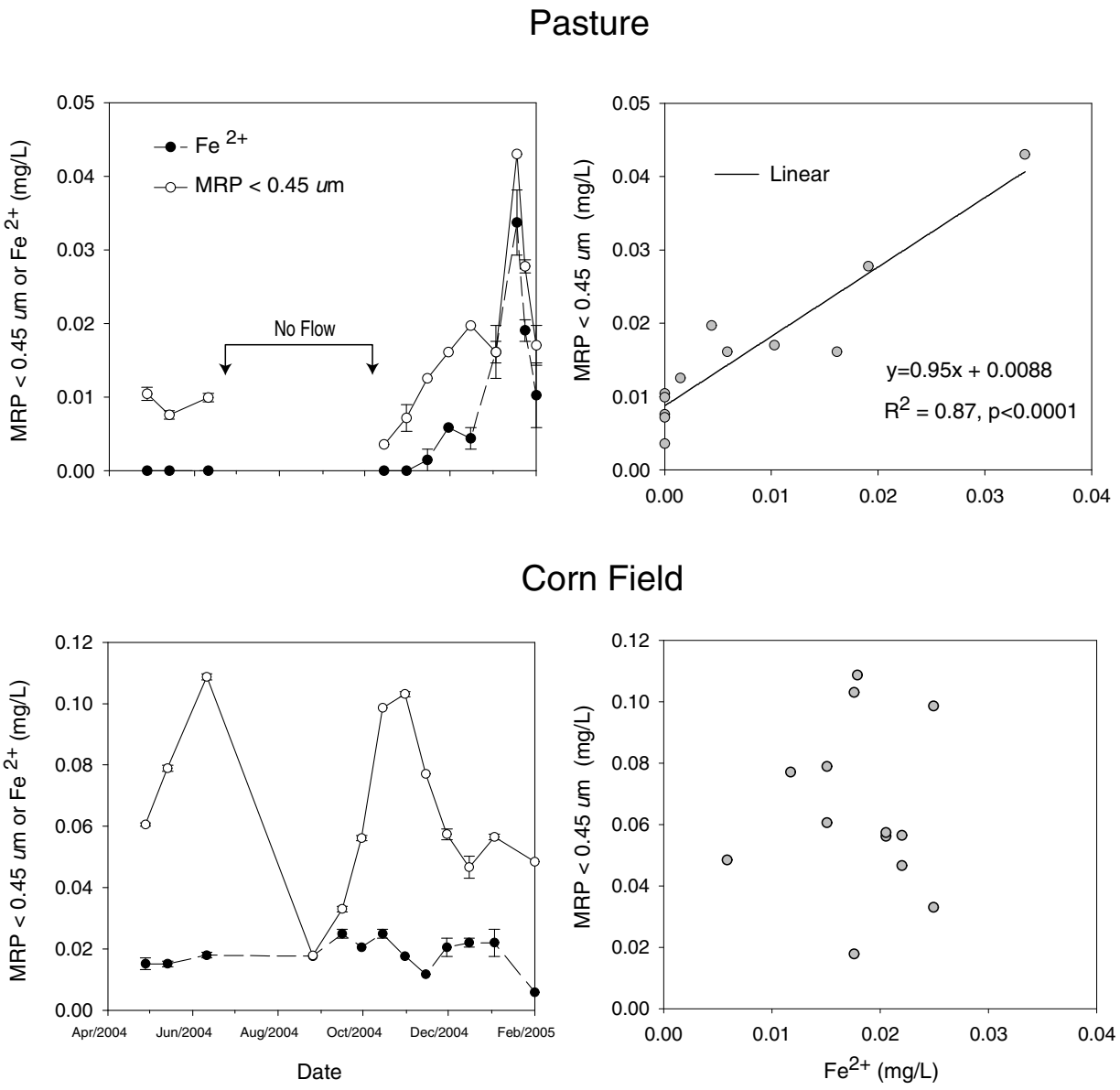

Figure 2.9: Variation of Fe^{2+} and $MRP_{<0.45}$ as a function of time. Relationship between Fe^{2+} and $MRP_{<0.45}$ for the pasture (top), and the corn field (bottom) at Everson. Error bars correspond to the standard errors (s.e.)

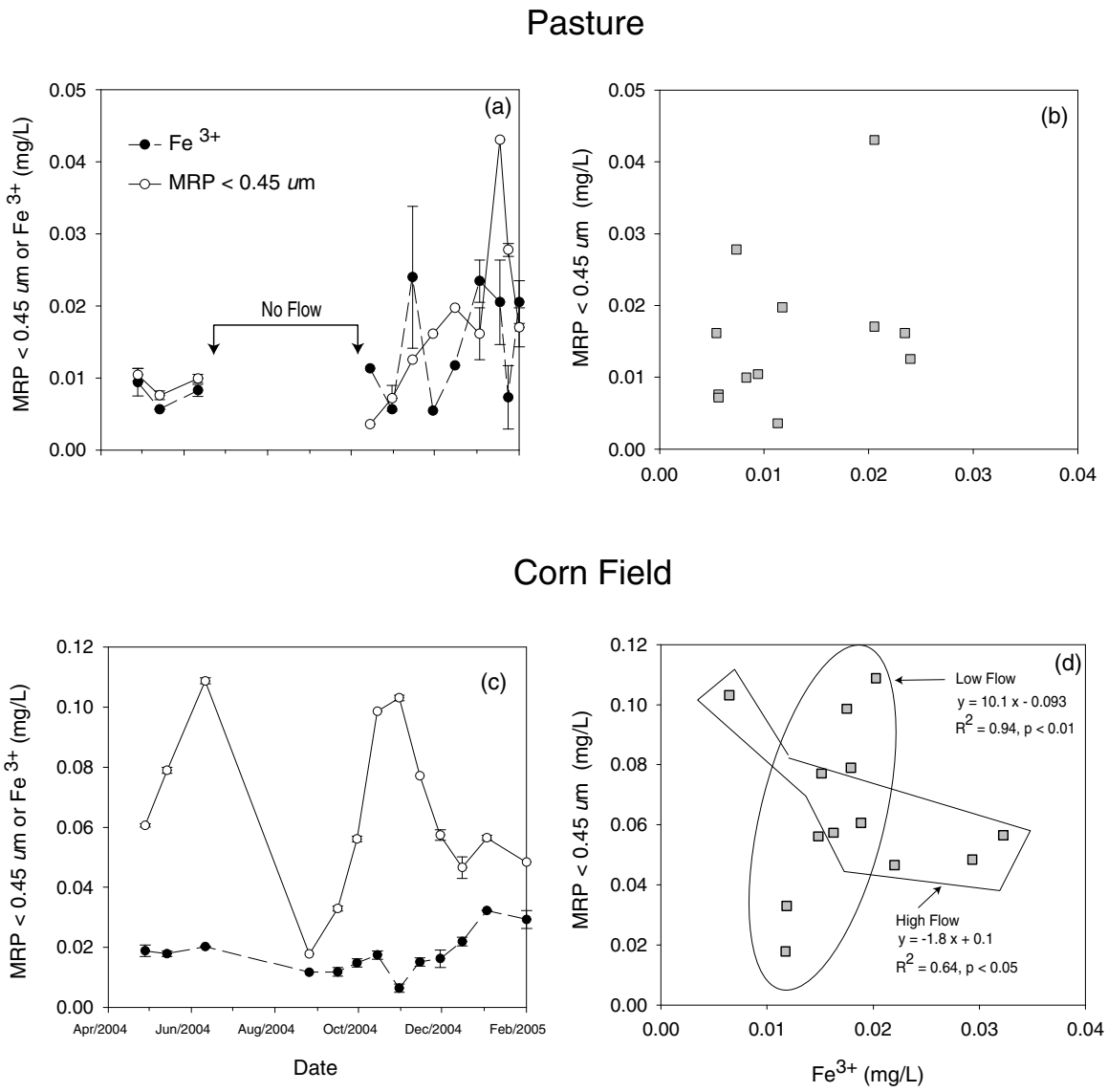

Figure 2.10: Variation of Fe^{3+} and $MRP_{<0.45}$ as a function of time for the pasture system (a) and for the corn field (c). Regression between Fe^{3+} and $MRP_{<0.45}$ for the pasture system (b) and in the corn field (d). Error bars correspond to the standard errors (s.e.).

Chapter 3

Phosphorus Transport through Ferrihydrite-coated Sand under Reducing Conditions

3.1 Abstract

Phosphorus (P) transport through soils is usually limited by strong sorption of P to iron or aluminum oxides. However, under conditions of reductive dissolution of Fe, P may be mobilized and transported in dissolved form through soils. This phenomenon has been well described in static systems but few studies have been conducted under dynamic conditions. We hypothesize that P, sorbed to iron (hydr)oxides, is released and leachable when the redox potential drops below the Fe^{3+}/Fe^{2+} redox couple. We set up an experiment to determine the effect of reduced conditions on P release and transport in a ferrihydrite-coated sand medium. Ferrihydrite-coated sand was packed into flow-through columns. Transport of P through these columns was studied under oxidized and reduced conditions in water-saturated sand columns. Bacteria (*She-*

wanella putrefaciens, CN-32) were used to induce reducing conditions, whereby Fe^{3+} was reduced to Fe^{2+}. Three systems were studied: an initially oxidized ferrihydrite-coated sand containing P that became reduced (experiment 1); P transport through an initially P-free system under reduced conditions (experiment 2), and P transport through oxidized conditions (oxidized control). Ferrous iron, P, pH, and redox potential were measured in the column outflow. In the initially oxidized column (experiment 1), 12% of the P in the system was released as a result of reductive dissolution of P during 100 pore volumes of throughflow. The reduced system (experiment 2), fixed more P than the oxidized control, but when the redox potential increased again, the system lost twice as much P as the oxidized control. Chemical equilibrium modeling indicated that, P release and fate in the experiment 2 was controlled by precipitation of vivianite ($Fe(II)_3(PO_4)_2{\cdot}8\ H_2O$), but not in experiment 1. This study demonstrated that an initially oxidized system saturated with P and under dynamic flow conditions can mobilize P after reductive dissolution of ferric iron. These results show that an initially reduced system presents a high affinity for P due to precipitation reactions, but the system turns unstable after the re-oxidative process, fixing less P than the oxidized control system. Reactive transport in the P-Fe-H_2O system, therefore, is determined by both adsorption and precipitation processes under reducing conditions.

3.2 Introduction

In soils, the stable form of P is orthophosphate. Orthophosphate in the form of phosphoric acid (H_3PO_4), has four dissociation states; however, for the pH range commonly found in soils (pH 4 to 7), $H_2PO_4^-$ and HPO_4^{2-} are the dominant species [*Lindsay,* 1979]. Orthophosphate sorbs to soil mainly by ligand exchange on iron or aluminum oxides/hydroxides forming binuclear surface complexes [*Goldberg and Sposito,* 1985]:

$$\mathrm{Fe - O - PO_2 - O - Fe} \tag{3.1}$$

These surface complexes are strong and therefore P does not readily desorb or leach from soils containing (hydro)oxides of Fe and Al. Thus, leaching has been of minor concern [*Sharpley et al.,* 1994] and most of the environmental problems related to P have been associated with erosion processes and surface runoff [*Smith et al.,* 1999]. Sorption of P to soil containing (hydro)oxides is controlled mainly by soil pH and redox potential. While many P sorption studies have been conducted, the influence of redox reactions on P chemistry and its potential impact on P mobility under dynamic conditions has not been investigated intensively.

Phosphorus sorbed to iron oxides may become soluble and may be leached through the soil profile due to a decrease in the redox potential. This leads to reduction of Fe^{3+} to Fe^{2+}, thereby releasing P into the soil solution [*Pant and Reddy,* 2001]. Enhanced leaching of P in such soils has been reported from several field studies [*Quang and Dufey,* 1997*; Sallade and Sims,* 1997*; Sims et al.,* 1998*; Scalenghe et al.,* 2002*; Pant*

et al., 2002]. Specific environments in which enhanced leaching has been observed include paddy fields [*Ponnamperuma,* 1972*; Shahandeh et al.,* 1994], marine sediments [*Slomp et al.,* 1996*; Anschutz et al.,* 1998], wetlands [*Novak et al.,* 2004], field lysimeter studies [*Villapando and Graetz,* 2001], and laboratory microcosms [*Young and Ross,* 2001].

The reductive transformation of iron–phosphates leading to P release can be described by:

$$\mathrm{Fe(III)PO_4}(s) \cdot 2\mathrm{H_2O}(l) + 2\mathrm{H^+}(aq) + e \rightleftharpoons \mathrm{Fe^{2+}}(aq) + \mathrm{H_2PO_4^-}(aq) + 0.5\mathrm{O_2}(g) \quad (3.2)$$

The Fe(III)-phosphate can be thought of as either a mineral, such as strengite, or an orthophosphate sorbed to an Fe(III)-oxide, such as ferrihydrite. In the presence of Fe^{2+} and P in solution, the controlling equilibrium solid phase becomes vivianite ($Fe(II)_3(PO_4)_2{\cdot}8\ H_2O$) [*Willett,* 1985]:

$$3\mathrm{Fe^{2+}}(aq) + 2\mathrm{H_2PO_4^-}(aq) + 8\mathrm{H_2O} \rightleftharpoons \mathrm{Fe(II)_3(PO_4)_2}(s) \cdot 8\mathrm{H_2O}(l) + 4\mathrm{H^+}(aq) \quad (3.3)$$

From Equations 3.2 and 3.3, we can see that the production and accumulation of Fe^{2+} will drive reaction 3.3 to the right, thereby limiting the reductive dissolution of Fe as vivianite-like Fe^{2+} phosphate precipitates [*Moore and Reddy,* 1994]. Indeed, *Roden et al.* [2000] argued that, in a batch experiment, the reduction of Fe is less pronounced than in dynamic flow systems, where the products of the reduction reaction are continuously carried away with the water flow. *Jensen et al.* [1999] postulated that the dynamics of P in sub-oxic environments follow two interrelated stages. Firstly, upon

iron reduction, the P is released from P-bearing ferric iron (hydr)oxides to pore water (loading). The second stage consists in the translocation of the P released via the percolating phase. *Jensen et al.* [1999] speculated that the reductive release of P associated with ferric iron was enhanced under dynamic flow conditions. Miscible displacement experiments therefore would allow us to obtain a more representative estimate of fate and transport of P in a reduced environment. Although evidence suggests that P can be mobilized upon reductive dissolution of ferric iron, this phenomenon has not been studied intensively in dynamic systems.

The objective of this study was to experimentally explore the effect of redox potential on P release and transport under dynamic flow conditions. An experimental setup was developed to simulate the effect of the water table on the transport of P resulting from reductive dissolution of P-bearing ferric iron (hydr)oxides. Specifically, we conducted experiments to simulate three typical cases of soils affected by cyclic flooding events: (i) P release from an initially oxidized system that becomes reduced, (ii) P transported through a reduced environment, and (iii) P transported through an oxidized environment, used as control (oxidized control).

3.3 Materials and Methods

3.3.1 General Experimental Approach

The effect of redox potential on P fate and transport was investigated using an idealized laboratory column flow-through system. We used ferrihydrite-coated sand as the porous medium and created reducing conditions using Fe-reducing bacteria. Phosphorus adsorption in soils is dominated by soil iron oxides, and ferrihydrite should therefore provide a representative model [*Borggaard,* 1983]. The column experiments were conducted under dark conditions at constant temperature of 10°C.

3.3.2 Synthesis of Ferrihydrite-coated Sand

Ferrihydrite ($5Fe_2O_3 \cdot 9H_2O$) was synthesized in a glass beaker, according to procedures described in Schwertmann and Cornell [*Schwertmann and Cornell,* 1991] (page 90). The ferrihydrite was coated onto a silica sand (J.T. Baker, lot A05673), which was previously fractionated to particle sizes between 250 and 500 μm. The silica sand was washed with 1 M of HCl by agitating in a end-over shaker overnight. The ferrihydrite was coated onto the sand grains following the method of *Brooks et al.* [1996].

The detailed procedure for ferrihydrite synthesis and sand coating was as follows: Ferrihydrite was synthesized by neutralizing 200 mL of 0.06 M of ferric chloride ($FeCl_3$) by adding 2 M NaOH dropwise until the pH was stable at 7.2. The solution was decanted overnight and the solution pH re-adjusted to 7.2. Two phases were clearly

identified: The supernatant solution free of oxide (clear part) was discarded and the bottom part (iron oxide) was dialyzed. Dialysis tubes of 25 mm flat width, 2mL/cm and with a molecular weight cut off value of 12,000-14,000 Da (Spectrum®) were filled with the iron oxide and placed in a plastic container with nanopure water. The water from the container was replaced every 12 h. This process eliminated the remaining content of salts from the oxide such as Na and Cl. The oxide was dialyzed until the electrical conductivity (EC) of the water reached a value of ≈ 3 μS/m. After dialysis, the ferrihydrite suspension was thoroughly mixed with 60 g of silica sand, and dried at room temperature for 3 days. The mixture was stirred twice a day to facilitate the drying process. Then the ferrihydrite-coated sand was washed several times with nanopure water and dried again at room temperature. The ferrihydrite-coated sand was heated for 24 h at 105°C to eliminate microbial contamination before the transport experiments. The specific surface area (1.11 m^2/g) was determined by B.E.T. analysis. The ferrihydrite obtained by this methodology was identified as a two-line ferrihydrite by x-ray diffraction (XRD) analysis (Figure 3.1). The ferrihydrite-coated sand was found to be stable after one year of storage both under dry conditions and immersed in nanopure water at room temperature (Figure 3.2).

3.3.3 Microorganisms used to Reduce Redox Potential

Iron-reducing bacteria (*Shewanella putrefaciens*, strain CN-32) were obtained from James Frederickson (Pacific Northwest National Laboratory, Richland, WA) and kept

at −70°C in a 20% glycerol stock solution. Bacteria were grown in a tryptic soy broth (TSB) suspension media at 25°C in an orbital shaker and harvested at late log-phase [*Frederickson et al.,* 1998]. When the late log-growth stage was reached (after 80 h), the bacteria were washed three times with a buffer solution (43 mM NaCl and 30 mM $NaHCO_3$, pH 7) [*Hansel et al.,* 2003]. The washing procedure consisted of shaking the bacteria with the buffer solution, centrifugation, and replacing the supernatant.

Shewanella putrefaciens is a "facultative, dissimilatory iron reducing bacterium (DIRB) that couples the incomplete oxidization of lactate to acetate with Fe^{3+} reduction" [*Hansel et al.,* 2003]. Figure 3.3 shows cells of *Shewanella putrefaciens* strain CN-32, growing in TBA agar medium at 25°C. A sample of the bacteria suspension was dried in dry ice and prepared for scanning electron microscopy (SEM). A scanning electron image of the bacteria used in this study is shown in Figure 3.4.

To determine the time for the bacteria to reach the late log-stage of growth, we measured the optical density (Hewlett Packard 8425A Diode array, at a wavelength of 500 nm) of the bacterial suspensions and the bacteria concentration as a function of time. To determine the bacteria concentration, bacteria were plate-counted. For plate counting a sample was incubated on TBA agar medium at room temperature for 72 h. The phosphorus consumption rate (k_b) at 25°C, was obtained in a separate batch reactor containing bacterial suspension media (TSB). After 10, 48, 72 and 96 h, 5 mL of media was centrifuged and analyzed for P by the molybdate blue method [*Murphy and Riley,* 1962]. Phosphorus changes as a function of time were assumed

to be the P bacteria consumption. Bacteria concentrations during incubation and optical densities as a function of time and bacteria P consumption rate are shown in Figure 3.5. The measured P consumption rate in batch experiments was found to decrease exponentially with time and at the time of harvest k_b approached zero. For this reason the bacterial P consumption was considered negligible in the P mass balance calculations.

Tests performed previous to the experiments indicated that the chemical composition of the mineral solution used in the transport experiments supports microbial growth of *S. putrefaciens* strain CN-32.

The following reactions can be expected to occur in an anoxic environment during the oxidation of lactic acid (Equation 3.4) by *Shewanella putrefaciens* in a FHO-coated sand in the presence of phosphate [*Frederickson et al.,* 1998].

$$4Fe(OH)_3(s) + CH_3CHOHCOO^-(aq) + 7H^+(aq) = 4Fe^{2+}(aq) + CH_3COO^-(aq) + HCO_3^-(aq) + 10H_2O(l) \quad (3.4)$$

$$2Fe(OH)_3(s) + Fe^{2+}(aq) = Fe_3O_4(s) + 2H_2O(l) + 2H^+(aq) \quad (3.5)$$

$$2Fe(OH)_3(s) + 4Fe^{2+}(aq) + A^{2-}(CO_3^{2-}, SO_4^{2-})(aq) + 9H_2O(l) = [Fe_4^{II}Fe_2^{III}(OH)_{12}][A^{2-} \cdot 3H_2O](s) + 6H^+(aq) \quad (3.6)$$

$$Fe^{2+}(aq) + HCO_3^-(aq) = FeCO_3(s) + H^+(aq) \quad (3.7)$$

$$3Fe^{2+}(aq) + 2HPO_4^{2-}(aq) + 8H_2O(l) = Fe_3(PO_4)_2 \cdot 8H_2O(s) + 2H^+(aq) \quad (3.8)$$

Equations 3.5, 3.6, 3.7 and 3.8 describe the formation of magnetite (Fe_3O_4), green rust ($[Fe_4^{II}Fe_2^{III}(OH)_{12}][A^{2-} \cdot 3H_2O]$), siderite ($FeCO_3^-$), and vivianite ($Fe_3(PO_4)_2 \cdot 8H_2O$), respectively.

3.3.4 Column Experiments

General Setup

Small glass columns of 1-cm i.d. and 7-cm length with 25 μm teflon frits in the end pieces (Omnifit, Cambridge, UK) were packed at a bulk density of 1.6 g/cm^3 with the ferrihydrite-coated sand. The column system was kept O_2-free by using an air-tight N_2 chamber. We kept a positive pressure of N_2 gas inside by flushing 99.99% N_2 gas into the chamber, controlled by a flow meter. Degassed water was poured in a compartment between the lid and the body of the box (Figure 3.6). The water layer interface (5 cm depth) was intended to avoid O_2 entering inside the chamber. This was based on the low diffusion rate of O_2 in water. Before each experiment, the box was flushed with N_2 for 30 min to take the O_2 out of the chamber. During the experiments, a positive pressure was maintained inside the chamber. It was checked periodically by the flow meter readings and the N_2 bubbles constantly escaping through the water interface to the outside of the chamber (Figure 3.6).

As the column itself is air-tight and was operated under completely water saturated conditions, we only placed inflow and outflow into the N_2 chamber. A constant upward-flow of eluent was maintained by a peristaltic pump at a flow rate of 0.035 cm/min (=0.5 m/d). Redox potential and pH were monitored in five minute intervals with in-line electrodes connected to flow-through cells. Sensor data were collected through a PC interface connected to an Orion 720A voltmeter (Orion Research Inc., Beverly, MA). Column outflow was collected in disposable glass culture tubes using a

Spectra/Chrom IS-95 interval sampler (Spectrum® Chromatography, Houston, TX). To each tube placed in the interval sampler, we added 0.05 mL of 6 M HCl to prevent P precipitation and iron oxidation caused by exposure to oxygen during chemical analysis. The whole system was set up inside of a temperature-controlled growth chamber at 10°C under dark conditions to mimic the soil environment. A schematic of the column setup is shown in Figure 3.6.

As stated before, three types of experiments were performed: In one type, P was sorbed to the ferrihydrite-coated sand under oxidizing conditions prior to the induction of reducing conditions; in the second experiment, P was injected into the ferrihydrite-coated sand column under reducing conditions; and in the third experiment, P was transported through the ferrihydrite-coated sand column under oxidizing conditions. The first experiment mimics an initially oxidized system containing P that becomes anoxic; the second experiment represents P transport through a reduced soil environment; and the third system considered P transported under oxidized conditions (oxidized control).

Experiment 1: Reduction of an Initially Oxidized System

A water saturated ferrihydrite-coated sand column was equilibrated with a non-degassed background electrolyte for nine pore volumes (pH 6.5 and redox potential of $\approx$ 350 mV). Then, 0.152 mM P as KH_2PO_4 was added to the inflow solution for 39 pore volumes, after which the inflow was switched back to the initial KCl background for

50 pore volumes until no P was detected in the outflow. This procedure deposited P inside the column, and a breakthrough curve of P was obtained in the column outflow. At this point, we assumed that we had a uniform coverage of P inside the column.

To reduce the redox potential inside the column, two pore volumes of bacteria ($\approx 10^8$ cells/mL) suspended in a mineral solution (3 mM lactic acid; 1.78×10^{-2} mM NH_4Cl; 6.72×10^{-2} mM KCl; 0.514 mM NaCl) were introduced as a pulse input, followed by elution of the mineral solution only. The sequence of column inputs and the composition of the mineral solution are summarized in the Table 3.1. To facilitate the bacteria input process, the original 25 μm pore size teflon frits in the inlet and outlet of the column were replaced by 53 μm pore size diameter nylon membranes (Gilson Company Inc., OH, USA).

We performed XRD analysis to determine the presence of secondary mineral formation. For the XRD sample preparation, the column was opened inside the chamber at the end of the experiment, and samples were collected in degassed water. The samples together with degassed water were introduced in a septa tube and N_2 gas was flushed inside to prevent oxidation of the material. Powder samples were obtained by sonicating the Fe-coated sand contained in the septa tubes for 10 minutes. The suspension was extracted from the tube using a 5 mL plastic syringe and replaced by the same volume of degassed nanopure water. This procedure was repeated three times. Then, the suspension containing the Fe-oxides was centrifuged and the supernatant was taken off by the same procedure and vacuum dried at room temperature.

The XRD patterns were collected with a Philips diffractometer (XRG 3100, Philips Analytical Inc., Mahwah NJ) at a scanning rate of $0.02^o 2\theta$.

Experiment 2: Reduced System

Ferrihydrite-coated sand was inoculated in a sterile glass beaker with the bacterial suspension using the same mineral solution listed on Table 3.1 . One column packing of sand was inoculated with the equivalent of two column pore volumes of bacteria suspension ($\approx 10^8$ cells/mL). After thorough mixing of the bacteria-sand slurry, the sand was packed into the column and equilibrated for one hour at 10°C without flow. Then a P-containing solution (0.32 mM) was fed through the column for 88 pore volumes, followed by elution with a P-free solution (Table 3.1). In this experiment we used the original 25 μm pore size teflon frits in the inlet and outlet of the column.

The porous media of the column was dissected in 1.75 cm increments at the end of the experiment. The material was extracted with 6 M HCl and the total Fe ($Fe_{Total} = Fe^{3+} + Fe^{2+}$) and P were measured colorimetrically as described in the section below.

Oxidized Control System

A bacteria free ferrihydrite-coated sand column was preconditioned with 9 pore volumes of non-degassed background electrolyte (pH 6.5 and redox potential of $\approx$ 350 mV) under saturated conditions. Then, 0.32 mM of P as KH_2PO_4 was added to the inflow solution for 21 pore volumes, after which the inflow was switched back to the initial KCl background for 25 pore volumes until no P was detected in the outflow.

A breakthrough curve of P was obtained in the column outflow (oxidized control in Table 3.1).

Analysis of Fe, P, and Bacteria in Column Outflow

Every six tubes, tubes from the interval sampler were capped inside the N_2 chamber. Column outflow was analyzed for Fe^{2+} with the ferrozine method [*Stookey*, 1970], P was analyzed with the molybdate blue method [*Murphy and Riley*, 1962], and turbidity (bacteria concentration) was determined spectrophotometrically. Redox potential was determined in the outflow with a combination ORP electrode (Cole Parmer, Cat. EW-05658-70, USA). The redox electrode was calibrated prior to each experiment by determining the redox potential in a buffer solution saturated with quinhydrone at pH 4 and 7. The redox readings were checked with a standard table provided by the manufacturer (Cole Parmer). In a similar way, the pH electrode (Cole Parmer, Cat. EW-05662-90 , USA) was calibrated using pH buffer standard solutions (pH 4 and 7).

3.3.5 Data Analysis and Interpretation of the Results

Data analysis consisted of mass balance and regression analyses. Mass balance analyses were performed for each system to study the net P retention and release. Regression analyses were performed by using SigmaPlot® 2002 version 8.0. Non-linear regressions were performed using the Solver utility provided by Microsoft Excel.

The results of the experiments were interpreted as follows: (i) the P transport in

the tailing portions of the P elution curves for experiment 2 and for the oxidized control system were predicted by the analytical solution of the advection dispersion equation (ADE) [*Manoranjan and Stauffer,* 1996]; and (ii) the secondary mineral formation inside the columns was modelled using the chemical equilibrium speciation model visual MINTEQ 2.15 [*Gustavsson,* 1999].

(i) Phosphorus Transport

The P transport through the ferrihydrite-coated sand medium for experiment 2 and for the oxidized control was described by the one-dimensional ADE

$$\theta\frac{\partial c}{\partial t} + \rho\frac{\partial q}{\partial t} = \theta D\frac{\partial^2 c}{\partial x^2} - \theta v\frac{\partial c}{\partial x} \tag{3.9}$$

where c is the solution-phase concentration, q the sorbed-phase, D is the dispersion coefficient, v is the pore water velocity, t is time, x is the distance, θ is the volumetric water content, and ρ is the bulk density. The P sorption was described by the Langmuir non-equilibrium sorption equation

$$\frac{\partial q}{\partial t} = k_f c(q_m - q) - k_r q \tag{3.10}$$

where q_m is the P sorption maximum, k_f is the sorption rate constant and k_r is the desorption rate constant.

Equations 3.9 and 3.10 are transformed into a coupled system of nonlinear ordinary differential equations with respect to z using the travelling wave coordinate $z = x - \alpha t$ as follows [*Manoranjan and Stauffer,* 1996]:

$$-\alpha\frac{dc}{dz} = \tilde{D}\frac{d^2 c}{dz^2} - \frac{dc}{dz} - w(-\alpha\frac{dq}{dz}) \tag{3.11}$$

$$-\alpha\frac{dq}{dz} = k_1bc - (k_1c + k_2)q \tag{3.12}$$

where, α is the constant speed at which the wave front is moving, $w = \rho/\theta$, $\tilde{D} = D/v$, $k_1 = k_f/v$, and $k_2 = k_r/v$. Combining Equations 3.11 and 3.12 we have

$$\frac{-\alpha\frac{dc}{dz} - \tilde{D}\frac{d^2c}{dz^2} + \frac{dc}{dz}}{-w} = k_1bc - (k_1c + k_2)q \tag{3.13}$$

but q can be obtained by integrating Equation 3.11

$$q = \frac{(-\alpha - \tilde{D}\frac{dc}{dz} + c)}{\alpha w} \tag{3.14}$$

Then Equations 3.13 and 3.14 are combined to obtain an expression in terms of c

$$\frac{-\alpha\frac{dc}{dz} - \tilde{D}\frac{d^2c}{dz^2} + \frac{dc}{dz}}{-w} = k_1bc - (k_1c + k_2)\frac{(-\alpha - \tilde{D}\frac{dc}{dz} + c)}{\alpha w} \tag{3.15}$$

Finally, using the Bernoulli equation, an analytical solution is obtained for Equation 3.15 in the form

$$c(x,t) = \frac{-(\frac{a_1}{a_2})}{[1 + \exp(-a_1(x - \alpha vt))]} \tag{3.16}$$

where a_1 (1/cm) and a_2 (L h/mmol cm^2) are constants related to solute desorption and adsorption, respectively. To obtain a positive concentration profile, α should be such that

$$0 < \alpha < 1; \alpha(1 - \alpha) > \tilde{D}k_2 \tag{3.17}$$

Estimating P desorption

We compared the desorption part of the P breakthrough curves for experiment 2 and for the oxidized control. The analytical solution of the ADE based on the traveling

wave front model [*Manoranjan and Stauffer*, 1996] was fitted to the experimental data describing the tailing parts of the P elution curves. The desorption rate constant k_r (t^{-1}) was estimated from:

$$k_r = \alpha v[a_1 + \frac{(1-\alpha)}{\tilde{D}}] \tag{3.18}$$

The adsorption rate constant k_f (L/mmolh^{-1}) is given by:

$$k_f = 2\alpha v a_2 \tag{3.19}$$

Desorption rate constants were attempted to quantify the differences in P release behavior between both systems.

A tracer experiment with bromide (Br^-) was conducted to determine D of the column system (Figure 3.7). A step input concentration of 0.2 mM of Br^- at pH 11, as KBr was flushed into the column previously equilibrated with 0.015 M KCl at pH 11. Bromine was analyzed spectrophotometrically at a wave length of 202 nm (HP 8452A, Hewlett Packard). The D was determined by fitting the one-dimensional advection-dispersion equation (ADE) to non-reactive solute breakthrough data using the CXTFIT code, version 2.1 [*Toride et al.*, 1999].

(ii) Chemical Speciation

The solubility equilibrium of the precipitates originating from the biogenic iron reduction and the stable solid mineral phases as a function of the pH and redox potential were predicted using MINTEQ 2.15 [*Gustavsson*, 1999], a Windows® version of MINTEQA2 [*Allison et al.*, 1991]. For these calculations, we used the solution concen-

trations, pH, and redox potential determined in the column outflow and assumed this to be representative for the resident concentration inside the column. The temperature was set to 10°C for all the calculations. The ionic strength was also estimated by the model. The chemical components used as input parameters are listed in Table 3.2. Three different cases were considered for modeling: for the experiment 1 three combinations of low, medium and high concentrations of P and Fe^{2+} were used for the calculations. In the experiment 2, we simulated the chemical speciation of solid phases in three different stages of the elution P curve. We considered the sorption part (4.7 pore volumes), the plateau (34.1 pore volumes), and the desorption phase of the curve (108.2 pore volumes).

3.4 Results and Discussion

P Transport in the Oxidized Control System

Experimental data obtained from the P transport in the oxidized system (oxidized control) are depicted in Figure 3.8. The initial pH of the solution was 6.5 but increased to neutral pH after three pore volumes. At this point the breakthrough curve showed the steepest slope, which is indicative of rapid saturation of the sorption sites. The increase in pH was assumed to be a result of ligand exchange reactions [*Goldberg and Sposito,* 1985]. After the saturation of sorption sites was attained, the sorption decreased in intensity and the pH started to decrease and stabilize at 6.5. Right after the P feeding

solution was shifted (after 30 pore volumes) to the original background solution the pH decreased below 6.5. The redox potential was stable at 200 mV throughout all the experiment suggesting the absence of oxidation or reduction reactions.

Experiment 1: P Transport by Reduction of an Oxidized System

The history of the column experiment is shown in Figure 3.9. The initial breakthrough of P was performed under oxidized conditions (redox potential > 240 mV). Under these conditions, no Fe reduction occurs and P chemisorbs to the ferrihydrite, as suggested by the shape of the P elution curve, which is similar of that obtained in the oxidized control.

The adsorption part of the P breakthrough curve is accompanied by an increase in pH as expected from binuclear bridging mechanisms between P and Fe-oxide [*McBride*, 1994]. After most of the P sorption has occurred the pH decreased up to background levels (pH=6.5). The desorption part of the P breakthrough curve is very steep, indicating an irreversibility of the sorption reaction. We introduced a total of 15.14 μmoles of P during 39 pore volumes and only about 10% (1.6 μmoles) was sorbed effectively inside the column (Table 3.4). This indicated that sorption capacity was relatively low.

After P was deposited inside the column and no P was detected in the outflow, the reduction part of the experiment was started by introducing the bacteria into the system (at 98 pore volumes). At this point, it was assumed that the system was

saturated with P because P broke through at C/Co $\approx$ 1. As Fe-reducing bacteria were introduced into the column, the redox potential started to drop after 105 pore volumes, suggesting a time lag (10 pore volumes) between introduction of bacteria and reduction. The pH correspondingly increased up to 7.5 as the redox potential dropped due to proton consumption during reduction of ferric iron as indicated in Equation 3.4. The bacteria decreased the redox potential efficiently and Fe^{2+} as well as P were detected in the column outflow.

The total P measured in the outflow after the bacteria input was 0.21 μmoles. Phosphorus concentration measured in the bacteria suspension before the start of the experiment was 0.0194 μmoles. This amount of P was considered to correct the mass balance analysis. Thus the net P leached out during the reductive part of the experiment 1 ($\approx$ 100 pore volumes) was 0.19 μmoles. In relative terms, the amount of P lost during the reductive part of the experiment represents the 12% of the total P content deposited inside the column during the oxidized part of the experiment.

Secondary Mineral Formation

Saturation indices (SI), a thermodynamic indication of mineral dissolution or formation, obtained for a series of potential precipitated phases are depicted in Table 3.3. A visual evidence of secondary mineral phase formation was observed after the 10 pore volumes of bacteria input. It consisted of a dark discoloration in the upper part of the column (outflow part) (Figure 3.10) and was evident until the end of the experiment.

The same phenomenon has been reported in other studies and attributed to magnetite formation ($Fe_2^{3+}Fe_2^{2+}O_4$) [*Hansel et al.,* 2003]. Indeed, the saturation indices, and Equation 3.5, indicate that magnetite may be present as a secondary mineral in this system. However, magnetite was not detected in the XRD analysis. There is evidence that upon reduction, the concentration of Fe^{2+} plays a fundamental role in the formation of magnetite [*Hansel et al.,* 2003]. *Hansel et al.* [2003], suggested that magnetite precipitation will occur when Fe^{2+} concentration increases above 0.3 mM. In this study the Fe^{2+} concentration was far less than this limit, so we believe this was an inhibiting factor of magnetite formation. It has been also reported that magnetite formation is inhibited by the presence of P [*Hansel et al.,* 2003]. The XRD identification of iron oxides is favored at concentrations >10% [*Wilson,* 1987]. Thus, the discoloration can be attributed to the presence of magnetite but at lower concentrations of this limit.

Secondary phases such as goethite, lepidocrocite, green rust, and vivianite have also been detected in this type of reduced system [*Benner et al.,* 2002]. According to the modeling results, the eluents were supersaturated with respect to magnetite, goethite, ferrihydrite, hematite, maghemite, lepidocrocite, and $Fe(OH)_{2.7}Cl_{0.3}$. Despite the several mineral phases that were predicted to be supersaturated by MINTEQ, none of those are associated with P. This supports the results obtained from mass balance calculations that P was released as result of the reductive dissolution of Fe^{3+} of the ferrihydrite-coated sand.

Experiment 2: Reduced System.

Phosphorus transport, Fe^{2+}, pH, and redox potential determined under reduced conditions are shown in Figure 3.11. The outflow solution pH was nearly constant at 7.5 during the period of P input (80 pore volumes). Right after the P input was stopped the pH decreased up to 6.5. Originally, the redox potential of the mineral solution was about 300 mV; however, right after the bacteria were mixed with the media, the redox potential decreased to 140 mV. The redox potential reached a minimum of 10 mV at 80 pore volumes and started increasing after the feeding P solution was shifted to the background electrolyte (after 80 pore volumes).

Ferrous iron reach a maximum first at 8 pore volumes and decreased gradually until 30 pore volumes. From 40 to 60 pore volumes Fe^{2+} was undetected. After 60 pore volumes the concentration reached $\approx$0.0005 mM, which coincided with stopping P input. Thereafter, Fe^{2+} decreased gradually again after the P input was shifted to the background electrolyte.

A comparison of the transport of P through the oxidized control and experiment 2 is shown in Figure 3.12. In both cases the breakthrough curves showed a sharp rise up to 20 pore volumes, and then the curve reached a plateau. In the oxidized control system the concentration rose up to the original feeding concentration of 0.32 mM. The P BTC observed under reduced conditions followed a similar pattern but never reached the original P concentration. Compared to the oxidized system, the P breakthrough showed a pronounced tailing.

The differences in the P breakthrough curves between the oxidized control and experiment 2, may be a result of precipitation and dissolution reactions.

Secondary mineral formation

The MINTEQ model outputs indicate the potential for the formation of vivianite as the only phase associated with P (Table 3.3). Solutions were supersaturated with respect to vivianite only during the sorption part of the P breakthrough curve of the experiment 2. The precipitation of vivianite would effectively reduce Fe^{2+} concentrations from solution as long as sufficient PO_4 is present [*Willett,* 1985]. This might also explain the higher P retention observed in the reduced column versus the oxidized control during the first 40 pore volumes. After P input was stopped (after 100 pore volumes) and the concentrations inside the column decreased, vivianite becomes undersaturated and consequently dissolves again. This was supported by the MINTEQ output results which indicate that vivianite was undersaturated after 80 pore volumes (plateau and desorption case in Table 3.2). This results in a release of P as well as Fe^{2+}. A pronounced Fe^{2+} peak was indeed detected coinciding with the decrease of P concentrations in the column outflow (Figure 3.11).

Phosphorus desorption in experiment 2 versus oxidized control

The desorption rate constant k_r estimated from Equation 3.18 showed that P was more tightly retained in the oxidized control. The desorption rate in the oxidized control was 2.86×10^{-7} h^{-1} versus 0.89 h^{-1} estimated for experiment 2. This indicates that,

in experiment 2, P continued being released after the P input stopped, supporting the idea that P in the reduced column was released as a result of dissolution processes which did not occur in the control. This process may correspond to vivianite dissolution as indicated by Equation 3.8 and the MINTEQ model outputs (Table 3.3).

The content of P and Fe_{Total} inside the column is depicted in Figure 3.13. Both P and Fe_{Total} variation inside the column were parallel. This can be explained by the fact, that upon reduction, Fe^{2+} may be transported and accumulated at the end of the column (column outflow) [*Hansel et al.,* 2003]. Dissolved phases of P and Fe^{2+} may have been transported upon reduction of Fe^{3+} and accumulated near the outflow end of the column, precipitating as vivianite in this portion of the column.

During the sorption part of the elution curve, a grater amount of P was retained by the reduced system in experiment 2 than the oxidized control. The inverse was true during the desorption part of the experiments. Mass balance analysis revealed that, in the reduced system (experiment 2), the P retained inside the column was 5% of the total P input (Table 3.4). On the other hand in the oxidized column (oxidized control) the P retained was 10% of the total P input. This suggests two things. First, the mechanism of sorption was different in both systems. Ligand exchange was most likely in the case of the oxidized conditions and vivianite precipitation apparently occurred in the reduced experiment (experiment 2). Second, the phosphate precipitated as vivianite seems to be relatively unstable. Small changes in the chemical conditions such as the switch back to the P-free solution during the desorption part, led to P

release due to the dissolution of vivianite. These results are in agreement with those obtained by *Patrick and Khalid* [1974].

These findings suggest that changes in redox potential during periodic flooded events may have significant effect in the P transport and fate.

3.5 Conclusions

In this study we provide evidence that P was released and mobilized upon ferric iron reduction under dynamic flow conditions. A reduced system retained more P than the oxidized column due to precipitation reactions. However, after P feeding was stopped, the redox potential increased causing the dissolution of precipitated phases. This explained the release of most of the P fixed inside the column.

Overall, a reduced environment immobilized less P than an oxidized environment. In this sense, P controlled by precipitated phases such as vivianite, may retain more P than oxic environments, but this retention may be temporary and is sensitive to change in P concentration.

These results confirm that redox processes are important mechanisms controlling P transport and fate in soils. Therefore, this study suggests that soils with elevated P and iron-bearing materials affected by anaerobic conditions constitute a potential risk for water quality impairment.

3.6 Tables and Figures

Table 3.1: Mineral composition and sequence of the type of feeding solution used in the experiments and in the control.

Pore Volumes	Solution Composition
	Experiment 1
0–9	Background electrolyte[‡]
9–48	Background electrolyte + 0.152 mM of P as KH_2PO_4
48–98	Background electrolyte
98–100	Bacteria, 10^8 cells/mL (suspended in mineral solution[§])
100–206	Mineral Solution
	Experiment 2
Inoculation	Bacteria + Mineral Solution + FHO-coated sand
Column Packing	column was left 1 h before start the flow
0–88	Mineral solution + 0.320 mM of P as KH_2PO_4
88-145	Background electrolyte
	Oxidized Control
0–9	Background electrolyte[‡]
9–30	Background electrolyte + 0.320 mM of P as KH_2PO_4
30-55	Background electrolyte

[‡] 15 mM KCl; pH 6.5; Eh 350 mV

[§] 3 mM Lactic Acid; 1.78×10^{-2} mM NH_4Cl; 6.72×10^{-2} mM KCl; 0.514 mM NaCl 14.3 mM $NaHCO_3$; pH 7.

Table 3.2: Cases used for MINTEQ calculations in Experiment 1: three concentrations of P and Fe^{2+} (mg/L) and in Experiment 2: three stages of the P elution curve in Experiment 2 at 10°C, .

	Experiment 1 cases[†]			Experiment 2 cases[§]		
Element	High	Medium	Low	Sorption	Plateau	Desorption
Fe^{2+}	0.00083	0.00014	0.000046	0.05	0.013	0.0023
PO_4^{3-}	0.58	0.31	0.06	13.98	27.45	3.07
pH	7.6	7.6	7.6	7.6	7.6	6.5
Eh (mV)	190	188	51.7	143	51	73

[†]Combination of the high, medium and the low Fe^{2+} and P concentrations determined in the column eluent

[§]selected from three different stages of the P elution curve: sorption, plateau, desorption.

Table 3.3: Predicted saturation indices (SI) for the mineral phases using MINTEQ for three concentrations of P and ferrous iron in Experiment 1 and for three stages of the P elution curve in Experiment 2 at 10°C.

	Experiment 1			Experiment 2		
	High[§]	Medium[§]	Low[§]	Sorption	Plateau	Desorption
Ferrihydrite	0.27	-0.51	-2.91	1.59	-0.56	-4.10
Goethite	3.09	2.31	-0.087	4.41	2.26	-1.28
Magnetite	9.54	7.23	2.47	14.32	9.52	-0.39
Hematite	8.51	6.94	2.15	11.14	6.85	-0.23
Maghemite	1.90	0.34	-4.45	4.53	0.24	-6.84
Lepidocrocite	2.77	1.99	-0.40	4.09	1.94	-1.59
$Fe(OH)_{2.7}Cl_{0.3}$	3.92	3.14	0.74	5.24	3.09	-0.12
Siderite	-2.90	-3.65	-3.62	-0.75	-1.26	-3.22
Vivianite	-8.97	-11.76	-12.72	0.25	-0.69	-7.76
Strengite	-2.81	-3.87	-6.79	-0.12	-1.97	-4.80

SI=(log IAP - log K_s), where IAP, Ion Activity Product and K_s, solubility constant

[§]Combination of the high, medium and the low Fe^{2+} and P concentrations determined in the column eluent

Table 3.4: Phosphorus mass balance analysis for Experiment 1, 2, and the control.

	Input	Output	Balance
	Mass of P (μmoles)		
	Experiment 1		
Before Bacteria input:			
Total P input	15.14 (100%)		
Total P output		13.53 (89.4%)	
Total P deposited inside the column			1.61 (10.6%)
After bacteria input:			
Total P input[‡]	0.0194		
Total P output		0.21	
Total P remaining in the column			1.42
Total P released by reductive dissolution			0.19 (12%)[♭]
	Experiment 2		
Total P input	60.81 (100%)		
Total P output		57.78 (95.01%)	
Total P deposited inside the column			3.03 (4.98%)
	Oxidized Control		
Total P input	25.92 (100%)		
Total P output		23.46 (90.5%)	
Total P deposited inside the column			2.46 (9.5%)

[‡]P content (μmoles) measured in the bacteria suspension

[♭]calculated as % of the total P deposited inside the column (0.19/1.61)

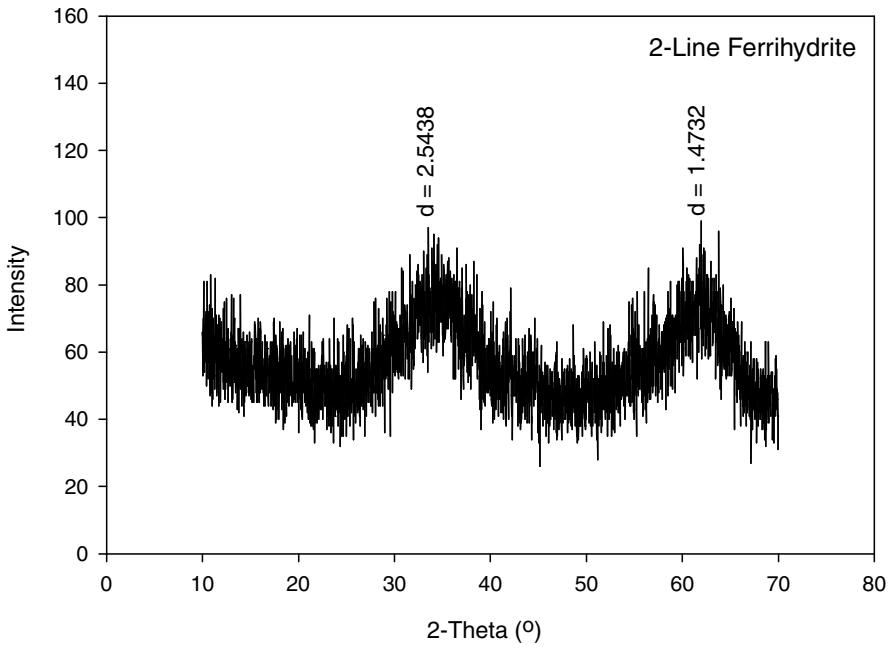

Figure 3.1: X-ray diffractogram of the 2-line ferrihydrite used for the coating process.

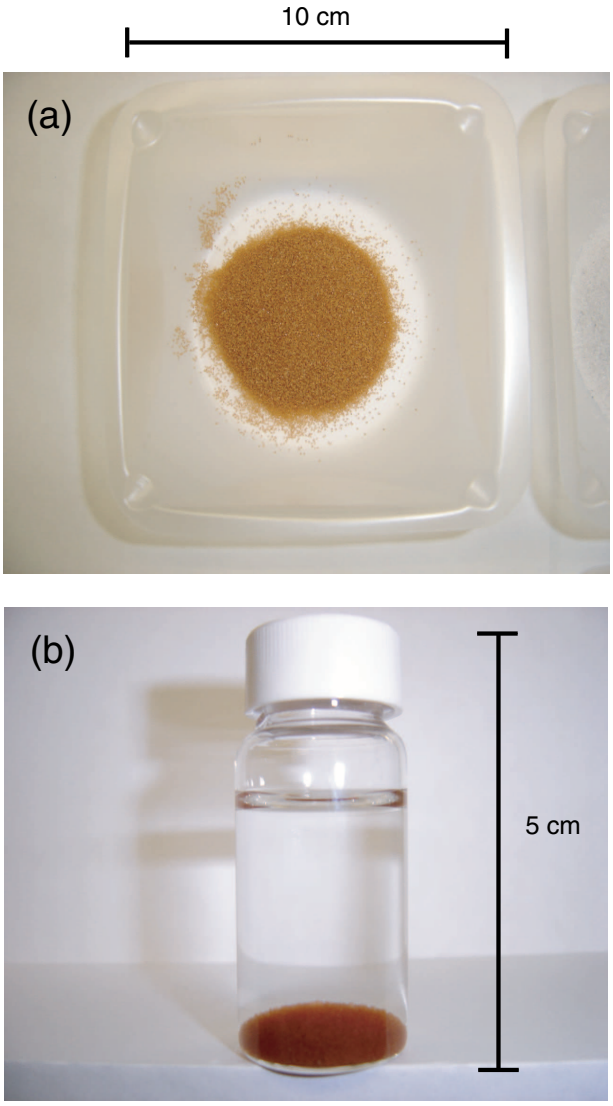

Figure 3.2: Ferrihydrite-coated sand stored for one year under dry conditions (a) and in nanopure water at room temperature (b).

Figure 3.3: Cells of *Shewanella putrefaciens* strain CN-32 growing in TBA agar medium at 25°C, 96 h after plating.

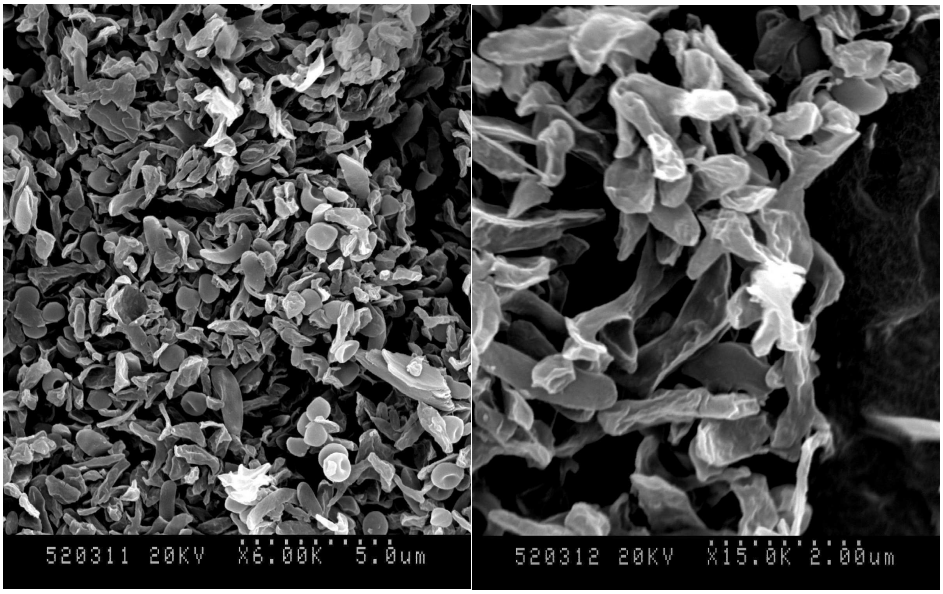

Figure 3.4: Scanning electron microscope image (SEM) of *Shewanella putrefaciens* CN-32 used in the experiments.

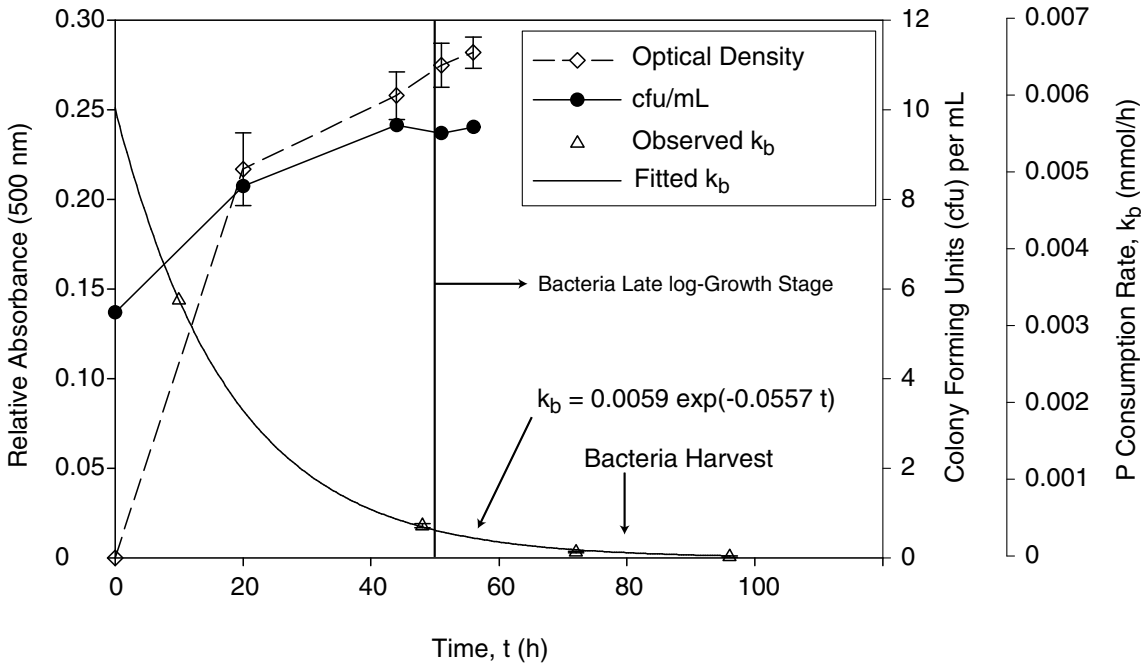

Figure 3.5: P consumption rate, bacteria plate counting (cfu/mL), and growth curve of *Shewanella putrefaciens* strain CN-32 used as iron reductive agent in the experiments. Error bars indicate the standard error (s.e.).

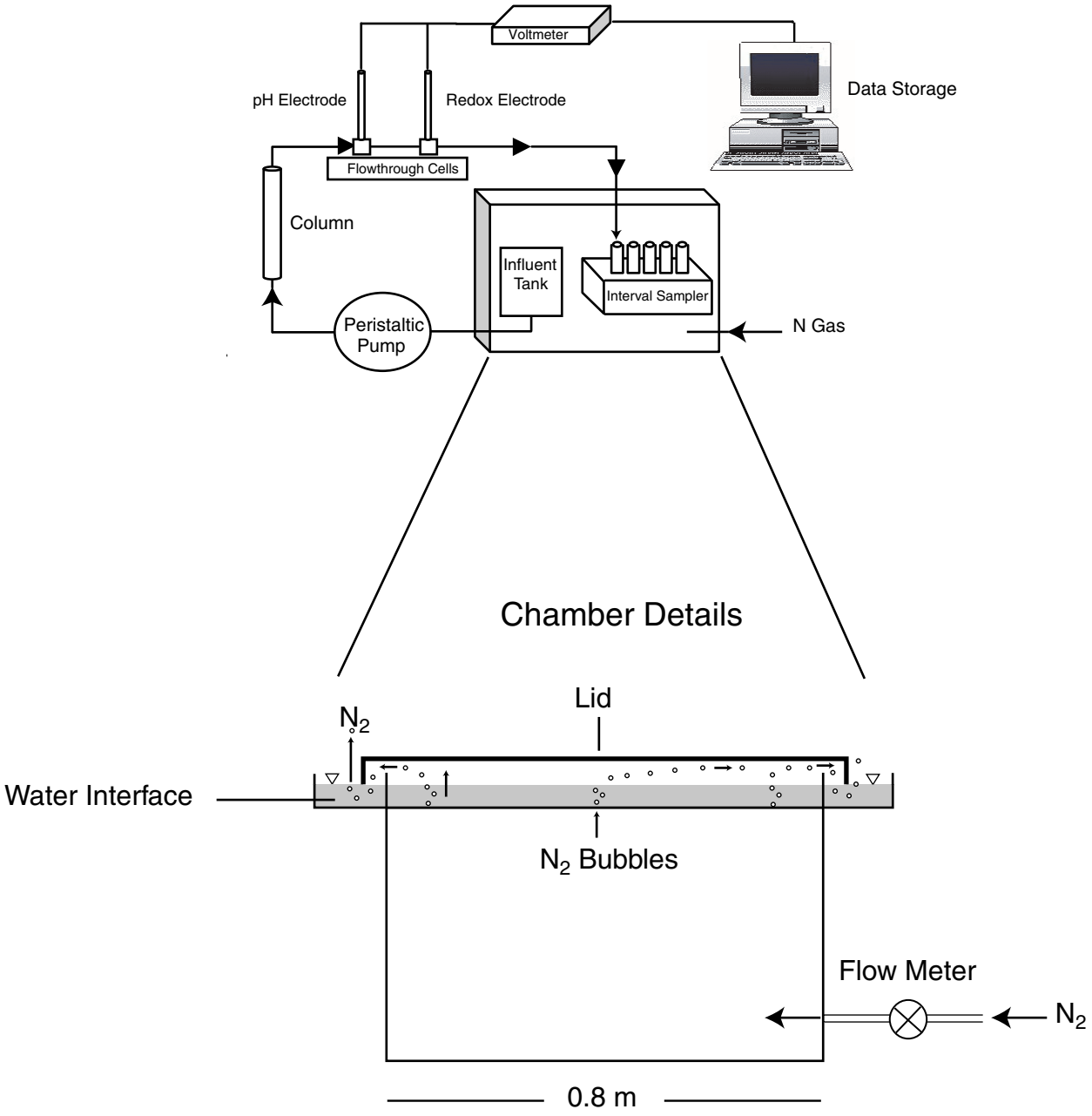

Figure 3.6: Schematic of column setup and details of the N_2 box, for P fate and transport studies under reducing conditions.

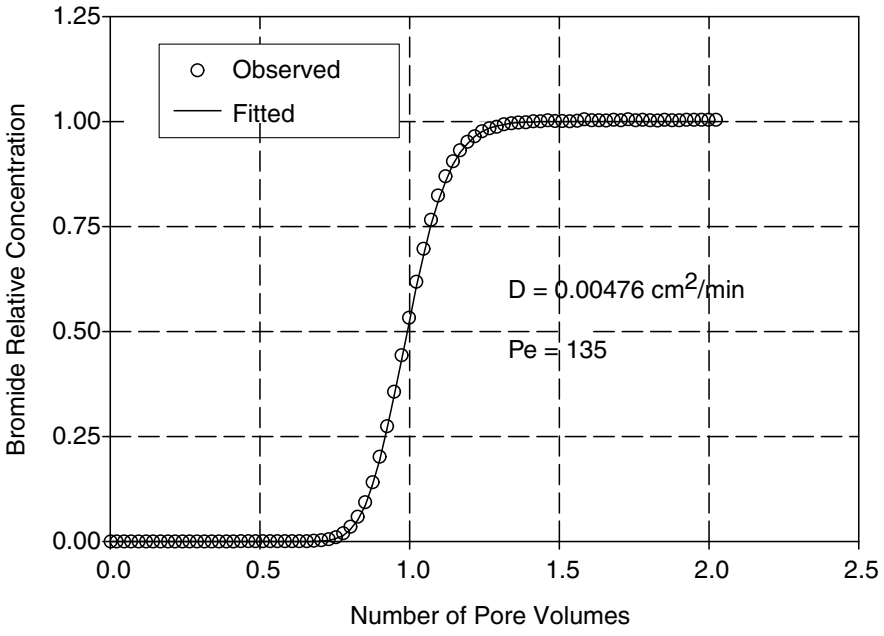

Figure 3.7: Experimental and fitted Br^- breakthrough curve for a saturated ferrihydrite-coated sand and the estimated hydrodynamic dispersion coefficient (D).

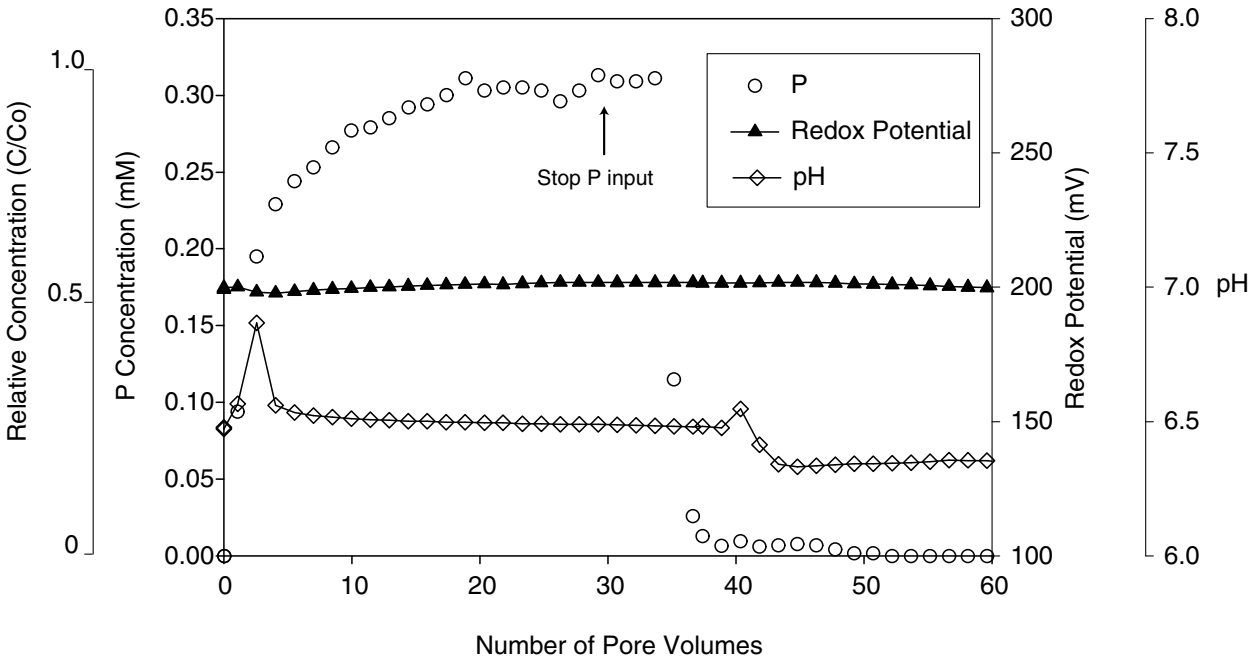

Figure 3.8: Experimental P breakthrough curve, redox potential (mV) and solution pH under oxidized conditions (oxidized control).

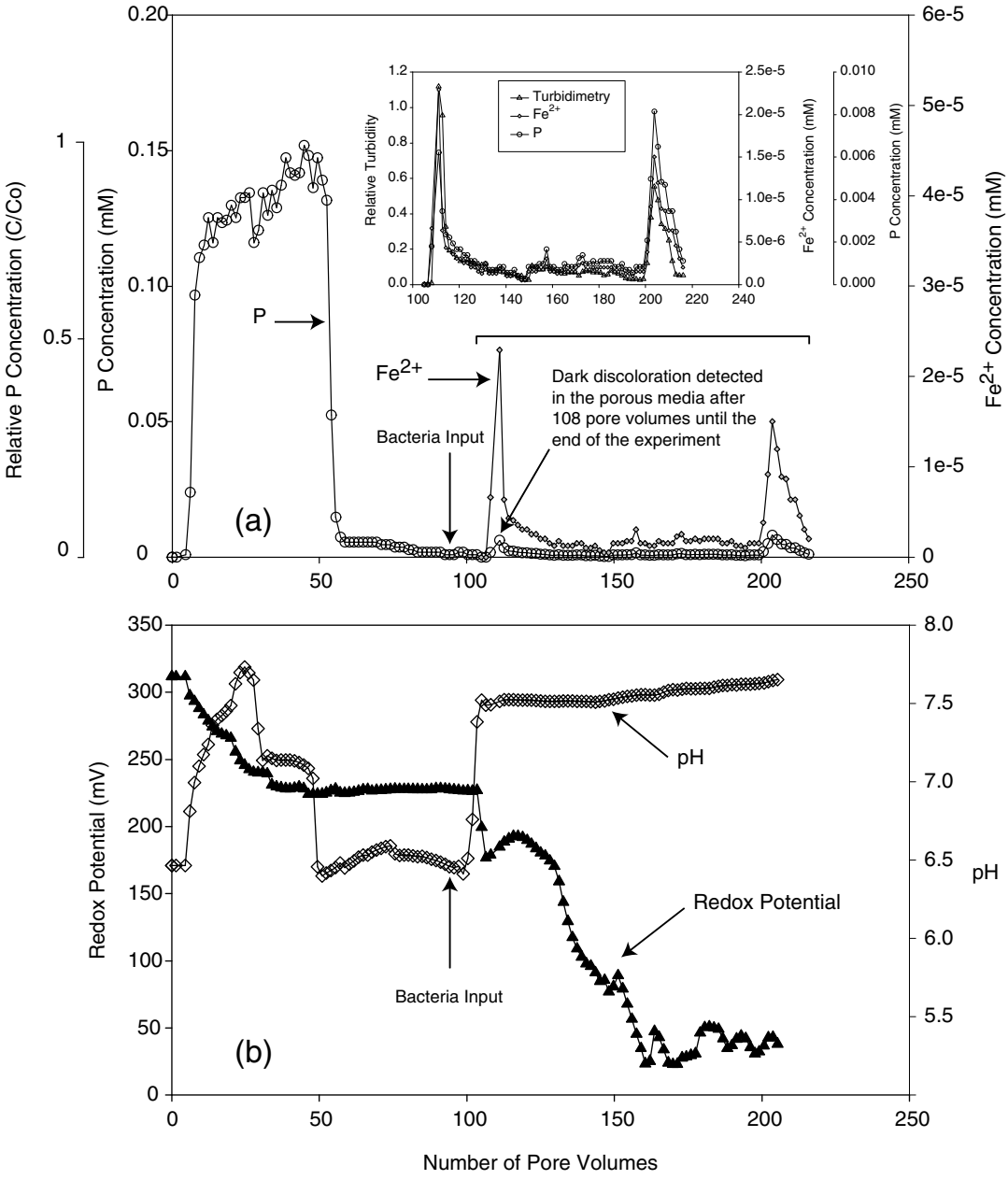

Figure 3.9: Elution curves for P, Fe^{2+}, bacteria (a), and redox potential and pH (b) (Experiment 1).

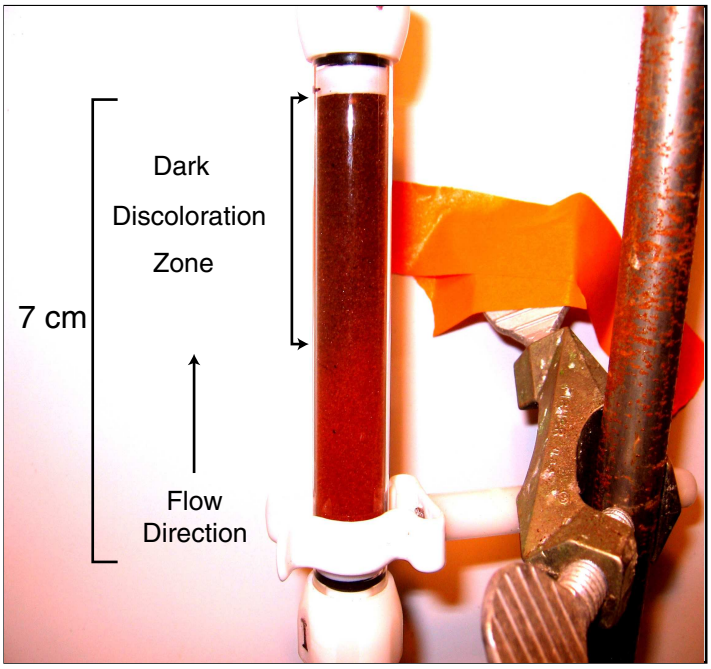

Figure 3.10: Visual evidence of the dark discoloration observed in the upper part of the column (outflow) 10 pore volumes after bacteria input in the experiment 1.

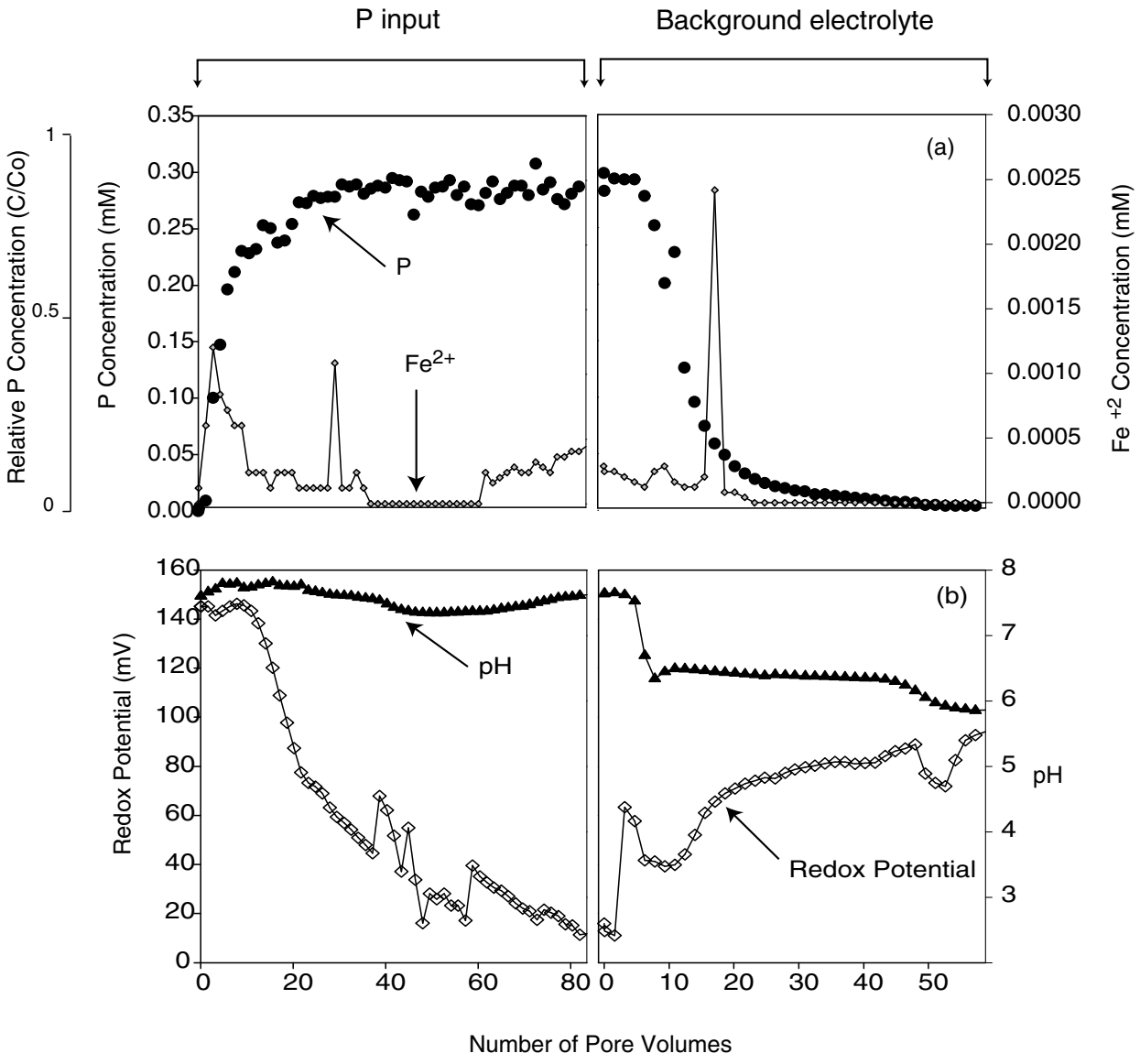

Figure 3.11: Phosphorus and Fe^{2+} breakthroughs for a saturated ferrihydrite-coated sand under reduced conditions (a). Redox potential (mV) and solution pH (b).

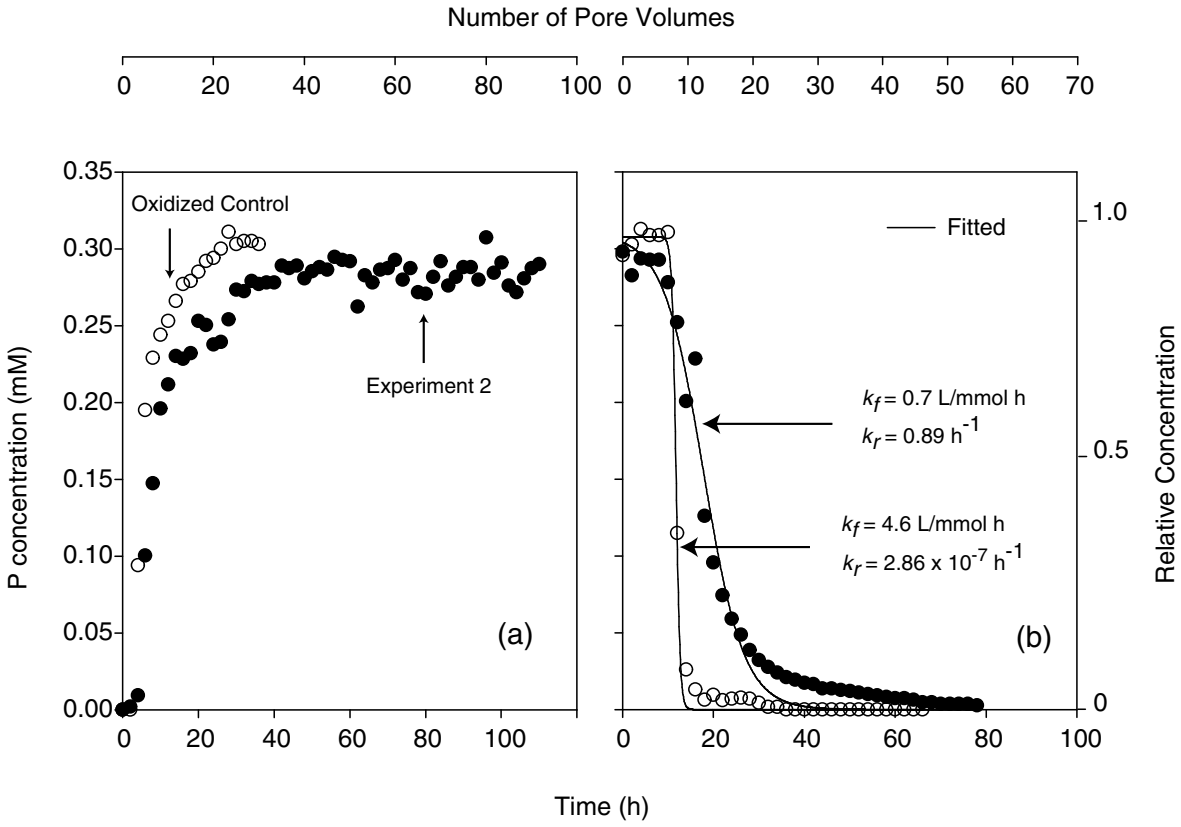

Figure 3.12: Experimental data of the P breakthrough curve under reduced conditions (experiment 2) compared to control under an oxic environment (oxidized control). Phosphorus sorption part of the curve (a) and P desorption after P input was shifted to the background electrolyte (b)

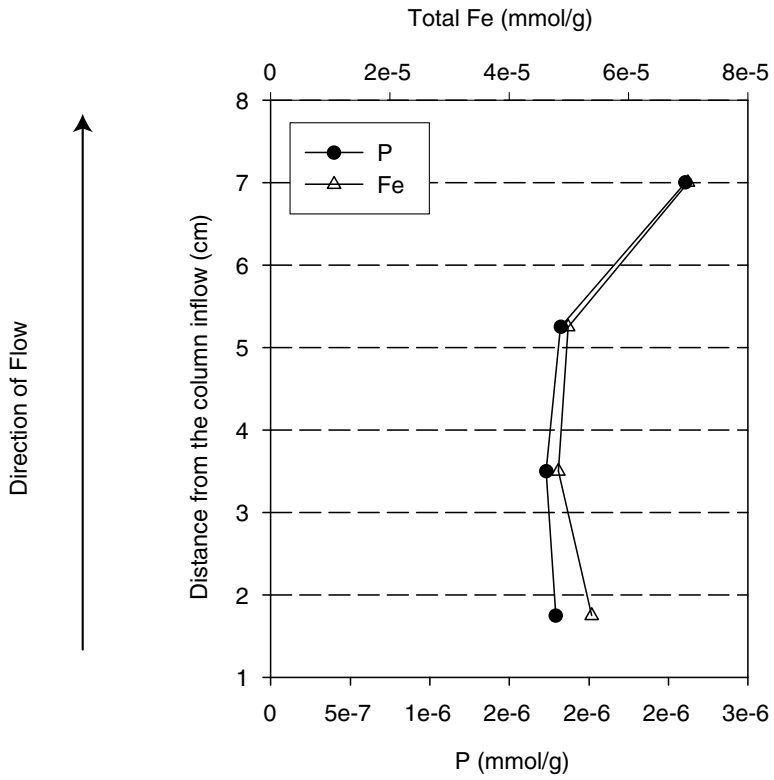

Figure 3.13: Total phosphorus and Fe (Fe^{2+} + Fe^{3+}) measured in 4 sections of the column after the Experiment 2.

Chapter 4

An Indicator to Assess Risk of Phosphorus Leaching in Manure-impacted Soils

4.1 Abstract

Diffuse contamination of surface water by P is one of the main water quality problems in the U.S. Agricultural soils receiving large amounts of phosphorus (P) may be susceptible to P loss via subsurface flow. Several indicators have been developed to determine the risk of P leaching. Recently, the slope of the Langmuir isotherm at lower solution P concentration ranges, has been used to predict enhanced P leaching in highly P-impacted soils; however, its use is limited because it needs to be estimated from a complete sorption isotherm. This study aimed to (i) obtain a similar estimate of the P sorption strength without developing a complete sorption isotherm; (ii) determine threshold levels of the indicator above which the P mobility may be enhanced; and (iii) provide a practical methodology to implement the use of the indicator. We provide theory and data to demonstrate that the inverse of the equilibrium P concen-

tration at zero sorption ($1/c_e$) is a valid estimate of the soil sorption strength. Soil samples from manure–impacted soils in northwestern Washington State were used as the experimental basis of this study. The $1/c_e$ was obtained in two ways: (1) using two points of the linear isotherm and (2) using the water-desorbable P (P_w). We demonstrated that $1/c_e$ is equivalent to the estimate of the sorption strength calculated from a complete sorption isotherm. A segmented model was used to determine a threshold level of $1/c_e$ below which P desorbability parameters were significantly enhanced. Values of $1/c_e$ were well predicted using two points of the isotherm and a good relationship was found with P_w. A threshold level of 0.71 L/mg was determined as a critical point of $1/c_e$ below which desorbability parameters (e.g. concentration of P in solution (P_s), P_w, calcium-chloride-extractable P (P_{CaCl_2}), desorption rate (k_d) increase significantly. Molybdate reactive P measured in drainage water from selected soils in this study was negatively correlated to $1/c_e$. The indicator $1/c_e$ is a meaningful estimate of the sorption strength that can be obtained without developing a complete sorption isotherm. It can be accurately calculated using only two points of the linear isotherm and also can be reasonably approximated by using $1/P_w$. The indicator $1/c_e$ can be implemented in a routine soil analytical procedure and, due to its nature, may be used in any soil type and management to predict/estimate the potential risk for P loss via subsurface flow.

4.2 Introduction

Phosphorus released from agricultural lands has a detrimental impact on surface water quality leading to algae proliferation and reduction of available oxygen for living aquatic organisms [*Sharpley et al.*, 1994; *Shober and Sims*, 2003; *Novak et al.*, 2004]. Phosphorus transfer from agricultural fields commonly occurs via surface runoff, whereby P is carried off site through sediment transport [*Sharpley et al.*, 1994]. However, in agricultural soils receiving high P inputs, P leaching has been identified as a serious environmental problem [*USEPA*, 2003].

Due to the increasing concern of subsurface P losses, the development of environmental indicators has been proposed to assess the risk of P leaching in agricultural soils [*Beauchemin and Simard*, 1999]. Soil test P (STP) [*Heckrath et al.*, 1995; *Maguire and Sims*, 2002] and the degree of soil P saturation (DPS) [*Beauchemin and Simard*, 1999; *Hooda et al.*, 2000] have been proposed to predict the risk of P mobilization via subsurface transport.

Soil test P, such as Olsen P, Mehlich-3 P, and Bray-P1, have been used as indicators of P availability to crops and for transport. *Heckrath et al.* [1995] reported good agreement between extractable soil P and P-leaching. For example, the P concentration in tile drainflow was significantly enhanced when the STP levels increased above 60 mg Olsen P/kg [*Hesketh and Brookes*, 2000]. The use of soluble and easily desorbable P in deionized water or in diluted salt solutions have also been proposed as environmental soil tests [*Hooda et al.*, 2000; *McDowell et al.*, 2001a]. For instance, extractable P in

0.01 M $CaCl_2$ and water soluble P have been well related to P leaching [*Hesketh and Brookes,* 2000*; McDowell and Sharpley,* 2001]. The use of STP as an environmental indicator is promising because the analyses are extensively used in agriculture. However, because the STP are site specific, they are not easily extrapolated to a different type of soil [*Pautler and Sims,* 2000].

On the other hand, DPS is calculated as the ratio between the actual P sorbed and an estimate of the P sorption capacity of the soil (PSC) [*Beauchemin and Simard,* 1999]. In the Netherlands, DPS is obtained as the ratio between P extracted with ammonium oxalate and the sum of the concentration of Al and Fe determined in the same extract (DPS_{ox}) [*van der Zee and van Riemsdijk,* 1988*; Breeuwsma et al.,* 1995]. A critical value of DPS_{ox}>25%, has been postulated as a critical level above which increased risk of P loss occurs in a range of agricultural soils [*Breeuwsma et al.,* 1995].

Even though, the use of DPS_{ox} has been applied successfully in sandy soils, this indicator fails in calcareous soils due to precipitation reactions between calcium and the oxalate used in the extracting solution [*McDowell et al.,* 2002a]. In highly manure-impacted soils, Fe and Al form binary complexes with the dissolved organic matter. Consequently, the PSC of the soil is overestimated and the value of DPS_{ox} is underestimated [*Sanchez and Uehara,* 1980].

The DPS has also been calculated as the ratio between STP such as Mechlich–1 and the Langmuir P sorption maximum (q_m) and related to the potential for P loss via leaching [*Pautler and Sims,* 2000]. In this case, P extracted by the Mechlich–1

method corresponds to the actual sorbed P, and q_m represents the PSC [*Beauchemin and Simard,* 1999]. However, as stated before, the indicators based on STP are site-specific and may not be easily generalized.

Recently, a more general approach (Equation 4.1) has been proposed using the sorption strength constant (k) from the Langmuir isotherm [*McDowell et al.,* 2002a]. The indicator ($\tilde{k}$) corresponds to the slope of the sorption isotherm curve evaluated at c_0, which is the equilibrium P concentration in solution, obtained when no P is added to the original solution. This point accounts for P desorption in highly P-impacted soils.

$$\tilde{k} = \frac{k}{(1 + kc_0)^2} \tag{4.1}$$

A value of $\tilde{k}$ lower than 0.07 (L/mg) was found to be a threshold level where the P movement in subsurface flow was significantly enhanced [*McDowell et al.,* 2002a]. This is a meaningful indicator that gives valuable information related to the potential for P leaching. However, its use is limited because the determination of k in Equation 4.1 requires that a complete sorption isotherm be obtained [*McDowell et al.,* 2002a].

Because sorption isotherms are linear in the lower range of P concentrations [*Hartikainen,* 1991] and c_0 lies in this range, the use of a complete sorption isotherm to obtain an estimate of the sorption strength in this region of the curve is unnecessary. The objectives of this study were to: (i) obtain an estimate of the P sorption strength without obtaining a complete sorption isotherm; (ii) determine threshold levels of the indicator above which the P mobility may be enhanced; and (iii) provide

a practical methodology to implement the indicator. This study provides theory to test the proposed indicator using data of selected soil samples collected from highly manure-impacted soils in northwestern Washington State.

4.3 Materials and Methods

4.3.1 Theory

Quantity/Intensity plots have been used as a simple methodology to describe the relationships between P in solution (intensity, I) and P sorbed onto the solid phase (quantity, Q) [*Hartikainen,* 1991]. These curves are obtained by reacting a known mass of soil with P solutions of different concentrations at constant temperature. At equilibrium, the decrease in the original P concentration is measured and assumed to be the amount of P sorbed onto the solid phase. The Q/I graphs are obtained by plotting the amount of P sorbed against the P remaining in solution [*Barrow,* 1978]. The first point of the Q/I plot (c_0) is obtained when no P is added to the original solution and its value is close to zero only in soils that are not heavily manured or fertilized with P.

In Q/I plots, the intercept of the curve with the abscissa is termed the equilibrium P concentration at zero sorption (c_e) and the intercept with the ordinate corresponds to the amount of instantly desorbable P (q_i) [*Taylor and Kunishi,* 1971*; Sims and Wolf,* 1994*; Zhou and Li,* 2001]. The parameter c_e denotes the concentration of P

in solution, at the point where no net P sorption or desorption occurs [*Taylor and Kunishi,* 1971]. This parameter has been widely recognized as a meaningful indicator to estimate the potential for a given soil to release P to water [*House and Denison,* 2000*; Yli-Halla et al.,* 2002]. The parameter q_i represents the potentially desorbable P [*Hartikainen,* 1991]. This parameter has been significantly related to the P loss in subsurface flow [*McDowell et al.,* 2001b]. Finally, the slope of the curve describes the sorption strength of the soil [*Hartikainen,* 1991].

Modeling the Q/I relationships

During sorption experiments conducted with highly P-impacted soils, desorption of P commonly occurs and has to be accounted for [*Scheinost and Schwertmann,* 1995]. Adsorption–desorption data from batch experiments can be treated according to the following mass balance [*House and Denison,* 2000]:

$$q_i + \frac{1}{m_s}[v_i c_i + m_p] = f(c) + \frac{c}{m_s}(V + v_i) \tag{4.2}$$

where, q_i is in mg/kg, m_s is the mass of soil used in the experiment (kg), v_i is the initial water volume (L) of the sample, c_i and c (mg/L) are the initial and final P contents in solution, respectively, m_p is the mass of P that has been added during the experiment (mg), $f(c)$ is a function describing the P sorbed after equilibration, and V is the volume of the solution (L) used for the sorption experiment. Because the soil is air dried before the experiment, the terms c_i and v_i can be neglected and the following

expression for the net P sorption (Δq) is obtained:

$$\Delta q = f(c) - q_i = \frac{1}{m_s}[m_p - cV] \tag{4.3}$$

Using the Langmuir model as $f(c)$ in Equation 4.3, yields:

$$\Delta q = \frac{kcq_{\mathrm{m}}}{1 + kc} - q_i \tag{4.4}$$

where k is the Langmuir sorption strength constant and q_m is the P sorption maxima. Dividing Equation 4.4 by q_i, a dimensionless expression is obtained

$$\frac{\Delta q}{q_i} = \frac{1}{q_i}\frac{kcq_{\mathrm{m}}}{(1 + kc)} - 1 \tag{4.5}$$

An expression for the parameter q_i can be obtained from Equation 4.4 when $\Delta q = 0$ and $c = c_e$.

$$q_i = \frac{kc_e q_m}{1 + kc_e} \mapsto c_e = \frac{q_i}{k(q_m - q_i)} \tag{4.6}$$

Combining Equations 4.5 and 4.6, q_m is eliminated and Equation 4.7 is suitable to model adsorption–desorption curves in Q/I plots (Figure 4.1).

$$\frac{\Delta q}{q_i} = \frac{c}{c_e}\frac{(1 + kc_e)}{(1 + kc)} - 1 \tag{4.7}$$

Parameters k, q_m, and q_i in Equation 4.4 were estimated by non-linear regression analysis using soil samples collected from five different fields as described below. The values of c_e were obtaining by solving Equation 4.6.

Obtaining the estimate of sorption strength

Differentiating Equation 4.7 with respect to c we obtain the slope of the sorption curve for the complete sorption isotherm. This expression is evaluated at c_0 as suggested by

McDowell et al. [2002a]:

$$\left[\frac{d(\frac{\Delta q}{q_i})}{dc}\right]_{c_0} = \frac{1 + kc_e}{c_e(1 + kc_0)^2} \tag{4.8}$$

Hence, the slope at c_0 is obtained in [L/mg] as an estimate of the sorption strength, similar to that proposed by *McDowell et al.* [2002a]; however, this still requires the development of a complete sorption isotherm to obtain k. Thus, following the same procedure, an alternative way to calculate the value of the slope is provided.

At low ranges of equilibrium P concentration, P sorption isotherms approximate to a linear function and can be described by the least squares model (Equation 4.9) (Figure 4.2) [*Koski-Vähälä and Hartikainen,* 2001].

$$\bar{q} = s\bar{c} + \bar{q}_i \mapsto \frac{\bar{q}}{\bar{q}_i} = \frac{s\bar{c}}{\bar{q}_i} + 1 \tag{4.9}$$

Where $\bar{q}$ is the sorbed or desorbed P, $\bar{q}_i$ is the instantaneously labile P determined linearly, $\bar{c}$ is the equilibrium P concentration, and s the linear sorption coefficient. Because, c_0 values lie in the lower range of the isotherm, it is expected that the slope calculated with the least squares fit model be similar to that calculated using Equation 4.8. Following the same methodology, Equation 4.9 is differentiated and the linear slope is obtained (L/mg).

$$\frac{d(\frac{\bar{q}}{\bar{q}_i})}{d\bar{c}} = \frac{s}{\bar{q}_i} \tag{4.10}$$

In analogy to the procedure to obtain q_i in Equation 4.6, this parameter is calculated from Equation 4.9 when $\bar{q} = 0$ and $c = \bar{c_e}$.

$$\bar{q}_i = s\bar{c_e} \tag{4.11}$$

Combining Equation 4.10 and Equation 4.11, the estimate of the sorption strength (indicator) is obtained. The inverse of the equilibrium P concentration at zero sorption (c_e), corresponds, in this study, to the proposed indicator as a predictor of risk of P leaching.

$$\frac{d(\frac{\bar{q}}{\bar{q}_i})}{dc} = \frac{1}{\bar{c_e}} \tag{4.12}$$

This is important because c_e has been recognized as an important parameter related to P desorption that describes the point where neither sorption nor desorption occurs. However, this study demonstrated that c_e is also a valid estimate of the sorption strength of the soil.

Methodology to Obtain $\bar{c_e}$

The indicator $1/\bar{c_e}$ was obtained using two approaches: (a) selecting two points of the linear isotherm (Equation 4.11), and (b) using Water-desorbable P (P_w).

Again, using the assumption that the isotherm is linear in the low P concentration range (0-10 mg/L), two points of the of the linear part of the isotherm were used to calculate the parameter $\bar{c_e}$ using Equation 4.13 (Figure 4.2).

$$\bar{c_e} = \frac{\bar{q_i}}{s} = c_0 - q_0 \frac{(c_1 - c_0)}{(q_1 - q_0)} \tag{4.13}$$

Finally, the indicator $1/\bar{c_e}$ is obtained:

$$\frac{1}{\bar{c_e}} = \frac{(q_0 - q_1)}{(q_0 c_1 - c_0 q_1)} \tag{4.14}$$

Where q_0 and q_1 are the amounts of sorbed P (mg/kg) that yield a solution concentration of c_0 and c_1 (mg/L) in a 0.01 M KCl extract solution (soil/solution ratio of 1:25

(w/v)) with original P concentrations of 0 and 5 mg/L of P added, respectively. Because there is evidence that the soil/solution ratio and the ionic strength have an effect on the P sorption in batch experiments [*Koopmans et al.,* 2002], a standard protocol for the determination of Q/I plots has to be adopted. We suggest the methodology proposed by Nair *et al.* [*Nair et al.,* 1984] as appropriate for the purpose of this paper.

For the purpose of simplifying the determination of c_e, we evaluate P_w as a predictor of c_e. Experimental details of the methodology of P_w determination are given in section 4.3.3 (Soil Analyses). Values of P_w were regressed against the c_e obtained from a complete sorption isotherm.

4.3.2 Sites and soils sampling

The sampling area is located in the western part of Washington State, focussing in those areas where dairy farming is a major activity. A total of five soils located in Whatcom, Skagit, and King counties constitute the physical basis of this work. The basic criteria were to choose fields that are under permanent pasture, are artificially drained using tiles and open ditches, and have received long-term dairy manure inputs.

Soil samples were collected by using an auger soil probe at two depths on August 2002 (0 - 30 cm and 30 - 60 cm). A stratified random sampling design was adopted in all sampling sites [*Webster and Oliver,* 1990]. Each site of about 5-7 ha was divided in five blocks and 10 sub-samples were taken randomly in each block. In each block, the sub-samples were lumped together to give a representative sample. At the end, five

composed samples (one from each block) were obtained for each surveyed site and for each depth. Composite soil samples were air-dried, ground, and sieved to pass through a $<$ 2-mm sieve before analysis.

4.3.3 Soil Analyses

Soil solution pH was determined with air-dried samples using the solution extracted from a 1:2 (w/v) soil:deionized water mixture. Total organic carbon (TOC) and total nitrogen (TON) were determined by combusting in a Leco FP2000 Nitrogen and Carbon Analyser, on air-dried samples ground to pass a 0.147 mm sieve.

Plant available P was measured in sub-samples with the Bray and Kurtz P-1 (Bray-P1) method. The Bray-P1 method (0.025 M HCl in 0.03 M NH_4F) was conducted according to standard procedures [*Kuo,* 1996]. The concentration of P in solution (P_s) was measured by shaking the soil sample with nano-pure water at a soil/solution ratio of 1:5 (w/v) for 15 min, equilibrating for 60 min, and then shaking again for a further 5 min [*Indiati and Sharpley,* 1998]. The determination of water-desorbable P (P_w) was determined by shaking soils with nano-pure water at a soil/solution ratio of 1:10 (w/v) and equilibrating for 60 min [*Kuo,* 1996]. Calcium-chloride-extractable P (P_{CaCl_2}) was obtained in a 1:10 ratio of soil to 0.01 M $CaCl_2$ with 60 min reaction time [*Kuo,* 1996].

Oxalate-extractable soil iron (Fe_{ox}), aluminum (Al_{ox}), and phosphorus (P_{ox}) were determined by the acid ammonium oxalate method [*Loeppert and Inskeep,* 1996]. In the extracts, Fe_{ox} and Al_{ox} were analyzed by atomic absorption spectrophotometry

(AAS) and oxalate extractable P (P_{ox}) was measured colorimetrically [*Wolf and Baker,* 1990].

All the extracts were filtered through a 0.45 μm cellulose-nitrate-acetate (CNA) membrane [*Haygarth and Sharpley,* 2000], and the phosphorus concentrations in the extracts were determined colorimetrically in the filtered solutions by the ammonium molybdate-blue method [*Kuo,* 1996]. All the procedures and extractions were performed at room temperature ($\approx 20 - 25°C$).

4.3.4 P sorption studies

A total of fifty samples corresponding to five soils, two depths, and 5 replications for each soil, were used in the P sorption studies. The standard procedure proposed by Nair and others was adopted [*Nair et al.,* 1984].

Phosphate sorption isotherms were obtained by equilibrating 1 g of an air-dried, $<$ 2-mm sieved soil with 25 mL of 0.01 M KCl P-free solution containing six levels of P (0, 0.01, 0.1, 5, 10 and 25 mg/L) as KH_2PO_4, in 50 mL centrifuge tubes. The tubes were placed horizontally on a mechanical shaker at 180 excursions per minute (epm) for a 24 h equilibration period. At the end of the equilibration time the soil samples were centrifuged for 10 min and the supernatant filtered through 0.45 μm CNA filter membrane. The filtrates were analyzed immediately and the P concentration was determined colorimetrically by the molybdate-blue method [*Murphy and Riley,* 1962]. Because, the soils have been intensively amended with animal manure, 0.01 mL of

chloroform was added to each tube to inhibit microbial activity. The phosphate not recovered in the solution after the equilibration period was assumed retained by the soil.

4.3.5 Kinetics of P desorption

A successive dilution methodology was adopted to study the kinetics of P desorption according to Hooda *et al.* [*Hooda et al.,* 2000]. The P desorption from soil as a function of time was obtained for each soil depth and for five replicates. One gram of soil was equilibrated with 20 mL of nano-pure water in 50 mL centrifuge tubes. Tubes were shaken for different periods of time (2, 10, 30, 120 and 1440 min). After each specific time, tubes were immediately centrifuged and 5 mL of supernatant were extracted and filtered through a 0.45 μm CNA membrane filter and analyzed for P. Thereafter, the remaining sample in the tubes was diluted by adding nano-pure water corresponding to the same volume of solution extracted before (5 mL). The remaining soil in the tubes was air dried and weighed to check for soil losses during the sequential extraction. Soil losses were considered negligible and changes in P concentrations were a function of P desorption rather than soil loss. A total of 50 curves corresponding to the five soils, two depths, and five replicates for each soil site were obtained. Desorption data were fitted using the expanded Elovich equation [*Polyzopoulos et al.,* 1986] (Equation4.15).

$$Q = \frac{1}{b}[\ln(ab) + \ln(t + d)] \tag{4.15}$$

where Q (mg/kg) is the amount of P released at time t (h) and a, b, and d are fitted parameters. And the rate of P desorption k_d (mg/kgh^{-1}) was determined from the slope of the fitted curve evaluated at t = 24 h (Equation 4.16).

$$\frac{dQ}{dt} = k_d(t) = \frac{1}{b}(t + d) \tag{4.16}$$

Twenty four hours was considered more than adequate because most significant P losses occur over a short time [*McDowell et al.*, 2001b].

4.4 Results and Discussion

4.4.1 Soil P status

Means, standard errors and range of selected chemical properties of the five soils included in this work, are given in Table 4.1. The TOC, TON, and soil solution pH were higher in surface soils than the subsoils. The same was true for the pH values. Long-term manure inputs are known to result in increasing soil organic matter content and pH [*Wood and Hattey*, 1995].

The range in plant available P determined by the Bray-P1 method in the sampled soils indicate excessive P build-up. A Bray-P1 value of 20-25 mg/kg is considered optimum for plant growth [*Sims*, 2000]. In this study, values for surface soils are ten times this optimum value. In addition, water-extractable P values were higher in all soils than the 0.2 mg/L adopted as adequate for plant growth [*Fox and Kamprath*, 1970]. The water extracted P (P_w) and P in solution (P_s) in the surface soils were also

higher than this value.

4.4.2 Phosphorus Sorption

Sorption curves showed L-type adsorption [*Giles et al.*, 1974] on all samples. The L-type isotherms were fitted with Equation 4.4 and the parameters k and q_m were determined by nonlinear regression analysis (Table 4.2). The subsoils showed much greater affinity for P (greater k) than the surface soils given the same P solution concentration. Lower P affinity in surface soils may result from organic anion competition for sorption sites and weaker sorption by metal sites in organic matter [*Sanchez and Uehara*, 1980]. Also it could result from a higher initial P in the surface soils as a result of manure application [*Holford et al.*, 1997].

Adsorption–desorption curves did not reach a plateau in the solution P concentration range tested (Figure 4.3). Generally, there was a 0.5-2 times increase in the initial slope (kq_m) for P sorption in the subsoils compared to topsoils. The inverse was true for the Buckley soil due to its higher q_m. A layer of gravelly sand beneath 30 cm depth in the Buckley soil was observed during sampling. It can be thought that this layer may account for the lower affinity for P than in the upper horizon.

The effect of the long–term manure application on sorption parameters of the soils is evident by the lower affinity for P (k) of the surface soils, higher values of TOC and TON, and the high levels of P (q_i, P_w, P_s, STP). These characteristics indicate that the soils under study represent a high risk for P loss and make them adequate for the

purposes of testing the proposed indicator $1/\bar{c_e}$.

4.4.3 Validation and interpretation of $1/\bar{c_e}$

Validation

Figure 4.4 shows that the indicator obtained from a complete sorption isotherm (Equation 4.8) was well correlated (1:1 plot, $R^2 = 0.99$, $p<0.001$) to the indicator calculated using c_e from Equation 4.6. This was expected because the slope of Equation 4.8 at c_0 corresponds to the linear range of the isotherm.

In a similar way, a good agreement was obtained (1:1 plot, $R^2 = 0.98$, $p<0.001$) between values of the sorption curve at c_0 using Equation 4.8 versus the indicator calculated using two points of the linear isotherm, $1/\bar{c_e}$ (Equation 4.14) (Figure 4.5). This was given by the good relationship found between c_e values calculated using Equation 4.6 and $\bar{c_e}$ obtained from Equation 4.13.

Regression analyses indicated that Pw and c_e from Equation 4.6 were also well correlated (1:1 plot, $R^2 = 0.99$, $p<0.001$) (Figure 4.6). This suggests that P extracted by water (P_w) was in equilibrium with the P originally sorbed by the soils [*Siemens et al.*, 2004] and can be used to approximate the value of c_e, using only a single soil analysis.

These results demonstrate that the proposed indicator $1/c_e$ is a valid alternative to estimate sorption strength using a complete sorption isotherm. Additionally, the data showed that the inverse of P_w is also an indicator of $1/c_e$.

Interpretation of $1/c_e$

The interaction of the parameters k, q_i and c_e determine the shape of the sorption/desorption curves. In order to interpret the concept of $1/c_e$ as an indicator of potential P leaching, three cases were studied. Values of $1/c_e$ were calculated for different combinations of k and q_i, using selected soil samples from this study.

In the first case, $1/c_e$ was compared between two soil samples with the same q_i (Figure 4.7a). A higher value of $1/c_e$ (10.4 L/mg) was obtained for the Skagit soil sample indicating a lower risk of P loss compared to the Briscot sample (2.66 L/mg). The higher value of $1/c_e$ in the Skagit sample can be attributed to its higher affinity parameter k (0.51 versus 0.24 L/mg). The value of P_w for this soil was twice as low as the Briscot sample, confirming its lower risk for P loss. The same can be seen when comparing the values of P_{CaCl_2}. In this case, two soils with the same q_i have different risks for P loss.

The second case consists of two soil samples with the same value of k (Figure 4.7b). In this example, the values of q_i are lower in the Skagit soil sample than those estimated for the Field sample. A lower value of $1/c_e$ (0.6 L/mg) was observed in the Field sample compared to the Skagit sample (1.9 L/mg). The higher values of P_w and P_{CaCl_2} are again in agreement with the lower $1/c_e$ values.

For the third case, $1/c_e$ was calculated for two soil samples with different values of k and q_i (Figure 4.7c). The value of $1/c_e$ was found to be higher for the Briscot than the Field soil sample (5.3 versus 0.56 L/mg). The higher value for the Briscot

soil was due to both its lower q_i and its higher affinity constant, k. The lower value of $1/c_e$ in the Field soil may indicate a higher risk for P transport in this soil. Values of P_w in the Field sample were seven times higher (2 mg/L) than those measured in the Briscot sample (0.27 mg/L). The same trend was observed for the P_{CaCl_2}.

These cases show that if an indicator is based on just one of these parameters (q_i or k), the potential risk for P loss can be biased. In general, it can be expected that a higher k will lower the risk of P loss; however, soil samples with the same k will not necessarily have the same risk. On the other hand, the parameter $1/c_e$ takes both quantity and intensity into account and appears as a reliable predictor of potential P loss.

Additionally, the same soil samples were compared in terms of the kinetics of P desorption. The parameter $1/c_e$ was, as before, negatively related to the rate of P desorption calculated at $t = 24$ h from Equation 4.16. Higher rates of P desorption were related to lower values of $1/c_e$ (Figure 4.8). This is a very important issue in predicting the risk for P loss. *McDowell et al.* [2001b] postulated that short P desorption events (no more than 24 h) are significantly more related to the P loss in subsurface flow than longer events. As shown here, the higher the value of $1/c_e$, the lower the P desorption rate and consequently, the lower the P mobilization into solution.

4.4.4 Determining $1/\bar{c_e}$ threshold levels

The risk for P loss in similar studies has been analyzed by defining threshold levels above or below which the P desorbability parameters increase significantly [*McDowell and Sharpley*, 2001]. The $1/c_e$ values were calculated in all of the soil samples using Equation 4.14 and regressed against P_w, P_s, P_{CaCl_2} and k_d, as parameters directly related to the P loss in subsurface flow [*Hooda et al.*, 2000; *Hesketh and Brookes*, 2000]. The curves were plotted using $1/c_e$ on the x axis and the desorbability parameter on the y axis. The curves were generally concave and fitted by a power model using nonlinear regression analysis (Figure 4.9). As suggested by *McDowell and Sharpley* [2001], a change point was estimated for each relationship using a segmented model (split line) [*Schabenberger and Pierce*, 2002].

$$m = f_1(\frac{1}{c_e} <= a_1) + f_2(\frac{1}{c_e} > a_1) \tag{4.17}$$

$$f_1 = b_0 + b_1 * (\frac{1}{c_e}) \tag{4.18}$$

$$f_2 = b_0 + b_1 * a_1 + b_2 * (\frac{1}{c_e} - a_1) \tag{4.19}$$

The model (m) describes two straight lines separated by the change point (a_1). The value of b_0 is the intercept and parameters b_1 and b_2 are the slopes of the straight line below and above the change point, respectively. Non–linear regression analysis was used to estimate the parameters b_0, b_1, b_2, and a_1 using the option *proc nlin* in SAS®.

The P desorption parameters increase as the indicator $1/c_e$ decreases. A change

point was evident in the curves and significantly determined ($p<0.001$) by the model. The selected P desorption parameters increased below the change point at ca. 0.71 L/mg indicating that enhanced P loss can occur from those soil samples. In a recent study, *Siemens et al.* [2004] used the indicator developed by *McDowell et al.* [2002a] to estimate $MRP_{<0.45}$ in drainage water and groundwater. These authors obtained a change point of 0.7 L/mg below which the $MRP_{<0.45}$ was enhanced substantially. These findings are in agreement with the threshold levels found in this study using $1/c_e$.

4.4.5 Evaluating $1/c_e$ with P concentration in tile drainage water

Independently from this study, another research team selected the same soils to monitor $MRP_{<0.45}$ in water samples from tile drains. The $1/c_e$ indicator calculated for the two soil depths using Equation 4.14 was compared with the concentration of $MRP_{<0.45}$ measured in that study (data courtesy of Joseph Harrison, Washington State University, Puyallup). Figure 4.10 shows that the higher the values of $1/c_e$, the lower the $MRP_{<0.45}$ concentration found in the water samples collected from the drain outflow. This is in agreement with the relationship found using the desorbability parameters.

In summary, given the high loads of P in manure, not all soils have the same potential risk to lose P by leaching. These results indicate that $1/c_e$ is able to reflect this characteristic. As the P input increases, the risk for P loss increases due to the

saturation of P sorption sites. As the P sites become saturated with P, the affinity of the soil to sorb more P decreases as indicated by the decrease in the affinity constant k. This means that the slope of the sorption curve at the lower P concentration range decreases, intersecting the x axis at higher values, and giving lower values of $1/c_e$. Because $1/c_e$ is an independent estimate of this slope, the risk for P leaching is predicted/estimated.

4.5 Conclusions

Theory and data from highly P-impacted soils show that the indicator $1/c_e$ is a valid estimate of the P sorption strength. The indicator can be obtained without developing a complete sorption isotherm, which allows its implementation in a routine soil analysis. In addition, $1/c_e$ can be reasonably approximated by $1/P_w$, simplifying even more its application. The indicator $1/c_e$ is not site specific which makes it superior to STP used as a P leaching indicators. The method to obtain $1/c_e$ is simpler than the oxalate extraction used to obtain DPS_{ox}. The $1/c_e$ indicator can be used in highly manured soils. The DPS_{ox} fails in organic soils and in calcareous soils as well.

Regression analysis between $1/c_e$ and desorbability parameters allowed us to determine a change point below which these parameters increased significantly. The $1/c_e$ values were also related to measured $\mathrm{MRP}_{<0.45}$ in drainage waters. The obtained change point represents a point below which the selected P desorbability parameters increase in a higher rate and may be applied to any soil and management regime.

This study shows that $1/c_e$ is a promising method that deserves further evaluation in different studies, such as lysimeter and field experiments. These studies, together with the definition of political environmental P limits, could be used to describe values of $1/c_e$ indicating low, medium or high risk of P leaching. The simple method provided to obtain $1/c_e$, makes this indicator a valid alternative to estimate the risk for P loss in agricultural soils.

4.6 Tables and Figures

Table 4.1: Mean (standard error) values of chemical and physical soil properties for the soils under study.

	Pangborn muck		Briscot		Skagit		Field		Buckley	
Soil Property	0-30 cm	30-60 cm	0-30 cm	30-60 cm	0-30 cm	30-60 cm	0-30 cm	30-60 cm	0-30 cm	30-60 cm
pH in water	5.1(0.1)	4.8 (0.05)	6.3(0.13)	6.3(0.15)	6.5 (0.05)	6.0 (0.1)	6.1 (0.09)	6.1 (0.08)	6.34(0.07)	6.15(0.05)
Total C %	27.9 (0.72)	27.7 (2.25)	1.8 (0.09)	1.1 (0.1)	2.5 (0.07)	1.2 (0.17)	1.9 (0.14)	0.6 (0.1)	7.8 (0.39)	2.2 (0.15)
Total N %	2.13 (0.038)	1.68 (0.115)	0.13 (0.006)	0.08 (0.006)	0.21 (0.007)	0.09 (0.013)	0.16 (0.014)	0.04 (0.07)	0.73 (0.033)	0.19 (0.013)
Bray-P1 (mg/kg)	346.6 (15)	223.9 (25)	123.6 (23)	32.4 (6)	182.1 (25)	69.2 (11)	359.3 (55)	58.3 (24)	264.4 (32)	93.5 (6)
P_{ox} (mmol/kg)	55.6 (10.3)	35.3 (5.7)	28.9 (2.4)	24.0 (4.0)	60.1 (1.6)	45.0 (5.1)	41.2 (3.6)	20.8 (2.5)	59.9 (8.3)	10.0 (2.1)
Al_{ox} (mmol/kg)	151.2 (8.9)	193.5 (21.7)	60.4 (2.7)	54.1 (1.6)	54.0 (2.5)	44.1 (2.6)	52.9 (3.8)	42.0 (5.5)	197.5 (23.3)	103.1 (6.8)
Fe_{ox} (mmol/kg)	114.9 (7.2)	106.3 (13.1)	100.5 (3.03)	102.8 (2.62)	149.1 (13.2)	164.7 (28.2)	68.3 (5.3)	67.5 (10.8)	96.2 (8.0)	73.6 (4.0)
P_w (mg/L)	5.1 (0.37)	3.5 (0.64)	0.6 (0.17)	0.1(0.006)	1.6 (0.3)	0.6 (0.13)	2.4 (0.5)	0.4 (0.3)	1.9(0.4)	0.3 (0.06)
P_s (mg/L)	3.43 (0.31)	1.83 (0.34)	0.25 (0.04)	0.05 (0.005)	1.12 (0.4)	0.37 (0.14)	1.50 (0.12)	0.05(0.02)	1.01(0.5)	0.15 (0.06)
P_{CaCl_2}(mg/L)	2.33 (0.32)	1.14(0.33)	0.05(0.0094)	0.00(0.000)	0.27 (0.099)	0.06 (0.027)	0.42(0.006)	0.01 (0.003)	0.37 (0.230)	0.03 (0.010))

Table 4.2: Mean (standard error) values of Langmuir sorption parameters determined by nonlinear parameter estimation.

	Pangborn muck		Briscot		Skagit		Field		Buckley	
Sorption Parameter	0-30 cm	30-60 cm	0-30 cm	30-60 cm	0-30 cm	30-60 cm	0-30 cm	30-60 cm	0-30 cm	30-60 cm
q_m (mg/kg)	2168.4(247.3)	2254.3(727.8)	299.4(11.8)	297.6(15.4)	443.1 (12.3)	368.9(32.8)	303.8(15.8)	230.1 (34.1)	739.5 (56.9)	407.8 (17.8)
k (L/mg)	0.06 (0.03)	0.10 (0.05)	0.25 (0.03)	0.54 (0.06)	0.25 (0.04)	0.36 (0.06)	0.31 (0.04)	0.48 (0.11)	0.35 (0.12)	0.51 (0.08)
c_e (mg/L)	5.9 (0.4)	3.7 (1.1)	0.5 (0.2)	0.02 (0.01)	1.2 (0.3)	0.2 (0.1)	1.4 (0.1)	0.4 (0.39)	1.2 (0.4)	0.1(0.03)
q_i	451 (99)	289 (48)	27 (5.2)	3.3 (1.2)	86 (10)	25 (1.4)	92 (23)	11.3 (7.6)	174 (25)	19 (4.6)
kq_m (L/kg)	115.6 (42.5)	164.9 (75.4)	73.7 (10.2)	159.1 (14)	108.6 (16.8)	138.7 (32.7)	104.9 (9.3)	118.8 (37.6)	273.5 (90.3)	212.1(42.7)

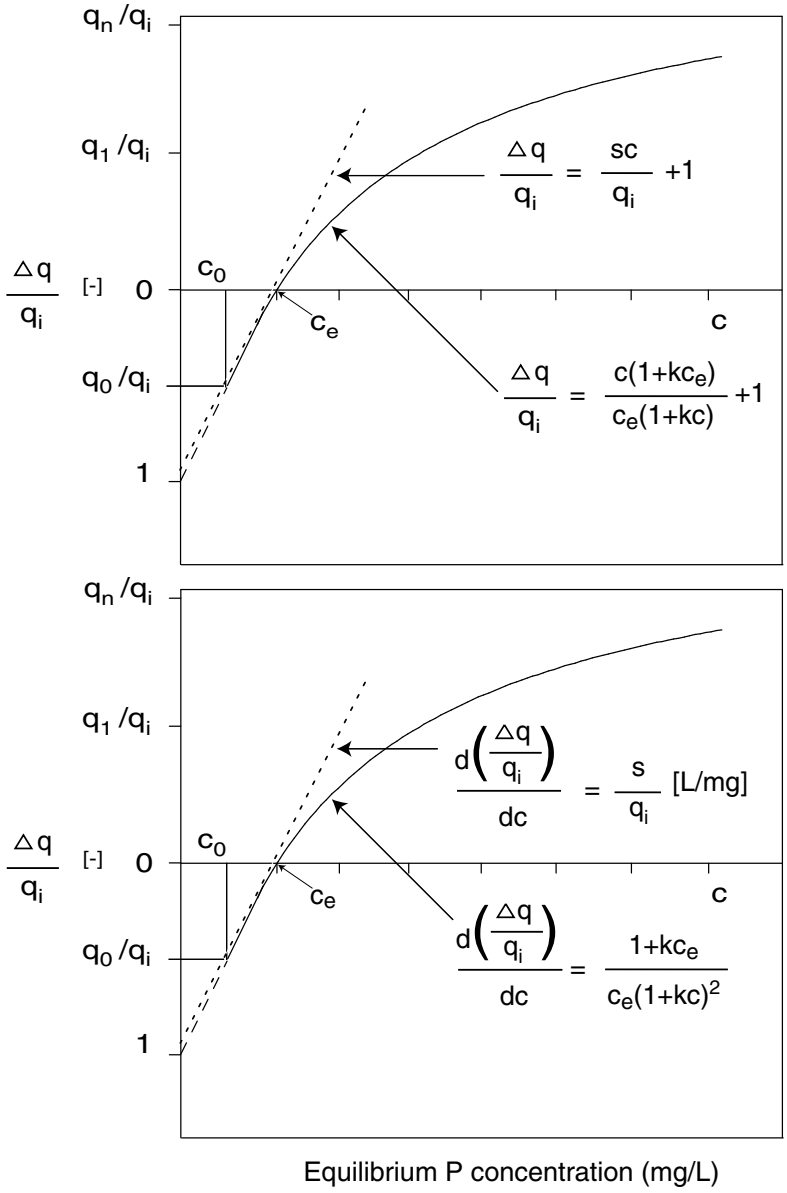

Figure 4.1: Schematic of the Q/I plot showing the modified Langmuir equation used to model adsorption–desorption curves. Schematic describing the least squares model used to describe sorption isotherm at low equilibrium P concentration range. Dashed line represents the least squares model and the solid line corresponds to the original isotherm.

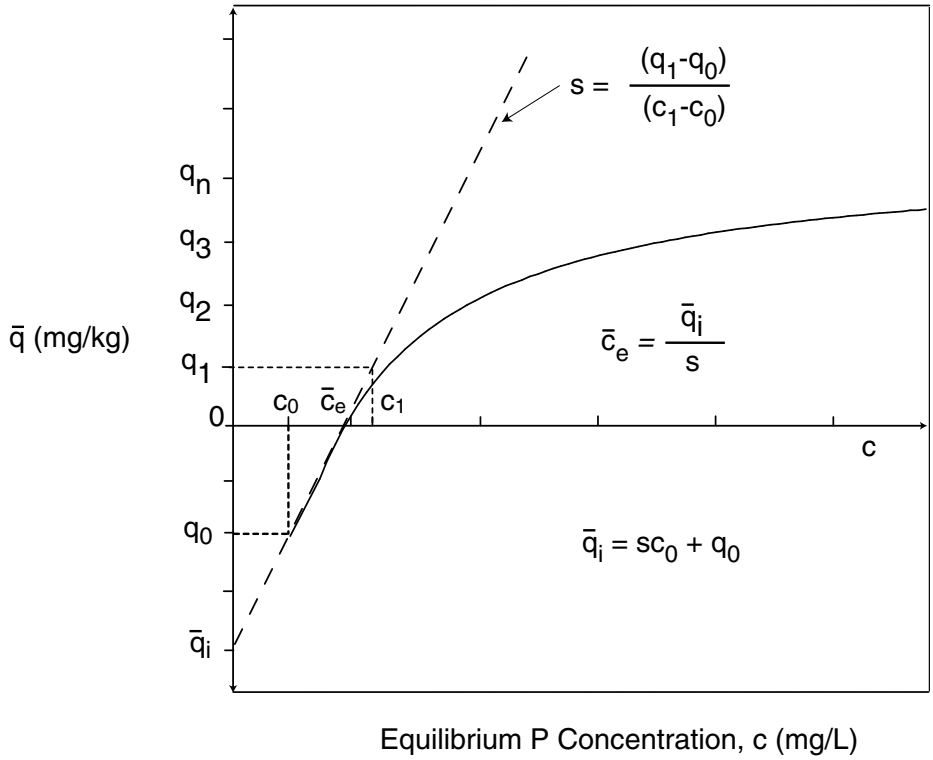

Figure 4.2: ,

[c_1, q_1]).]Schematic describing the use of the least squares model to obtain c_e and q_i using only two points of the isotherm ([c_0, q_0], [c_1, q_1]). Dashed line represents the straight line passing through the two points and the solid line corresponds to the original isotherm.

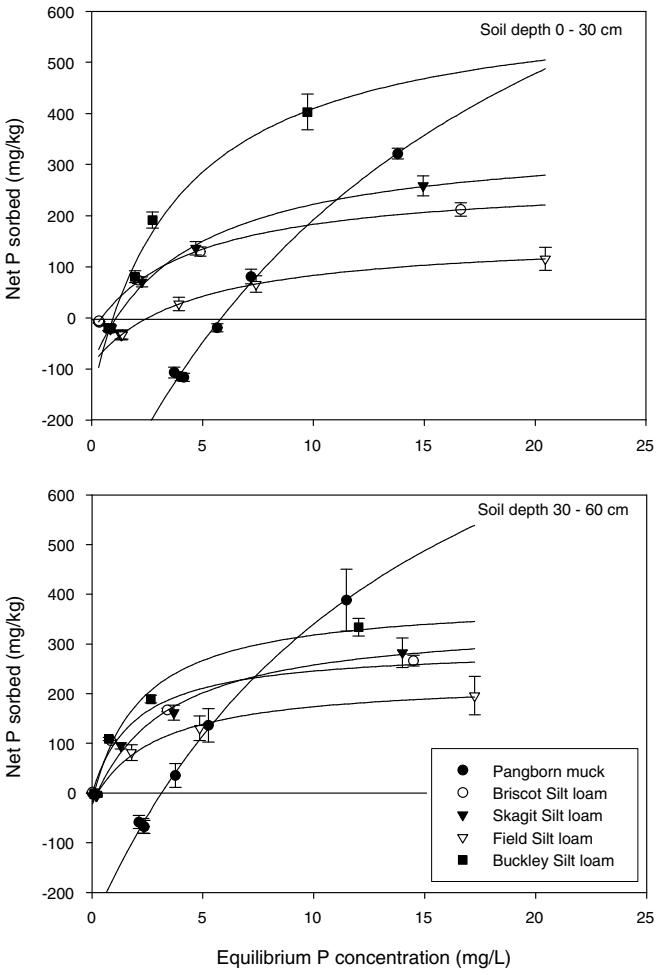

Figure 4.3: P Sorption/desorption plots of top (0-30 cm) and subsoils (30-60 cm) of of five soils in western Washington. The curves represent sorption and desorption data fitted to the modified Langmuir equation (Equation 4.4). Points are a mean of five replications and the vertical error bars on each point indicate the standard error (s.e).

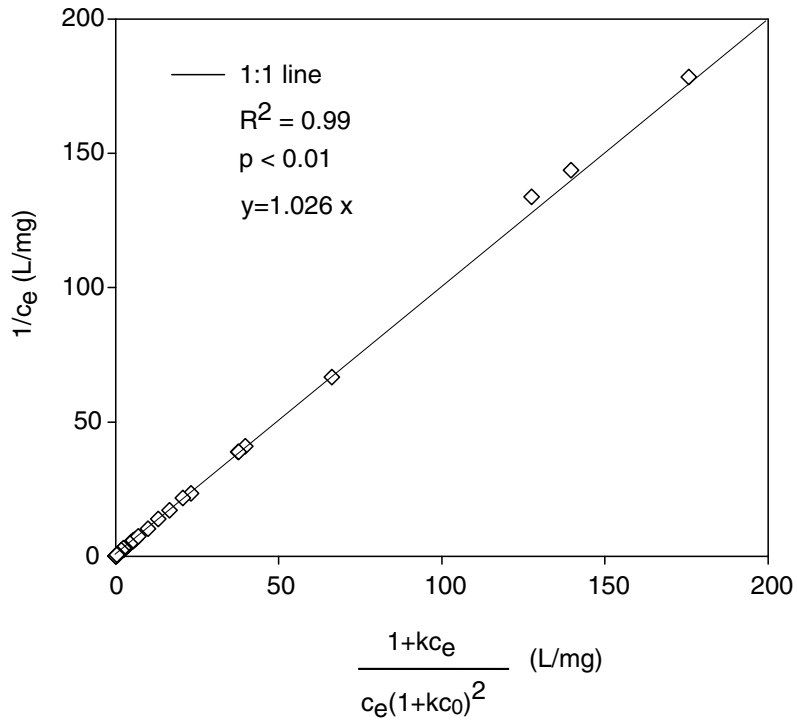

Figure 4.4: Relationship between c_e obtained from a complete sorption isotherm (Equation 4.8) and c_e calculated using Equation 4.6.

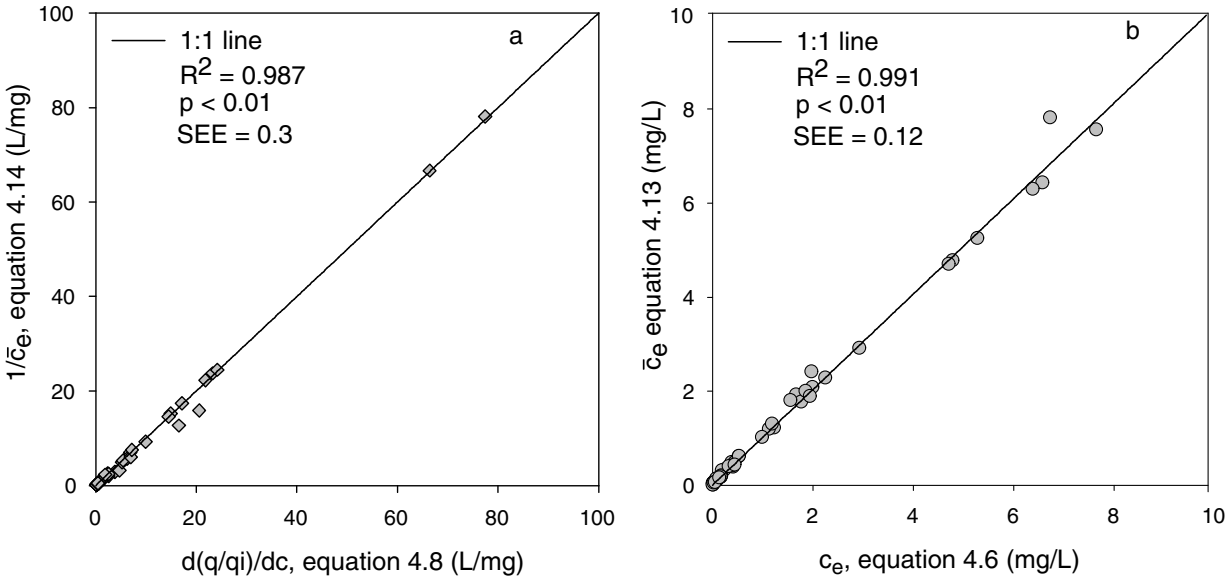

Figure 4.5: Relationship between $1/c_e$ (Equation 4.14) and $d(q/qi)/dc$ obtained from Equation 4.8 (a). Relationship between $\bar{c_e}$ values calculated using Equation 4.13 and c_e from Equation 4.6 (b).

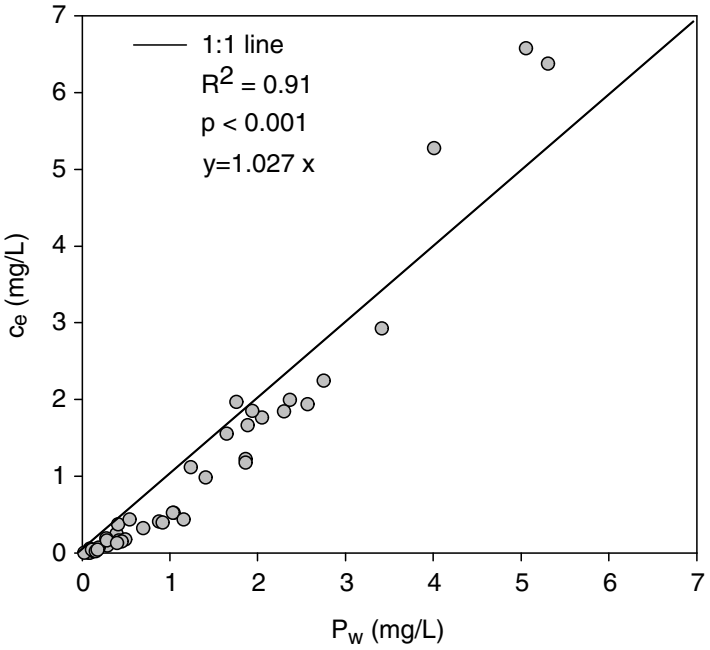

Figure 4.6: Relationship between c_e calculated from Equation 4.6 and P_w.

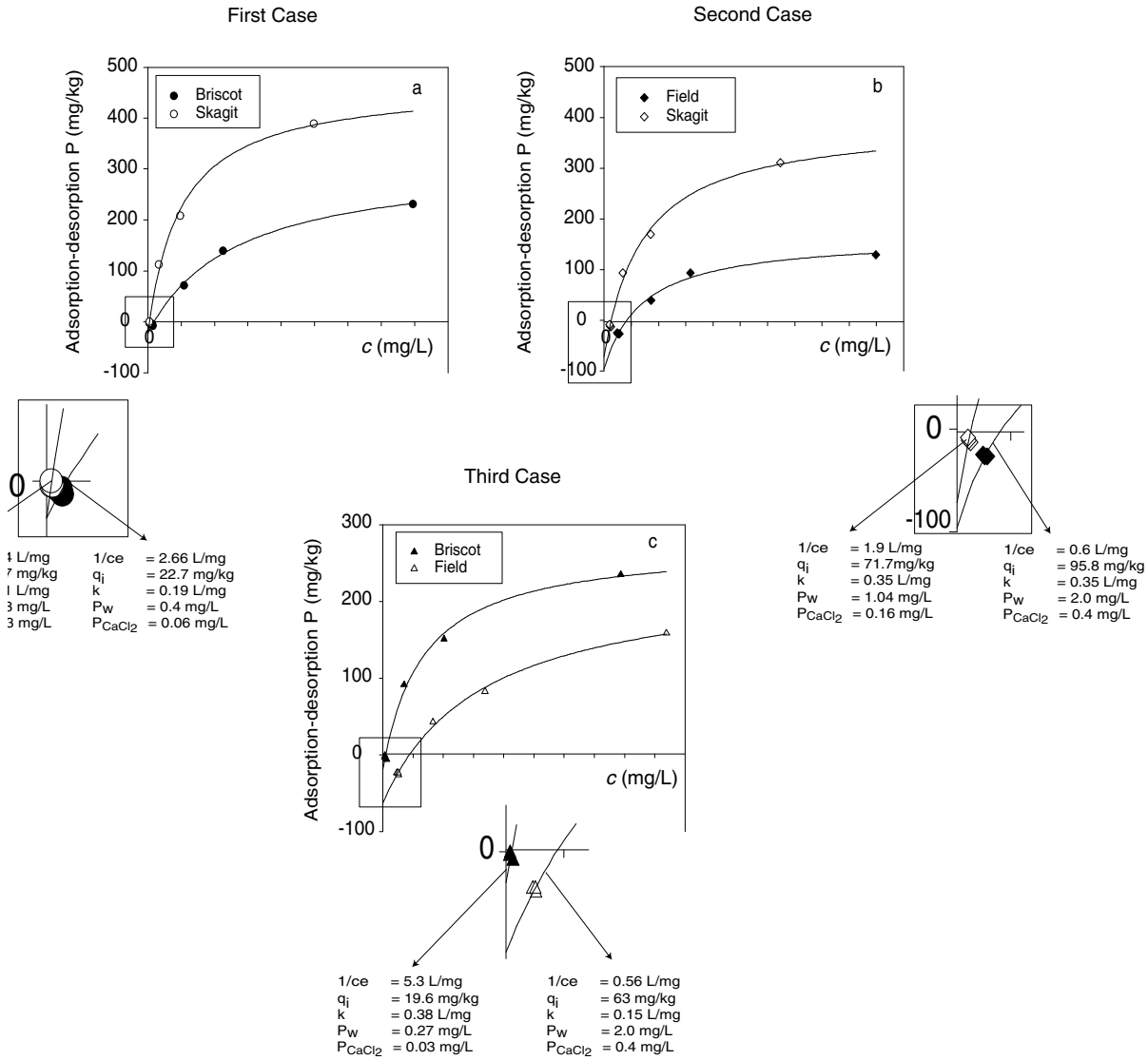

Figure 4.7: Adsorption–desorption curves of selected soil samples with detailed picture of the intercepts. Different combinations of k and q_i (cases) were used to illustrate the concept of $1/c_e$. Two soil samples with the same amount of q_i (a). Two soil samples with same affinity parameter k (b) and two soil samples with different k and q_i (c). Solid lines represent sorption data fitted to Equation 4.4.

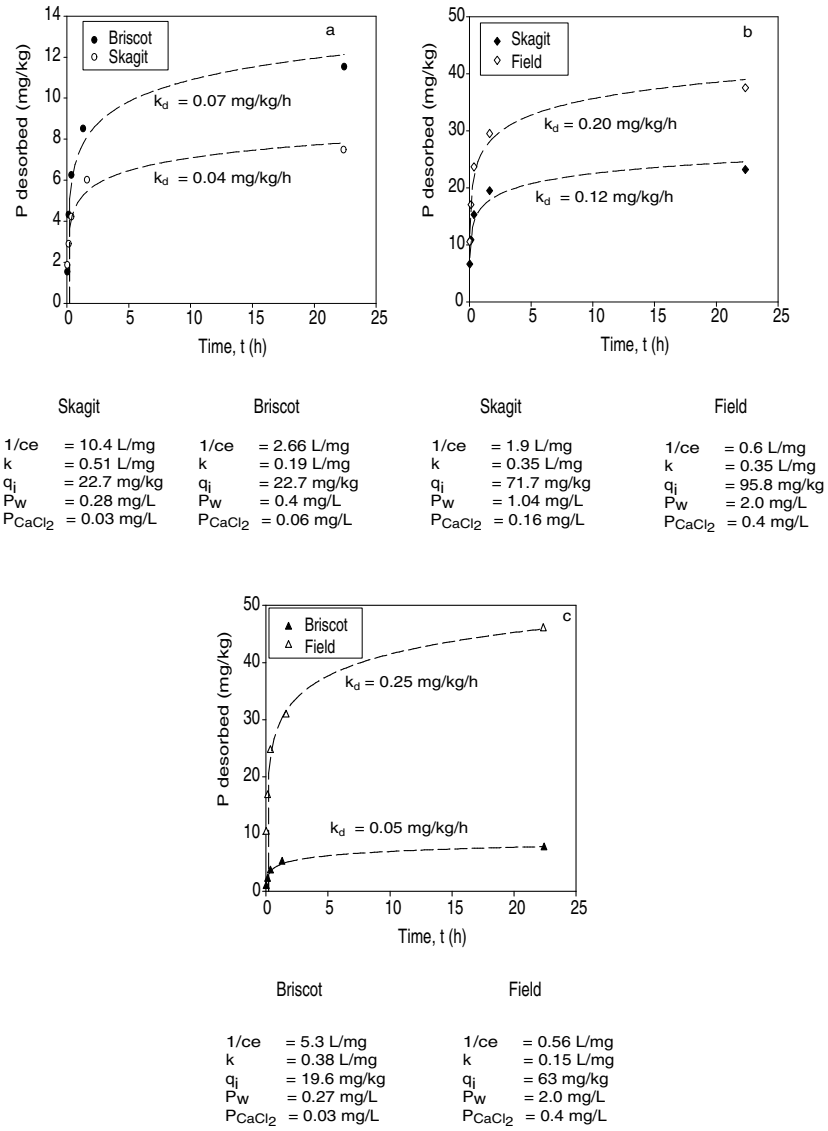

Figure 4.8: Desorption P curves obtained by successive dilution method and the corresponding k_d values. The calculated indicator $1/c_e$ is listed together with the P_w, and P_{CaCl_2} values for each soil sample. Two soil samples with the same amount of q_i (a). Two soil samples with the same affinity parameter k (b) and two soil samples with different k and q_i (c). Solid lines represent desorption data fitted to the expanded Elovich equation.

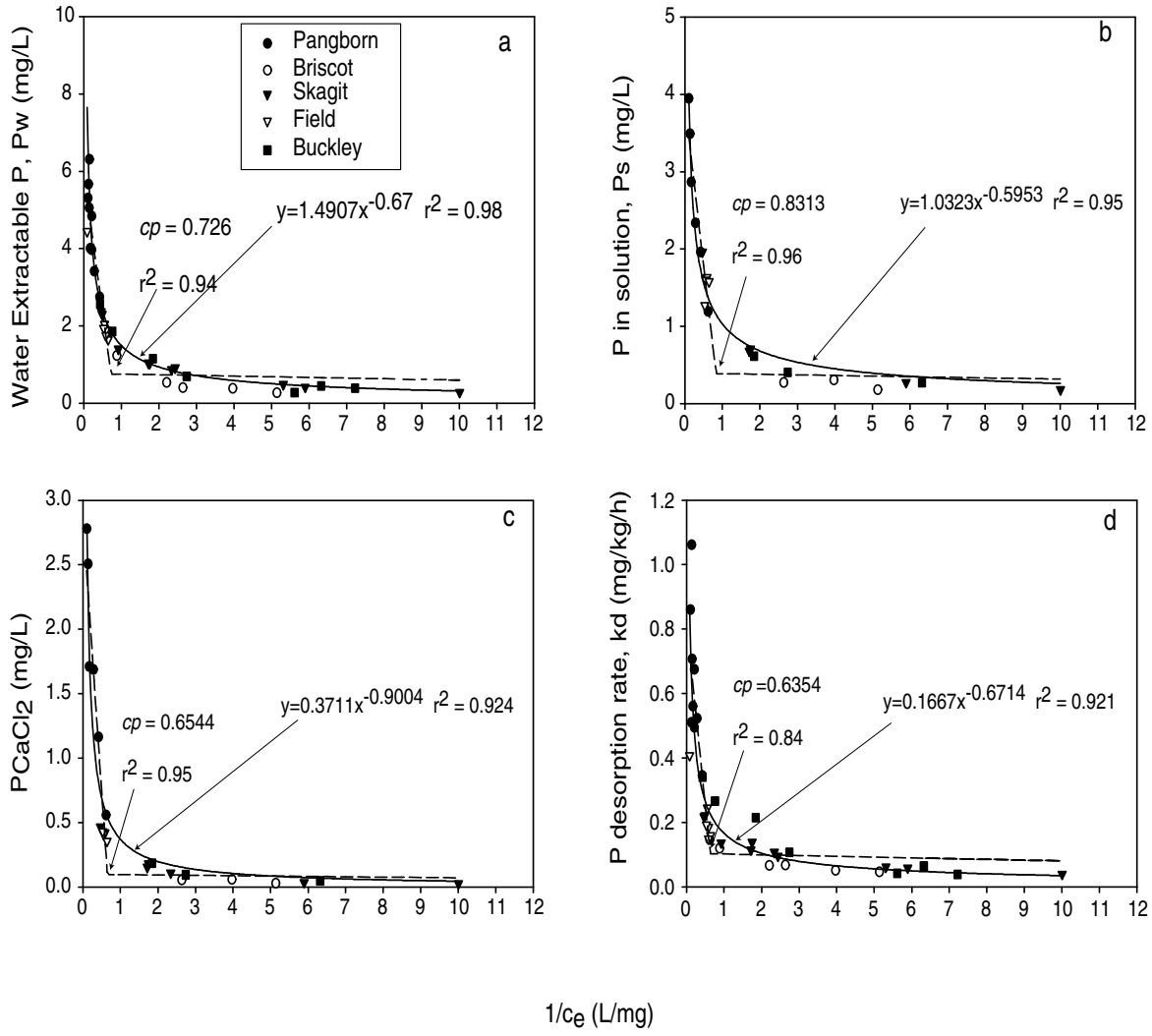

Figure 4.9: Relationships between $1/c_e$ and P_w (a), P_s (b), $\mathrm{P_{CaCl_2}}$ (c) and k_d (d). The solid line represents fitting of the power model significant at the $p < 0.001$ level. Dashed lines correspond to the fit of the segmented model (Equation 4.17) indicating the change point (cp).

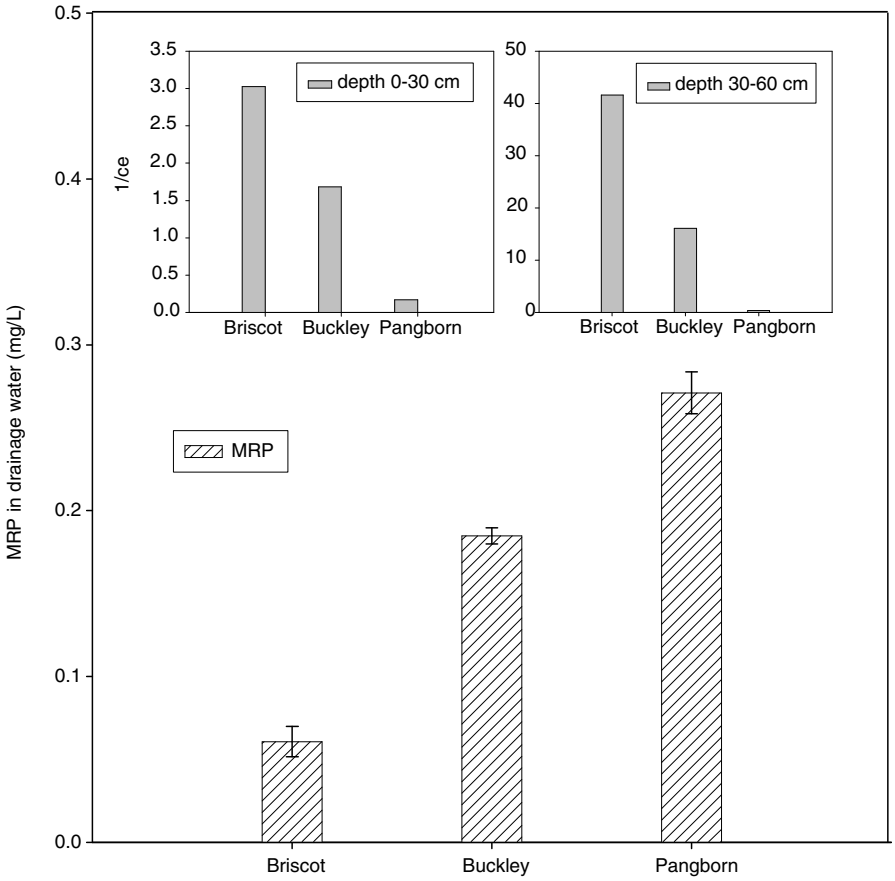

Figure 4.10: Concentration of MRP $_{<0.45}$ in tile drain water and $1/c_e$ values for two depths (0-30 cm and 30-60 cm) of three soils affected by high P inputs. Vertical error bars represent the standard error (s.e.) of the measured MRP$_{<0.45}$.

Chapter 5

Summary and Conclusions

From a field study (Chapter 2), we conclude that, in the pasture system, P lost in tile drainage was associated with reductive dissolution of Fe. A different mechanism led to the P release in the corn field. Cultivation of a soil with elevated DPS levels could favor Fe(III)-DOM complexes and P as a ternary complex with these by (i) stimulating oxidation of Fe or suppressing its reduction; or (ii) enhancing the mineralization of soil organic matter. So that we believe that P and iron were transported as ternary complexes with dissolved organic matter (DOM).

In a column study (Chapter 3), we demonstrated that an initially oxidized system saturated with P and under dynamic flow conditions can mobilize P after reductive dissolution of ferric iron. These results revealed that an initially reduced system presents a high affinity for P due to precipitation reactions, but the system turns unstable after the P concentrations decreased. At the end, a reduced system fixed less P than the oxidized control system. These findings suggest that changes in soil redox potential play an important role in subsurface P transport.

The last study (Chapter 4) provides theory and data to obtain a P leaching indicator in highly P impacted soils. This study demonstrated that the inverse of the equilibrium P concentration at zero sorption ($1/c_e$) is a meaningful estimate of the sorption strength that can be obtained without developing a complete sorption isotherm. It can be accurately calculated using only two points of the linear isotherm and also can be reasonably approximated by using the inverse of water-desorbable P ($1/P_w$). The indicator $1/c_e$ can be implemented in a routine soil analytical procedure and used in any soil type and management to predict/estimate the potential risk for P loss via subsurface flow.

Overall, this research demonstrates that soils with excessive P content and affected by fluctuating water tables may release P and contribute to P enrichment of ground and surface waters. The indicator developed in this study can be useful to estimate the risk of P losses by leaching under these conditions.

Bibliography

Allison, J. D. A., D. S. Brown, and K. J. Novo-Gradac, *MINTEQA2/PRODEFA2. A geochemical assessment model for environmental systems: Version 3 User's Manual*, Report No. EPA/600/3-91/021. 113 pp. U. S. Environmental Protection Agency, USA, 1991.

Anschutz, P., S. Zhong, B. Sundby, A. Mucci, and C. Gobeil, Burial efficiency of phosphorus and the geochemistry of iron in continental margin sediments, *Limnol. Oceanogr.*, *43*, 53–64, 1998.

Barrow, N., The description of phosphate adsorption curves, *J. Soil Sci.*, *29*, 447–462, 1978.

Beauchemin, S., and R. R. Simard, Soil phosphorus saturation degree: Review of some indices and their suitability for P management in Québec, Canada, *Can. J. Soil Sci.*, *79*, 615–625, 1999.

Beauchemin, S., R. Simard, and D. Cluis, Forms and concentrations of phosphorus in drainage water of twenty-seven tile drained soils, *J. Environ. Qual.*, *27*, 721–728,

1998.

Benner, S. G., C. M. Hansel, V. W. Wielinga, T. M. Barber, and S. Fendorf, Reductive dissolution and biomineralization of iron hydroxide under dynamic flow conditions, *Environ. Sci. Technol.*, *36*, 1705–1711, 2002.

Blake, G. R., and K. H. Hartge, Particle density, in *Methods of soil analysis. Part 1. Physical and Mineralogical Methods*, edited by A. Klute, pp. 377–382, American Society of Agronomy, Madison, Wisconsin, 1986.

Borggaard, O. K., The influence of iron oxides on phosphate adsorption by soil, *J. Soil Sci.*, *34*, 333–341, 1983.

Breeuwsma, A., J. G. A. Reijerink, and O. F. Schoumans, Impact of manure on accumulation and leaching of phosphate in areas of intensive livestock farming, in *Animal waste and the land-water interface*, edited by K. Steele, pp. 239–249, CRC/Lewis Publishers, Boca Raton, Florida, 1995.

Brookes, P. C., G. Heckrath, J. De Smet, G. Hofman, and J. Vanderdeelen, Losses of phosphorus in drainage water, in *Phosphorus loss from soil to water*, edited by H. Tunney, O. T. Carton, P. C. Brookes, and A. E. Johnston, pp. 253–271, CAB International, Wallingford, UK, 1997.

Brooks, S. C., D. L. Taylor, and P. M. Jardine, Reactive transport of EDTA–complexed cobalt in the presence of ferrihydrite, *Geochim. Cosmochim. Acta*, *60*, 1899–1908, 1996.

Carey, B. M., *Groundwater, soil, and crop nitrogen at a field where dairy waste is used as fertilizer in Whatcom County*, Washington State Department of Ecology. Publication 04-03-112, Olympia, WA, 2004.

Cox, S., and S. Kahle, *Hydrogeology , Ground-Water Quality , and Sources of Nitrate in Lowland Glacial Aquifers of Whatcom County, Washington and British Columbia, Canada*, US Geological Survey Water-Resources Investigations Report 98-4195, Reston, VI, 1999.

Dolfing, J., W. J. Chardon, and J. Japenga, Association between colloidal iron, aluminum, phosphorus, and humic acids, *Soil Sci.*, *164*, 171–179, 1999.

Fox, R. L., and E. J. Kamprath, Phosphate sorption isotherms for evaluating the phosphate requirements of soils, *Soil. Sci. Soc. Am. Proc.*, *34*, 902–907, 1970.

Frederickson, J. K., J. M. Zachara, D. W. Kennedy, H. Dong, T. C. Onstott, N. W. Hinman, and S. M. Li, Biogenic iron mineralization accompanying the dissimilatory reduction of hydrous ferric oxide by a groundwater bacterium, *Geochim. Cosmochim. Acta*, *62*, 3239–3257, 1998.

Giles, C. H., D. Smith, and A. Huitson, A general treatment and classification of the solute adsorption isotherm. I. Theoretical, *J. Colloid Interface Sci.*, *47*, 755–765, 1974.

Goldberg, S., and G. Sposito, On the mechanism of specific phosphate adsorption by hydroxylated mineral surfaces: A review, *Commun. Soil Sci. Plant. Anal.*, *16*, 801–821, 1985.

Goldin, A., *Soil Survey of Whatcom County Area, Washington*, USDA-SCS, U.S. Governmental Printing Office, Washington D.C., 1992.

Gustavsson, J. P., *Visual MINTEQ*, Department of Land and Water Resources, Royal Institute of Technology, Sweden, accessed July 15, 2000 (http://www.lwr.kth.se/english/OurSoftware/vminteq), 1999.

Hansel, C. M., S. G. Benner, J. Neiss, A. Dohnalkova, R. Kukkadapu, and S. Fendorf, Reactive transport of edta–complexed cobalt in the presence of ferrihydrite, *Geochim. Cosmochim. Acta*, *67*, 2977–2992, 2003.

Hartikainen, H., Potential mobility of accumulated phosphorus in soil as estimated by the indices of Q /I plots and by extractant, *Soil Sci.*, *152*, 204–209, 1991.

Haygarth, P. M., and A. N. Sharpley, Terminology for phosphorus transfer, *J. Environ. Qual.*, *29*, 10–15, 2000.

Haygarth, P. M., and S. C. Jarvis, Transfer of phosphorus from agricultural soils, *Adv. Agron.*, *66*, 195–249, 1999.

Heathwaite, A. L., and R. M. Dils, Characterising phosphorus loss in surface and subsurface hydrological pathways, *Sci. Total Environ.*, *251/252*, 523–538, 2000.

Heckrath, G., P. C. Brookes, P. R. Poulton, and K. W. T. Goulding, Phosphorus leaching from soils containing different phosphorus concentrations in the broadbalk experiment, *J. Environ. Qual.*, *24*, 904–910, 1995.

Hens, M., and R. Merckx, Functional characterization of colloidal phosphorus species in the soil solution of sandy soils, *Environ. Sci. Technol.*, *35*, 493–500, 2001.

Hens, M., and R. Merckx, The role of colloidal particles in the speciation and analysis of "dissolved" phosphorus, *Water Res.*, *36*, 1438–1492, 2002.

Hesketh, N., and P. C. Brookes, Development of an indicator for risk of phosphorus leaching, *J. Environ. Qual.*, *29*, 105–110, 2000.

Holford, I. C. R., C. Hird, and R. Lawrie, Effects of animal effluents on the phosphorus sorption characteristics of soils, *Aust. J. Soil Res.*, *35*, 365–373, 1997.

Hooda, P. S., A. R. Rendell, A. C. Edwards, P. J. A. Withers, M. N. Aitken, and V. W. Truesdale, Relating soil phosphorus indices to potential phosphorus release to water, *J. Environ. Qual.*, *29*, 1166–1171, 2000.

House, W. A., and F. H. Denison, Factors influencing the measurement of equilibrium phosphate concentrations in river sediments, *Wat. Res*, *34*, 1187–1200, 2000.

Hutchison, K. J., and D. Hesterberg, Dissolution of phosphate in a phosphorus-enriched ultisol as affected by microbial reduction, *J. Environ. Qual*, *33*, 1793–1802, 2004.

Ilg, K., J. Siemens, and M. Kaupenjohann, Colloidal and dissolved phosphorus in sandy soils as affected by phosphorus saturation, *J. Environ. Qual.*, *34*, 926–935, 2005.

Indiati, R., and A. N. Sharpley, Changes in soluble and equilibrium phosphate concentration in selected soils from italy, *Commun. Soil Sci. Plant. Anal.*, *29*, 2429–2440, 1998.

Jensen, M. B., H. C. B. Hansen, N. E. Nielsen, and J. Magid, Phosphate leaching from intact soil column in response to reducing conditions, *Water Air Soil Pollut.*, *113*, 411–423, 1999.

Kleinman, P. J. A., B. A. Needelman, A. N. Sharpley, and R. W. McDowell, Using soil phosphorus profile data to assess phosphorus leaching potential in manured soils, *Soil Sci. Soc. Am. J.*, *67*, 215–224, 2003.

Koopmans, G. F., R. W. McDowell, W. J. Chardon, O. Oenema, and J. Dolfing, Soil phosphorus quantity-intensity relationships to predict increased soil phosphorus loss to overland and subsurface flow, *Chemosphere*, *48*, 679–687, 2002.

Koski-Vähälä and H. Hartikainen, Assessment of the risk of phosphorus loading due to resuspended sediment, *J. Environ. Qual.*, *30*, 960–966, 2001.

Kuo, S., Phosphorus, in *Methods of Soil Analysis. Part 3. Chemical Methods*, edited by D. L. Sparks, pp. 869–920, American Society of Agronomy, Madison, Wisconsin, 1996.

Lindsay, W. L., *Chemical Equilibria in Soils*, second ed., John Wiley & Sons, New York, 1979.

Loeppert, R. H., and W. P. Inskeep, Iron, in *Methods of soil analysis. Part 3. Chemical methods*, edited by D. L. Sparks, pp. 639–665, American Society of Agronomy, Madison, Wisconsin, 1996.

Maguire, R., and T. Sims, Soil testing to predict phosphorus leaching, *J. Environ. Qual*, *31*, 1601–1609, 2002.

Manoranjan, V. S., and T. B. Stauffer, Exact solution for contaminant transport with kinetic Langmuir sorption, *Water Resour. Res.*, *32*, 749–752, 1996.

McBride, M. B., *Environmental Chemistry of Soils*, Oxford University Press, New York, 1994.

McDowell, R. W., A. N. Sharpley, and P. Withers, Indicator to predict the movement of phosphorus from soil to subsurface flow, *Environ. Sci. Technol.*, *36*, 1505–1509, 2002a.

McDowell, R. W., A. N. Sharpley, P. Brookes, and P. Poulton, Relationship between soil test phosphorus and phosphorus release to solution, *Soil Sci.*, *166*, 137–149, 2001a.

McDowell, R. W., A. N. Sharpley, P. J. A. Kleinman, and W. J. Gburek, Hydrological source management of pollutants at the soil profile scale, in *Agriculture, Hydrol-*

ogy and Water Quality, edited by P. M. Haygarth, and S. C. Jarvis, pp. 197–220, CAB International, Devon, UK, 2002b.

McDowell, R. W., and A. N. Sharpley, Soil phosphorus fractions in solution: influence of fertilizer and manure, filtration and method of determination, *Chemosphere*, *45*, 737–748, 2001.

McDowell, R. W., S. Sinaj, A. N. Sharpley, and E. Frossard, The use of isotopic echange kinetics to assess phosphorus availability in overland flow and subsurface drainage waters, *Soil Sci.*, *166*, 365–373, 2001b.

Miller, M. H., Contribution of nitrogen and phosphorus to subsurface drainage water from intensively cropped mineral and organic soils in Ontario, *J. Environ. Qual.*, *8*, 42–48, 1979.

Mitchell, R. J., R. S. Babcock, S. Gelinas, L. Nanus, and D. E. Stasney, Nitrate distributions and source identification in the Abbotsford Sumas Aquifer, Northwestern Washington State, *J. Environ. Qual.*, *32*, 789–800, 2003.

Moore, P. A., and K. R. Reddy, Role of Eh and ph on phosphorus geochemistry in sediments of Lake Okeechobee, Florida, *J. Environ. Qual*, *23*, 955–964, 1994.

Murphy, J., and J. P. Riley, A modified single solution method for the determination of phosphate in natural waters, *Anal. Chem. Acta*, *27*, 31–36, 1962.

Nair, P. S., T. J. Logan, A. N. Sharpley, L. E. Sommers, M. A. Tabatabai, and T. L. Yuan, Interlaboratory comparison of a standardized phosphorus adsorption procedure, *J. Environ. Qual.*, *13*, 591–595, 1984.

Novak, J. M., K. C. Stone, A. A. Szogi, D. W. Watts, and M. H. Johnson, Dissolved phosphorus retention and release from a coastal plain in-stream wetland, *J. Environ. Qual.*, *33*, 394–401, 2004.

NRCS *Hydric soils list, Whatcom County area, Washington: Detailed soil map legend [Online]*, U.S. Department of Agriculture., http://www.or.nrcs.usda.gov/pnw_soil/wa_reports.html, Accessed May, 2005, 2005.

Olila, O. G., K. R. Reddy, and D. L. Stites, Influence of draining on soil phosphorus forms and distribution in a constructed wetland, *Ecol. Eng.*, *9*, 157–169, 1997.

Pant, H. K., and K. R. Reddy, Hydrologic influence on stability of organic phosphorus in wetland detritus, *J. Environ. Qual.*, *30*, 668–674, 2001.

Pant, H. K., V. D. Nair, K. R. Reddy, D. A. Graetz, and R. R. Villapando, Influence of flooding on phosphorus mobility in manure-impacted soil, *J. Environ. Qual.*, *31*, 1399–1405, 2002.

Patrick, W. H., and R. A. Khalid, Phosphate release and sorption by soils and sediments: effect of aerobic and anaerobic conditions, *Science*, *186*, 53–55, 1974.

Pautler, M., and J. T. Sims, Relationships between soil test phosphorus, soluble phosphorus, and phosphorus saturation in delaware soils, *Soil. Sci. Soc. Am. J.*, *64*, 765–773, 2000.

Petruzzelli, L., L. Celi, and F. Ajmone-Marsan, Effects of soil organic fractions on iron oxide biodissolution under anaerobic conditions, *Soil Sci.*, *170*, 102–109, 2005.

Polyzopoulos, N. A., V. Z. Keramidas, and A. Pavlatou, On the limitaions of the simplified elovich equation in describing the kinetics of phosphate sorption and release from soils, *J. Soil Sci.*, *37*, 81–87, 1986.

Ponnamperuma, F. N., The chemistry of submerged soils, *Adv. Agron.*, *24*, 29–97, 1972.

Pote, D. H., and T. C. Daniel, Analyzing for dissolved reactive phosphorus in water samples, in *Methods of Phosphorus Analysis for Soils, Sediments, Residuals, and Waters.*, edited by G. M. Pierzynski, pp. 91–93, Southern Cooperative Series Bulletin Nr. 396, Manhattan, KS, 2000.

Quang, V. D., and J. E. Dufey, Phosphate desorption from flooded and reoxidized soils as compared with adsorption characteristics, *Commun. Soil Sci. Plant. Anal.*, *28*, 885–898, 1997.

Roden, E. E., M. M. Urrutia, and C. J. Mann, Bacterial reductive dissolution of crystalline Fe (III) oxide in continuous-flow column reactors, *Appl. Environ. Microbiol.*, *66*, 1062–1065, 2000.

Rowell, D. L., Oxidation and Reduction, in *The chemistry of soil processes*, edited by D. J. Greenland, and M. H. B. Hayes, pp. 401–461, John Wiley & Sons, Belfast, Ireland, 1981.

Sallade, Y. E., and J. T. Sims, Phosphorus transformations in the sediments of Delaware's agricultural drainageways: II. effect of reducing conditions on phosphorus release, *J. Environ. Qual.*, *26*, 1579–1588, 1997.

Sample, E. C., R. J. Soper, and G. J. Racz, Reaction of phosphate fertilizers in soils, in *The role of phosphorus in agriculture*, edited by F. E. Khasawneh, E. C. Sample, and E. J. Kamprath, pp. 263–310, ASA–CSSA–SSSA, Madison, WI, 1980.

Sanchez, P. A., and G. Uehara, Management considerations for acid soils with high phosphorus fixation capacity, in *The role of phosphorus in agriculture*, edited by F. E. Khasawneh, E. C. Sample, and E. J. Kamprath, pp. 471–514, ASA–CSSA–SSSA, Madison, WI, 1980.

Scalenghe, R., A. C. Edwards, F. Ajmone Marsan, and E. Barberis, The effect of reducing conditions on the solubility of phosphorus in a diverse range of European agricultural soils, *Eur. J. Soil Sci.*, *53*, 439–447, 2002.

Schabenberger, O., and F. J. Pierce, *Contemporary statistical models for the plant and soil sciences*, CRC Press LLC, Boca Raton, FL, 2002.

Scheinost, A. C., and U. Schwertmann, Predicting phosphate adsorption–desorption in a soilscape, *Soil Sci. Soc. Am. J.*, *59*, 1575–1580, 1995.

Schwertmann, U., and R. M. Cornell, *Iron oxides in the laboratory. Preparation and characterization*, VCH, Weinheim, 1991.

Shahandeh, H., L. R. Hossner, and F. T. Turner, Phosphorus relationships in flooded rice soils with low extractable phosphorus, *Soil Sci. Soc. Am. J.*, *58*, 1148–1189, 1994.

Sharpley, A. N., S. C. Chapra, R. Wedephohl, J. T. Sims, T. C. Daniel, and K. R. Reddy, Managing agricultural phosphorus for protection of surface waters: Issues and options, *J. Environ. Qual.*, *23*, 437–451, 1994.

Sharpley, A., T. Daniel, T. Sims, J. Lemunyon, R. Stevens, and R. Parry, *Agricultural Phosphorus and Eutrophication*, USDA–ARS, USA, 1999.

Shober, A. L., and J. T. Sims, Phosphorus restrictions for land application of biosolids: Current status and future trends, *J. Environ. Qual.*, *32*, 1955–1964, 2003.

Siemens, J., K. Ilg, F. Lang, and M. Kaupenjohann, Adsorption controls mobilization of colloids and leaching of dissolved phosphorus, *Eur. J. Soil Sci.*, *55*, 253–263, 2004.

Sims, J. T., and D. C. Wolf, Poultry waste management: Agricultural and environmental issues, *Adv. Agron.*, *52*, 1–83, 1994.

Sims, J. T., R. R. Simard, and B. C. Joern, Phosphorus losses in agricultural drainage: Historical overview and current research, *J. Environ. Qual.*, *27*, 277–293, 1998.

Sims, T., Soil test phosphorus: Bray and Kurtz P-1, in *Methods of phosphorus analysis for soils, sediments, residuals, and waters*, edited by G. M. Pierzynski, pp. 13–14, Bulletin No. 396, Southern Cooperative Series, Manhattan, KS, 2000.

Slomp, C. P., S. J. van der Gaast, and W. van Raaphorst, Phosphorus binding by poorly crystalline iron oxides in north sea sediments, *Marine Chem.*, *52*, 55–73, 1996.

Smith, V. H., G. Tilman, and J. C. Nekola, Eutrophication: impacts of excess nutrient inputs on freshwater, marine, and terrestrial ecosystems, *Environmental Pollution*, *100*, 179–196, 1999.

Stamm, C., H. Flühler, R. Gächter, J. Leuenberger, and H. Wunderli, Preferential transport of phosphorus in drained grassland soils, *J. Environ. Qual.*, *27*, 515–522, 1998.

Stookey, L. L., Ferrozine a new spectrophotometric reagent for iron, *Anal. Chem.*, *42*, 779–781, 1970.

Stumm, W., and L. Sigg, Kolloidchemische Grundlagen der Phosphor-elemination in Fällung, Flockung und Filtration, *Zeitschrift für Wasser-und Abwasser-Forschung*, *2 /79*, 73–83, 1979.

Szilas, C. P., O. K. Borgaard, and C. B. Hansen, Potential iron and phosphate mobilization during flooding of soil material, *Water Air Soil Pollut.*, *106*, 97–109, 1998.

Taylor, A. W., and H. M. Kunishi, Phosphate equilibria on stream sediment and soil in a watershed draining an agricultural region, *J. Agr. Food Chem.*, *19*, 827–831, 1971.

Theis, T. L., and P. C. Singer, Complexation of iron (II) by organic matter and its effect on iron (II) oxygenation, *Environ. Sci. Technol.*, *8*, 569–573, 1974.

Toride, N., F. J. Leij, and M. T. van Genuchten, *The CXTFIT Code for estimating transport parameters from laboratory or field tracer experiments*, vol. Research Report No 137, U.S. Salinity Laboratory, Agricultural Research Service, U.S. Department of Agriculture, Riverside, California, 1999.

Torrent, J., Interactions between phosphate and iron oxide, *Advances in Geoecology*, *30*, 321–344, 1997.

Turner, B. L., and P. M. Haygarth, Phosphorus forms and concentrations in leachate under four grassland soil types, *Soil Sci. Soc. Am. J.*, *64*, 1090–1097, 2000.

USEPA *National Management Measures for the Control of Nonpoint Pollution from Agriculture*, National Service Center for Environmental Publications, Cincinnati, OH, 2003.

van der Zee, S. E. A. T. M., and W. H. van Riemsdijk, Model for long-term phosphate reaction kinetics in soil, *J. Environ. Qual.*, *17*, 35–41, 1988.

Villapando, R. R., and D. A. Graetz, Water table effects on phosphorus reactivity and mobility in a dairy manure-impacted spodosol, *Ecol. Eng.*, *18*, 77–89, 2001.

Webster, R., and M. A. Oliver, *Statistical Methods in Soil and Land Resource Survey*, Oxford University Press, Oxford, 1990.

Willett, I. R., The reductive dossolution of phosphated ferrihydrite and strengite, *Aust. J. Soil Res.*, *23*, 237–244, 1985.

Wilson, M. J., X-ray powder diffraction methods, in *A handbook of determinative methods in clay mineralogy*, edited by M. J. Wilson, pp. 26–98, Blackie & Son Limited, New York, 1987.

Wolf, A. M., and D. E. Baker, Colorimetric method for phosphorus measurement in ammonium oxalate soil extracts, *Commun. Soil Sci. Plant Anal.*, *21*, 2257–2263, 1990.

Wood, C. W., and J. A. Hattey, Impact of long-term manure applications on soil chemical, microbiological, and physical properties, in *Animal waste and the land-water interface*, edited by K. Steele, pp. 419–428, CRC/Lewis Publishers, Boca Raton, Florida, 1995.

Yli-Halla, M., H. Hartikainen, and P. Väätäinen, Depletion of soil phosphorus as assessed by several indices of phosphorus supplying power, *Eur. J. Soil Sci.*, *53*, 431–438, 2002.

Young, E. O., and D. S. Ross, Phosphate release from seasonally flooded soils: A laboratory microcosm study, *J. Environ. Qual.*, *30*, 91–101, 2001.

Zhou, M., and Y. Li, Phosphorus sorption characteristics of calcareous soils and limestone from the Southern Everglades and adjacent farmlands, *Soil Sci. Soc. Am. J.*, *65*, 1404–1412, 2001.